

# **Nucleation and Growth of Crystals of Pharmaceuticals on Functionalized Surfaces**

by

**Kasim Biyikli**

A Thesis

Submitted to the Faculty

of the

WORCESTER POLYTECHNIC INSTITUTE

in partial fulfillment of the requirements for the

Degree of Master of Science

in

Chemistry

February 2006

APPROVED :

Prof. John C. MacDonald, Research Advisor

Signature: \_\_\_\_\_ Date: \_\_\_\_\_

Prof. James W. Pavlik, Head of Department

Signature: \_\_\_\_\_ Date: \_\_\_\_\_

## **ABSTRACT**

A series of hydrophobic and hydrophilic self-assembled monolayers (SAMs) were deposited by the adsorption of 1-dodecanethiol (SAM I), 11-mercapto-1-undecanol (SAM II), 16-mercaptohexadecanoic acid (SAM III), 5-(10-mercaptodecyloxy)benzene-1,3-dioic acid (SAM IV) and 4-(10-mercaptodecyloxy)-pyridine-2,6-dicarboxylic acid (SAM V) on gold substrates. Crystallization experiments were carried out on SAMs I-V, on control surfaces (bulk gold, glass and PDMS (polydimethylsiloxane)) and in microfluidic devices to screen the polymorphs of two well known drugs, acetaminophen and barbital. Microfluidic devices consist of PDMS (polydimethylsiloxane) patterned with microchannels and then bonded to self-assembled monolayers (SAMs) of organic molecules on gold substrates. The crystallization of acetaminophen was carried out under thermodynamic conditions from solutions at room temperature and under kinetic conditions by rapid cooling. The results of crystallization experiments and the influence of self-assembled monolayers (SAMs) in controlling polymorphism by acting as nucleation sites, or templates, are discussed.

## **ACKNOWLEDGEMENTS**

I would like to sincerely thank my advisor, Professor John C. MacDonald for his support, patience and guidance.

I would also like to thank Professor W. Grant McGimpsey and Professor Venkat Thalladi for use of equipment in their labs.

I also would like to thank all my colleagues in the department. In particular, I would like to thank Eftim Milkani, Branko Zugic, Jason Cox, Salim G. Adilov, Marta Dabros, Chuchawin Changtong and Taner Gokcen.

I also would like to thank my parents, brothers and friends for encouraging me and supporting me over years.

## TABLE OF CONTENTS

ABSTRACT.....	1
ACKNOWLEDGMENTS.....	2
TABLE OF CONTENTS.....	3
LIST OF FIGURES.....	5
LIST OF TABLES.....	9
1. INTRODUCTION.....	10
2. POLYMORPHISM.....	12
2.1 What is polymorphism?.....	12
2.2 How does polymorphism occur?.....	14
2.3 Stability of polymorphs .....	15
2.4 Can Polymorphism be controlled?.....	16
2.5 Model systems for studying nucleation and growth of polymorphs of pharmaceuticals on surfaces.....	24
2.5.1 Barbitol (5,5-diethylbarbituric acid).....	25
2.5.2 Acetaminophen (Paracetamol).....	32
3. Self-Assembled Monolayers.....	35
3.1 Introduction and background on self-assembled monolayers.....	35
3.2 SAMs used for crystallization.....	38
3.3 Preparation of SAMs.....	43
3.3.1 Experimental procedures used to prepare SAMs on gold.....	45
3.4 Characterization of SAMs.....	45
3.4.1 Contact Angle Goniometry.....	45
3.4.2 Ellipsometry.....	48
3.4.3 Grazing angle FT-IR.....	49
3.4.4 Cyclic Voltammetry.....	51
4. Crystallization on SAMs.....	53
4.1 Crystallization on SAMs on bulk surfaces.....	53
4.1.1 Method I.....	56
4.1.2 Method II.....	57
4.1.3 Method III.....	58



4.2	Crystallization on SAMs in microfluidic channels.....	58
4.2.1	Fabrication of microfluidic devices.....	59
4.2.2	Crystallization of barbital in microchannels.....	62
4.2.2.1	Method 1.....	62
4.2.2.2	Method 2.....	63
4.3	Characterization of crystals.....	63
4.3.1	Melting point.....	64
4.3.2	Optical microscopy.....	65
4.3.3	Infrared Spectroscopy.....	66
4.3.4	<sup>13</sup> C CP/MAS NMR.....	70
4.3.5	X-Ray Powder Diffraction.....	72
4.4	Results and Discussion.....	73
4.4.1	Acetaminophen.....	76
4.4.1.1	Bulk Surfaces.....	76
4.4.1.1.1	Ethanol.....	76
4.4.2	Barbital.....	81
4.4.2.1	Bulk surfaces.....	81
4.4.2.1.1	Ethanol.....	81
4.4.2.1.2	Water.....	89
4.4.2.1.3	Ethyl Acetate.....	93
4.4.2.2	Microfluidic Device.....	98
4.4.2.2.1	Ethanol.....	99
4.4.2.2.2	Water.....	103
4.5	Conclusions.....	106
4.6	References.....	108

## LIST OF FIGURES

<b>Figure 2.1:</b> Polymorphism in molecular crystals arises when molecules pack in different conformations (right) or in different orientations (left).....	15
<b>Figure 2.2:</b> Model for crystallization of polymorphs.....	18
<b>Figure 2.3:</b> Structure of barbital (5,5-diethylbarbituric acid).....	26
<b>Figure 2.4:</b> Possible hydrogen-bonded dimer pair combinations between barbituric acids. Dimer pairs related through a center of symmetry are indicated by a dot (•).....	27
<b>Figure 2.5:</b> Hydrogen-bonding motifs observed in the crystals structures of barbituric acids. X represents an O or S atom and L represents a range of organic substituent groups.....	28
<b>Figure 2.6:</b> Structure of form I of barbital (a) and the hydrogen-bonding motif of form I (a linear ribbon) illustrated with a ChemDraw diagram (b) and crystal packing diagram (c).....	30
<b>Figure 2.7:</b> Structure of form II of barbital (a) and the hydrogen-bonding motif of form II (a linear tape) illustrated with a ChemDraw diagram (b) and crystal packing diagram (c).....	31
<b>Figure 2.8:</b> Structure of form IV of barbital and the hydrogen-bonding motif of form IV (a sheet) illustrated with a ChemDraw diagram (b) and crystal packing diagram (c). .....	32
<b>Figure 2.9:</b> Structure of acetaminophen.....	32
<b>Figure 2.10</b> Structure of form I <sup>76</sup> of acetaminophen and the hydrogen-bonding motif of form I illustrated with a ChemDraw diagram (b) and crystal packing diagram (c).....	34

<b>Figure 2.11</b> Structure of form II <sup>76</sup> of acetaminophen and the hydrogen-bonding motif of form II (a sheet) illustrated with a ChemDraw diagram (b) and crystal packing diagram (c).....	35
<b>Figure 3.1:</b> (a) Chemical structures of SAMs I-V deposited on gold substrates for experiments. (b) Chemical structures used for control experiments.....	39
<b>Figure 3.2:</b> a) Hydrogen-bonding donor and acceptor groups on barbital and acetaminophen. b) Examples of different hydrogen-bonding motifs that result from homomeric (self) assembly of barbital. c) Examples of different hydrogen-bonding motifs that can result from heteromeric assembly of barbital with carboxylic acids and alcohols.....	41
<b>Figure 3.3:</b> Illustration of different modes of hydrogen bonding interactions between barbital and SAMs terminated with COOH and OH groups.....	42
<b>Figure 3.4:</b> Preparation of SAMs of alkanethiols on gold.....	44
<b>Figure 3.5:</b> Example of a contact angle measurement.....	46
<b>Figure 3.6:</b> Images of 1µL drops of water on SAMs I-V and bare gold viewed through a microscope equipped with a goniometer: (a) SAM I; (b) SAM II; (c) SAM III; (d) SAM IV; (e) SAM V and (f) bare gold.....	47
<b>Figure 3.7:</b> Grazing angle FT-IR spectra of SAMs that were used for crystallization experiments. (a) SAM I. (b) SAM IV. (c) SAM III. (d) SAM II. (e) SAM V.....	51
<b>Figure 3.8:</b> Cyclic Voltammograms of SAMs I-V and bare gold.....	53
<b>Figure 4.1:</b> (a) Crystallization experiment set up for method I (solvent at the bottom of Petri dish). (b) Method II. (c) Method III.....	55

<b>Figure 4.2:</b> (a) Microfluidic device with a single channel (1 mm x 18 mm x 0.2 mm). (b) Microfluidic device with ten channels (0.7 mm x 18 mm x 0.1 mm).....	60
<b>Figure 4.3:</b> Fabrication of microfluidic device and growth of crystals.....	61
<b>Figure 4.4:</b> Crystal pictures of form I, II and IV for barbital.....	65
<b>Figure 4.5:</b> Crystal pictures of form I and II for acetaminophen <sup>76</sup> .....	66
<b>Figure 4.6:</b> (a) IR spectra for forms I, II and IV of barbital. (b) Expanded IR spectra of zone 1. (c) Expanded IR spectra of zone 2.....	68
<b>Figure 4.7:</b> (a) IR spectra for forms I and II of acetaminophen. (b) Expanded IR spectra of zone 1. (c) Expanded IR spectra of zone 2. (d) Expanded IR spectra of zone 3.....	69
<b>Figure 4.8:</b> <sup>13</sup> C CP/MAS NMR spectra of forms I, II and IV of barbital.....	70
<b>Figure 4.9:</b> X-ray powder diffraction traces of forms I, II and IV of barbital (a-c, respectively). The dotted lines mark the positions of the more intense peaks in the trace of form I (a). Overlap of these peaks with peaks in the trace of form IV (c) indicate contamination of form IV by approximately 5% of form I.....	73
<b>Figure 4.10:</b> Forms I, II and IV of barbital from different substrates.....	75
<b>Figure 4.11:</b> Forms I and II of acetaminophen from different substrates.....	75
<b>Figure 4.12:</b> Examples of acetaminophen crystal pictures on each surface for each method.....	79
<b>Figure 4.13:</b> Results of acetaminophen crystallization experiments for each method...	81
<b>Figure 4.14:</b> Hypothesis for the explanation of how form IV appears on hydrophilic surface.....	84
<b>Figure 4.15:</b> Examples of barbital crystal pictures on each surface for each method from ethanolic solution.....	85

<b>Figure 4.16:</b> Results of barbital crystallization experiments for each method from ethanolic solution.....	88
<b>Figure 4.17:</b> Examples of barbital crystal pictures on each surface for each method from water solution.....	90
<b>Figure 4.18:</b> Results of barbital crystallization experiments for each method from water solution.....	91
<b>Figure 4.19:</b> Examples of barbital crystal pictures on each surface for each method from ethyl acetate solution.....	96
<b>Figure 4.20:</b> Results of barbital crystallization experiments for each method from ethyl acetate solution.....	97
<b>Figure 4.21:</b> Examples of barbital crystal pictures in microchannels from ethanolic solution.....	101
<b>Figure 4.22:</b> Results of barbital crystallization experiments in microchannels from ethanolic solution. The distribution of forms I, II and IV that grew on bulk Au, glass and PDMS substrates are shown for comparison.....	102
<b>Figure 4.23:</b> Examples of barbital crystal pictures in microchannels from water solution.....	104
<b>Figure 4.24:</b> Results of barbital crystallization experiments in microchannels from water solution. The distribution of forms I, II and IV that grew on bulk Au, glass and PDMS substrates are shown for comparison.....	105

## LIST OF TABLES

<b>Table 2.1:</b> Melting point, crystal system and shape of forms for barbital.....	30
<b>Table 2.2:</b> Melting point, crystal system and shape of forms for acetaminophen.....	33
<b>Table 3.1:</b> Contact angle measurements of SAMs.....	48
<b>Table 3.2:</b> Thickness of SAMs.....	49
<b>Table 4.1:</b> Concentration of barbital and acetaminophen solutions used for crystallization.....	55
<b>Table 4.2:</b> Concentration of barbital solutions used for crystallization in microfluidic devices.....	62
<b>Table 4.3:</b> Chemical shifts from $^{13}\text{C}$ CP/MAS NMR spectra of forms I, II and IV of barbital.....	71

## 1. INTRODUCTION

The design and preparation of crystalline materials with desired properties is one of the principal aims for chemists. The existence of polymorphic forms of molecular solids offers a special chance for examining structure-property relationships because the main difference between polymorphs arises from variation in molecular packing arrangements within crystals rather than differences in molecular structure. Crystallization of drug molecules from solution as polymorphs—that is, different crystal forms in which the molecules adopt alternate packing arrangements—remains a persistent problem for crystal engineering.<sup>1,2</sup> Polymorphism is particularly problematic in the development of pharmaceuticals because polymorphs of a single compound legally are classified as different drugs. Consequently, there is a need to develop methods to screen for the incidence of polymorphs and control which polymorphs form. Control over the polymorphic behavior of drugs, identification of different polymorphic forms of drugs and prediction of new polymorphs are major hurdles in the development and marketing of all pharmaceuticals that form crystalline solids. In the pharmaceutical industry, 70% of barbiturates, 60% of sulfonamides and 23% of steroids exist in different polymorphic forms. Polymorph screening is an especially important part in the development of drugs because polymorphs impact the process at many levels that include patent protection, polymorph identification and characterization,<sup>3</sup> development and process control to achieve consistent crystallization results.<sup>4</sup>

While considerable effort has been spent investigating how factors such as concentration, temperature, solvent and pH influence nucleation and growth of polymorphs, considerably less is known about the influence of thin molecular films such

as self-assembled monolayers (SAMs) in this regard. While crystallization of inorganic minerals,<sup>5-11</sup> organic compounds<sup>12-16</sup> and proteins<sup>17,18</sup> on SAMs, langmuir layers and other substrates have been reported, few studies have focused on the use of SAMs in controlling the incidence of polymorphs.<sup>19,20</sup> Fewer studies still have focused on the use of microfluidic devices to carry out crystallization on small quantities of solution (e.g., nanoliters) in microchannels,<sup>21,22</sup> although control of polymorphism has been studied in micropores and capillaries recently.<sup>23-25</sup> In our research, we have focused on the questions of whether nucleation and growth of polymorphs of pharmaceuticals such as barbital (5,5'-diethylbarbituric acid) and acetaminophen can be promoted and controlled on SAMs on gold substrates both on bulk surfaces and in microchannels. We have begun to investigate microfluidic devices that contain multiple channels as a means to develop high throughput methods to screen for polymorphism.<sup>26</sup> Goals of this research included determining (1) whether crystals of barbital and acetaminophen will nucleate on SAMs of gold substrates and in microchannels, (2) if nucleation of polymorphs occurs preferentially in microchannels on surfaces functionalized with a range of hydrophobic and hydrophilic organic groups, (3) whether the incidence of specific polymorphs—particularly those that are less stable—can be controlled on different SAMs on bulk surfaces and in microchannels, and (4) whether microfluidic devices with multiple channels can be used to screen for polymorphs.

Our strategy was to crystallize barbital and acetaminophen on a series of SAMs that contain nonpolar and polar groups exposed at the surface. We anticipated that assembly of barbital and acetaminophen molecules onto the surface of different SAMs via



hydrogen bonding might generate molecular aggregates that would serve as nucleation sites, or templates, that lead to different polymorphs during crystallization.

## **2. Polymorphism**

### **2.1 What is polymorphism?**

Polymorphism is the ability of a substance to exist in two or more crystalline phases, or polymorphs, that have different arrangements and/or conformations of molecules in the solid state.<sup>1</sup> Although the molecules in polymorphs have identical structure and properties in the solution phase, the physical properties of polymorphs generally differ, often quite dramatically. Different crystal modifications or crystal structures of the same molecule are referred to as polymorphs or forms. The stabilities of polymorphs, especially those that appear together, or concomitantly, generally are close with lattice energies that differ by no more than approximately 5 kcal/mol. One polymorph is the thermodynamically most stable form at any specific temperature except at temperatures where two polymorphs are in equilibrium. As the difference in lattice energy between two polymorphs becomes greater, the less stable polymorph is more likely to undergo a phase transformation either converting into the more stable form or a new form with greater stability. W. C. McCrone established in 1965 that polymorphic phase transformations of one crystalline form into a different crystalline form can occur exclusively in the solid phase without the solid first melting.<sup>27</sup>

Polymorphism has been studied with a variety of commercially important materials ranging from silica, alumina, and metals to complex molecular compounds such as drugs, dyes, and plastics.<sup>27</sup> Polymorphism is particularly problematic in the pharmaceutical industry because polymorphs of drugs differ in their physical properties (e.g., melting

point, solubility, and bioavailability). An important consequence of this variability is that all polymorphs of a given pharmaceutical compound legally are regarded as different drugs. As such, pharmaceutical companies spend considerable expense and effort to identify and patent as many polymorphs as possible. For example, the anti-ulcer drug Zantac (ranitidine hydrochloride) is a histamine receptor antagonist that works by decreasing the amount of acid produced in the stomach. Zantac has two known polymorphs that have been patented and sold commercially.<sup>28</sup> Polymorphism in pharmaceutical solids, as in all molecular solids, is attributed to different packing arrangements that arise predominately based on differences in intermolecular interactions between molecules during crystal nucleation. Of all the different types of non-covalent interactions<sup>29-32</sup> (i.e., hydrogen bonding, van der Waals interactions,  $\pi$ - $\pi$  stacking, electrostatic interactions, etc.) present in polymorphic solids, hydrogen bonding generally is the most important type of interaction because hydrogen bonds have the greatest strength and are directional.<sup>33</sup>

The possibility of polymorphism exists for virtually any compound regardless of structure or size. The conditions necessary to obtain polymorphs, however, are not usually obvious. Often it is necessary to crystallize a compound under a broad range of conditions and then screen bulk samples of crystals in order to find polymorphs. Even when polymorphs are observed, it is difficult to know if additional polymorphs are accessible and under what conditions. McCrone adroitly explained the occurrence of polymorphism by stating: "It is at least this author's opinion that every compound has different polymorphic forms and that, in general, the number of forms known for a given compound is proportional to the time and money spent in research on that compound."<sup>27</sup>

## 2.2 How does polymorphism occur?

Figure 2.1 illustrates how polymorphism can result during the process of crystal nucleation or during a phase transformation from one crystal form to another. As shown on the right, two polymorphs result when molecules crystallize separately in two different conformations. Polymorphs that result from changes in molecular conformation are referred to as conformational polymorphs. For example, biphenyl is a well-known example of a compound that exhibits conformational polymorphism. In the stable form, the phenyl rings twisted about the central C-C bond  $10^\circ$ , while in the metastable form, the phenyl rings are coplanar.<sup>36</sup> As shown on the left in Figure 2.1, polymorphs also result when molecules crystallize separately in different relative orientations or packing arrangements. For example, hexachloro-ketodihydrobenzene,  $C_6Cl_6O$ , is a conformationally rigid molecule that crystallizes in two different polymorphic forms.<sup>37</sup> The two forms differ in that the molecules pack in two different arrangements. In this case, the two polymorphs crystallize concomitantly under the same conditions, which indicate that the two polymorphs have similar lattice energy and, therefore, stability.

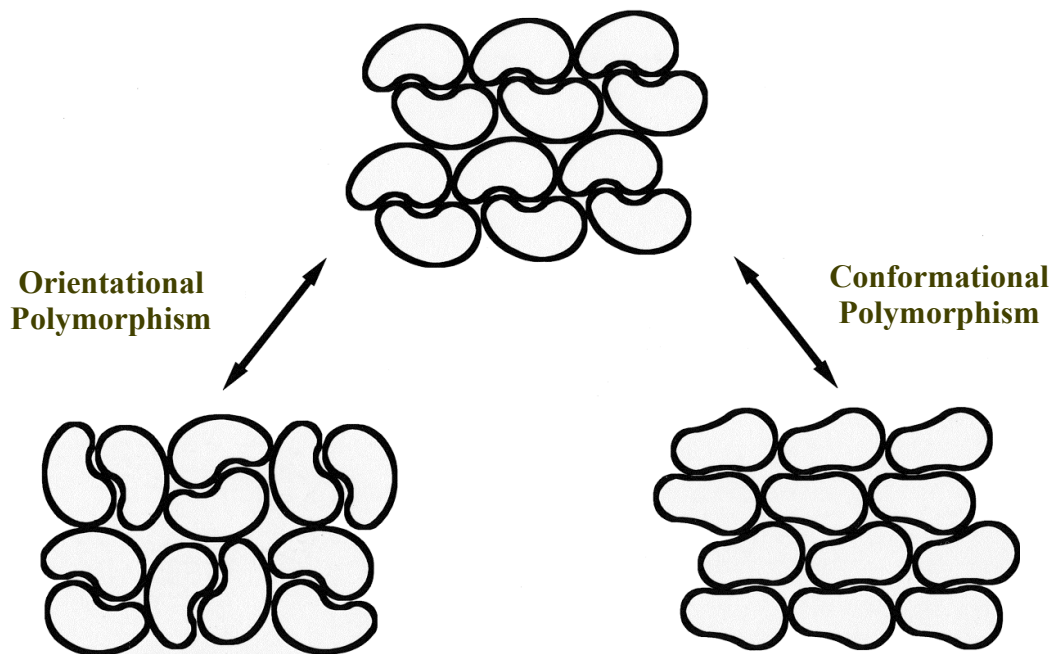


**Figure 2.1** Polymorphism in molecular crystals arises when molecules pack in different conformations (right) or in different orientations (left).

### 2.3 Stability of polymorphs

Polymorphic phase transformations can occur when the difference in lattice energy between a metastable form and a more stable form is greater than several kcal/mol. Phase transformations can occur spontaneously in solution or in air. In many cases, external stimuli such as heating or mechanical grinding are required, however, to induce polymorphic transformation in order to provide enough activation energy to initiate molecular rearrangement in the solid. For example, the metastable form of biphenyl undergoes a polymorphic transformation to the stable form upon cooling. Competition between conjugation of double bonds in the two rings and the steric repulsion of the ortho-hydrogen atoms causes biphenyl to crystallize in the stable form with the phenyl rings twisted and in the metastable form with the phenyl rings coplanar. In crystals, the twisted and planar conformations are in equilibrium with the twisted form being more

stable than the planar form by about  $1.5 \text{ kcal mol}^{-1}$ .<sup>36</sup> The energy of a given polymorph is related to the Gibbs free energy. Lattice energy usually is taken as an estimate for Gibbs free energy. The relative stability of the two polymorphs depends on their free energies (lattice energies) with the more stable polymorph having the lowest lattice energy. The differences in free energies of different polymorphs might be very small ( $1\text{-}2 \text{ kcal mol}^{-1}$ ). If two or more polymorphs have energetically equivalent structures or structures that are within  $\sim 1 \text{ kcal/mol}$ , the different crystal forms can and frequently do appear at the same time under identical conditions. Polymorphs that appear simultaneously are referred to as concomitant polymorphs.<sup>1</sup> The concept of concomitant polymorphs is illustrated by the drug barbitol (5,5'-diethylbarbituric acid), which has three known polymorphs (forms I, II and IV) that form concomitantly when barbitol is crystallized by slow evaporation from solutions in ethanol.<sup>65,71</sup> Forms I and II of barbitol are both stable in air under ambient conditions, while metastable form IV slowly transforms to form I over days or weeks on standing in air.

#### **2.4 Can Polymorphism be controlled?**

Crystallization is the name of the process when upwards of  $10^{20}$  molecules or ions spread essentially randomly throughout a fluid medium coalesce and naturally form a solid with a well-defined structure.<sup>1</sup> How crystallization begins and how it proceeds are questions that are not completely understood. Models for crystallization have been developed to explain the different stages leading to the formation of molecular crystals.<sup>68-</sup><sup>70</sup> The first stage of crystallization is known as nucleation. Nucleation occurs when molecules in solution aggregate, typically on a surface, to form a nucleus consisting of an ordered arrangement of molecules that serves as a site in the crystallization medium from

which crystals may grow. It is important to note that the packing arrangement of molecules in bulk crystals is defined by the arrangement of molecules present in a nucleus. Thus, a nucleus can be considered as an ordered aggregate, or template, containing the minimum number of molecules necessary to define the crystal structure. The number of molecules in a stable crystal nucleus differs depending on the structure and size of the molecule and typically ranges from 10 to 1000.<sup>71,72</sup> Once a nucleus forms, growth occurs by subsequent addition of molecules from solution to propagate the arrangement of molecules present in the nucleus. Growth is a dynamic process in which molecules come into contact and bind to the surface of a growing nucleus. Under typical equilibrium conditions, molecules can remain bound or leave from the surface. For growth to occur, molecules must interact with other molecules on the surface in the appropriate orientation to maximize energetically favorable interactions (e.g., van der Waals interactions, hydrogen bonds, etc.) that prevent molecules from leaving the surface. In particular, hydrogen bonds frequently play an important role during nucleation because they are the strongest and most directional of all intermolecular interactions.<sup>7</sup> The selectivity of different organic functional groups in forming specific hydrogen-bonding motifs (e.g., dimers between carboxylic acids) often results in specific aggregates that lead to different polymorphs. In some cases, hydrogen bonding leads to supramolecular aggregates with identical hydrogen bonding that form polymorphs by crystallizing in different arrangements.<sup>38</sup>

The incidence of polymorphism can be attributed directly to the formation of molecular aggregates with different structures that lead to stable nuclei with different packing arrangements. Thus, each different stable aggregate that forms in solution has the

potential to serve as a nucleus for a unique polymorphic form. This concept is illustrated in Figure 2.2. Formation of different molecular aggregates generally occurs in response to competition between kinetic and thermodynamic factors during crystallization. Consider the hypothetical crystallization shown in Figure 2.2 in which two different aggregates promote nucleation and growth of four polymorphic forms, I-IV, where form I is the most stable and form IV is the least stable. Under thermodynamic conditions, the polymorph that is most stable (form I) will predominate regardless of the rate at which aggregates 1 and 2 form; whereas, under kinetic conditions, the predominant polymorph or polymorphs will be determined by the aggregate that forms at the fastest rate. For example, even if form 1 is the thermodynamically most stable polymorph, forms 3 and/or 4 will be the only polymorphs obtained if aggregate 2 nucleates crystal growth faster than aggregate 1. Any change that shifts the balance between thermodynamics and kinetics even slightly can have a significant impact on the polymorphs that appear. Consequently, the most common strategy to obtain new polymorphs or alter the distribution of polymorphs is to vary the conditions of crystallization (e.g., solvent, temperature, concentration, method of crystallization, etc.).

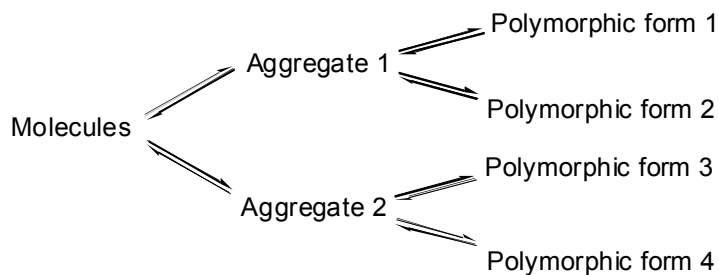


**Figure 2.2** Model for crystallization of polymorphs.

Previous studies have established that factors such as solvent, temperature, concentration, pH and surfaces in contact with growth solutions influence nucleation and growth of crystals.<sup>4,39-41</sup> The influence of each of these factors is summarized below.

**i. Solvent:** It is generally accepted that solvents influence crystallization by preferential adsorption onto the different surfaces or facets of crystals as they develop thus hindering the deposition of solute molecules differentially on the different surfaces.<sup>73,75</sup> For polar crystals, the effect of different solvents on crystal morphology can be observed easily. The variation in the rate of growth of two opposite faces that lie along the same polar direction is considered to result from solvent effects. For example the (010) face of N-n-octyl-D-gluconamide when exposed to polar solvents (e.g., methanol) grows about five times slower than the  $(0\bar{1}0)$  face under the same conditions.<sup>76</sup> Growth kinetics of N-n-octyl-D-gluconamide in a polar solvent fully support that the slowest growing face is indeed the more hydrophilic one. Different solvent systems also can lead to the appearance of different polymorphs. For example, 2,6-dihydroxybenzoic (DHB) acid has two known polymorphs, forms 1 and 2.<sup>78,79</sup> These two forms contain different arrangements of molecules that arise from two different hydrogen bonding motifs. Form 1 features discrete carboxylic acid dimers that are packed in a herringbone motif, while form 2 contains infinite hydrogen-bonded chains of carboxylic acids. It has been shown that dimerization in toluene solutions is the most effective means of maximizing the solute-solute interactions while minimizing the unfavorable polar-nonpolar interactions between toluene and DHB. In the presence of chloroform, however, formation of carboxylic acid dimers is hindered sterically due to the interaction of chloroform with the



carboxylic acid groups. It has been proposed that dimers do not form under those conditions because dimers would not be solvated effectively due to the unfavorable proton contacts as molecules of chloroform seek to maximize the number of favorable Cl $\cdots$ H-O interactions.<sup>80</sup>

**ii. Temperature:** Temperature often controls nucleation and crystal growth by manipulating the solubility and supersaturation of the sample.<sup>43-45</sup> Slow cooling often is used for saturated solutions if the compound is more soluble at high temperature. Alternatively, slow warming can be used if the compound is less soluble at higher temperatures. Slow cooling or warming allows the thermodynamically most stable polymorph to form under conditions where the selectivity is highest for nucleation and growth of that most stable form. In contrast, rapid cooling frequently leads to nucleation and growth of several different polymorphs, particularly when the solubilities of the different polymorphs are close. In general slow crystallization under thermodynamic condition gives larger crystals than fast crystallization under kinetic conditions.

**iii. Concentration:** The time it takes for crystals to nucleate and begin growth depends on the concentration and the rate at which solvent evaporates. To reach the supersaturation point for a given solution to initiate crystallization requires either that the amount of solvent be reduced (e.g., evaporation of solvent) or that the solubility of the solute be reduced. Accordingly, evaporation of solvent is one of the more commonly used methods for crystallizing compounds. Ostwald demonstrated that unstable polymorphic forms have a greater solubility than the more stable forms in a particular

solvent.<sup>46</sup> Therefore, crystallization by slow evaporation generally results in formation of the most stable polymorph.

**iv. pH:** pH is another important factor that can affect crystallization and the appearance of polymorphs, especially for protein crystallization. In aqueous solution, a protein with hydrophilic groups on its surface is covered with surface-bond water molecules. Addition of ions to solution results in removal of some water molecules that leaves some sites on the surface of the protein free to bind to other protein molecules. Thus, aggregation of proteins and subsequent nucleation and growth of crystals often can be promoted simply by changing the pH of the solution.<sup>47</sup> For example, glycine molecules pack as zwitterions in each of its three polymorphic forms ( $\alpha$ ,  $\beta$  and  $\gamma$  glycine). Accordingly, the charge of glycine molecules will change depending on the pH range of the solution. It has been reported that glycine crystallizes in the  $\alpha$  form by forming centrosymmetric dimers in solutions with pH values between 3.8 and 8.9.<sup>35</sup> Outside of this range, singly charged glycine molecules do not form dimers, but instead crystallize by forming polar chains that give the  $\gamma$  form of glycine.<sup>35</sup>

**v. Surface:** Once a nucleus forms, growth units (atoms, ions or molecules) can diffuse from solution to the surface of the nucleus and incorporate into the lattice resulting in crystal growth.<sup>81</sup> Adsorption of the growth units on the surface of a growing crystal may occur at three possible sites: 1) ledge sites having only one surface in contact with the growth unit, 2) step sites having two surfaces in contact, or 3) kink sites having three sites in contact. Because growth units with the greatest number of contacts are

bound most strongly to the surface, a kink site is the most favorable energetically. Thus, substrates that promote molecular aggregation and nucleation of crystals frequently have high energy three-dimensional surfaces that feature many kink sites. For example, formation of snowflakes as a result of nucleation of ice crystals on the high energy surface of dust particles is a well known example from nature of this principle. Similarly, scratching the bottom of a glass beaker with a glass rod to induce crystallization and distribute the resulting crystal nuclei throughout solution is a well established method for crystallization. The composition and structure of substrates on which nucleation occurs play an important role in directing selectivity toward different polymorphs. Such selectivity suggests that the availability of hydrogen-bonding functionality at the nucleation interface plays an important role.<sup>3</sup>

Many studies have been carried out examining the effect of temperature and solvents on polymorphism. Far fewer studies have examined the influence of surfaces and modification of the chemical functionality presented at surfaces as a means to control polymorphism. Several studies have shown that soluble “tailor-made” small-molecule additives or polymeric additives, single crystals, Langmuir monolayers and self-assembled monolayers (SAMs) can behave as nucleation sites or templates that promote nucleation and growth of molecular crystals.<sup>5-12,14-17,48-57</sup>

Self-Assembled Monolayers (SAMs) are ordered assemblies of molecules the thickness of a single molecule formed by adsorption of molecules from solution or a gas onto a solid surface. The molecules in SAMs are highly ordered and oriented and can incorporate a wide range of groups both in the alkyl chain and at the chain termini. The ability to tailor both head and tail groups of the constituent molecules makes SAMs ideal

systems to understand competition between intermolecular, molecular-substrate and molecule-solvent interactions. Surfaces other than SAMs also have been shown to induce oriented growth of crystals, but crystallization could not be controlled easily because the structures of these surfaces were neither homogenous nor well-defined.<sup>34,171-179</sup>

Crystallization of inorganic compounds have been especially well studied on SAMs.<sup>5-</sup>  
<sup>11</sup> Aizenberg and Whitesides showed that using SAMs on metal surfaces as substrates for crystallization of calcite makes it possible to obtain a high level of control over crystal orientations.<sup>10</sup> Swift, Varney and Hiremath showed the ability to influence nucleation and oriented growth of polar crystals of 4-iodo-4-nitrobiphenyl on SAMs with different functionalities.<sup>57</sup> Studies focusing on crystallization of organic compounds on SAMs also have been reported.<sup>14</sup> For example, crystallization of malonic acid on SAMs terminated with carboxylic acids, esters, and alkyl groups.<sup>14</sup> That study demonstrated that the rate of at which crystals of malonic acid nucleate increased on SAMs with hydrogen-bonding functionality provided by terminal carboxylic acid groups when compared to other surfaces.

Recently a study was carried out to examine the effect of solids of polymers in influencing heterogeneous nucleation of polymorphs of acetaminophen and other drug molecules.<sup>51</sup> The important findings of that study were that crystallization of acetaminophen in the presence of different polymer solids resulted in the formation of form I or form II or a mixture of forms I and II of acetaminophen. Although the authors were not able to predict *a priori* which polymorphs would nucleate on given solid polymer, the polymorphs that formed did so reproducibly. This work demonstrated that it is possible to use heterogeneous nucleation on solids with different surface energies to

promote formation of different polymorphs of acetaminophen. More importantly, that work established that heterogeneous nucleation on polymer solids can be used to obtain the less stable form of acetaminophen. This study in particular provided much of impetus for our work investigating the influence of SAMs as templates for controlling nucleation of polymorphs.

## **2.5 Model systems for studying nucleation and growth of polymorphs of pharmaceuticals on surfaces**

For the purposes of this study, we sought two different polymorphic drug systems with the following requirements: (1) at least two polymorphs are known to be stable at room temperature; (2) the molecular structures have two or more functional groups capable of hydrogen bonding; (3) the compound is soluble both in organic solvents and water; and (4) the polymorphic forms can be distinguished both visually and spectroscopically. In addition, we wanted to find one system with concomitant polymorphs having similar lattice energies and stabilities. Our reasoning was that such systems would be useful in probing the effect of subtle variations in the interaction energies on different surfaces in controlling nucleation. By choosing polymorphs with similar lattice energies, we hoped to demonstrate that selectivity for one polymorph over another results predominantly from surfaces acting as templates for nucleation, rather from inherent differences in the stabilities of the polymorphs. For the second system, we tried to find a drug with stable polymorphs that do not form concomitantly in order to study the selectivity of surfaces in promoting nucleation of less stable or even metastable polymorphs.

A survey reported in 1999<sup>58</sup> found 321 polymorphic systems in the Cambridge Structural Database of which 291 were dimorphic, 27 trimorphic, 3 had four polymorphs, and none had five or more. Many more examples of polymorphic systems are known, however, where the crystal structure of only one polymorph has been reported. Substituted barbituric acids are the one of the more extensively studied families of compounds that exhibit polymorphism extensively.<sup>59-64</sup> For our research we selected to investigate barbital (5,5-diethylbarbituric acid), which has three known polymorphs (forms I, II and IV),<sup>65</sup> and acetaminophen, which has two known polymorphs (forms I and II) that have been studied broadly.<sup>66-70</sup>

### **2.5.1 Barbital (5,5-diethylbarbituric acid)**

We identified the family of drugs known as barbituric acids as a good source for polymorphs and chose barbital in particular as a model system for this study. The structure of barbital is shown in Figure 2.3. Our choice was based on previous work in which we established that barbituric acids are prone to polymorphism because the arrangement of amide groups in barbituric acids give these compounds considerable variability in their hydrogen-bonding associations.<sup>72</sup> The presence of two N-H donors and three carbonyl acceptors introduces the potential for variability in the hydrogen-bonding motifs based on hydrogen-bonded dimers. For example, shown in Figure 2.4 are ten possible barbituric acid dimer configurations consisting of different centrosymmetric and noncentrosymmetric configurations that can form when substituents  $R_1$  and  $R_2$  are different. Considering that the energies of the hydrogen bonds in each dimer are similar, and that each dimer has additional sites at either end to form additional amide-amide

hydrogen bonds, it is not surprising that barbituric acids form a variety of different hydrogen-bonding motifs that frequently lead to different polymorphs during crystallization. To emphasize this point, shown in Figure 2.5 are six different hydrogen-bonding motifs present in twenty-three crystal structures of barbituric acids from the Cambridge Structural Database that we reported previously.<sup>72</sup> The molecules of barbituric acids formed two tape motifs (I and II), two ribbon motifs (I and II), and two layer motifs (I and II). Of those, tapes were the most common motif, occurring in fifteen structures.

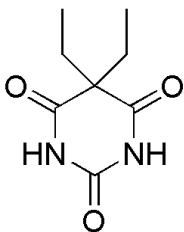


**Figure 2.3** Structure of barbital (5,5-diethylbarbituric acid).

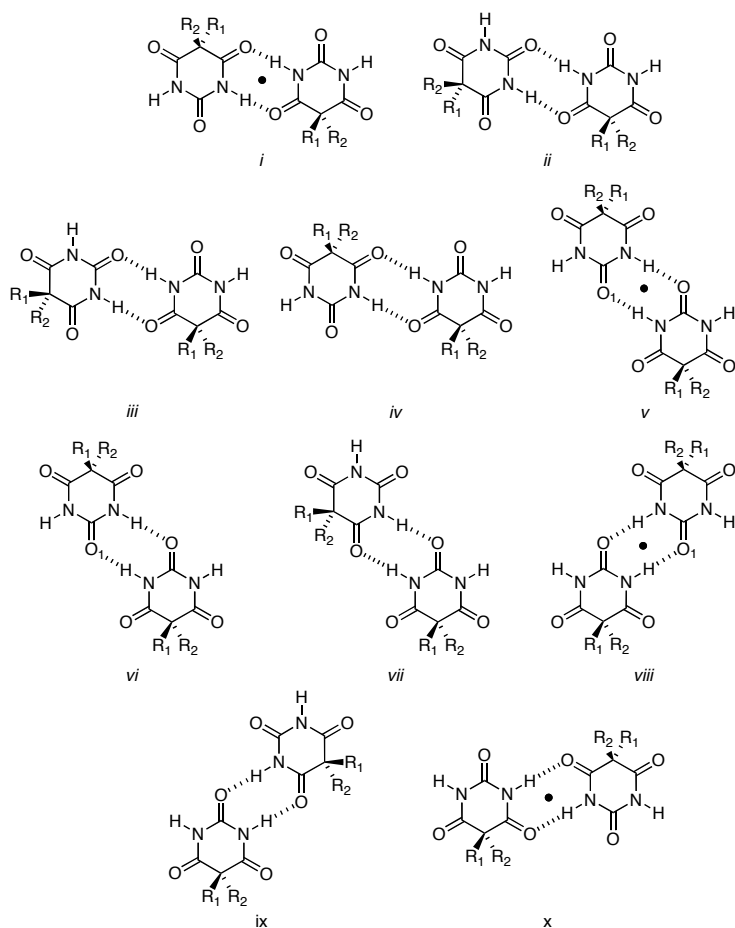


**Figure 2.4** Possible hydrogen-bonded dimer pair combinations between barbituric acids. Dimer pairs related through a center of symmetry are indicated by a dot (•).



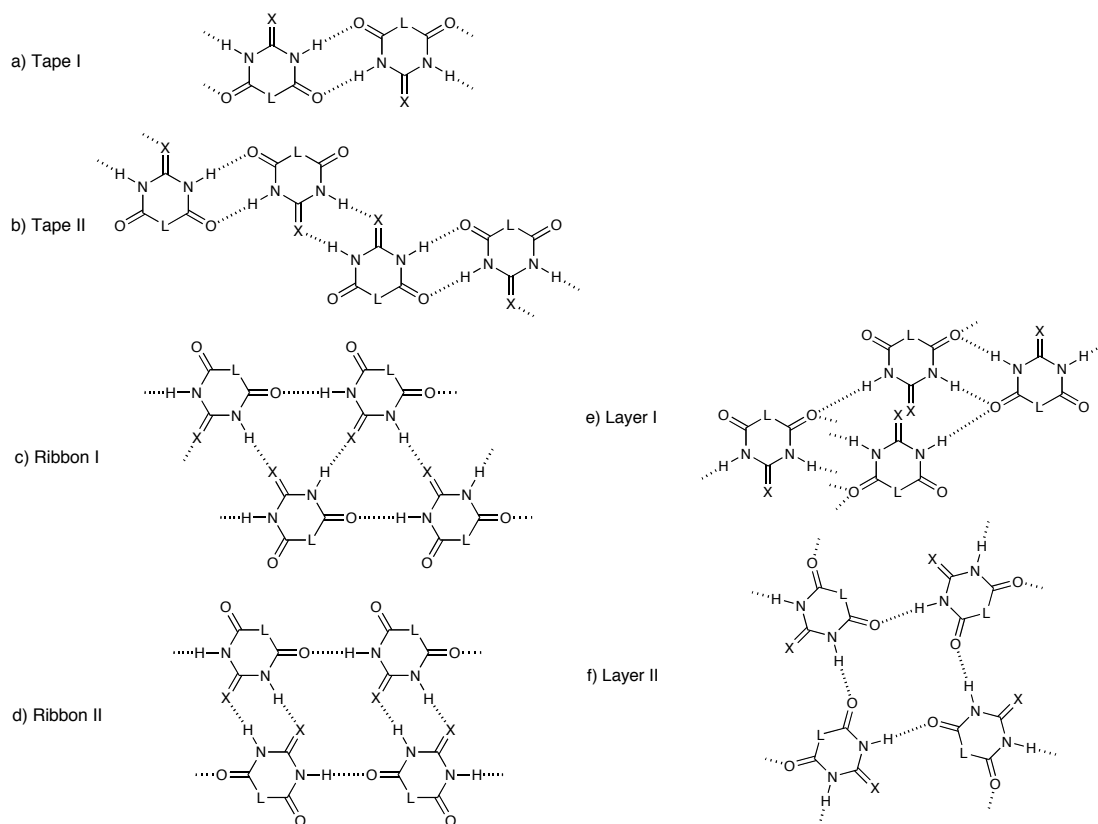


**Figure 2.5** Hydrogen-bonding motifs observed in the crystals structures of barbituric acids. X represents an O or S atom and L represents a range of organic substituent groups.

Several studies of polymorphism in substituted barbituric acids have been reported.<sup>150-154</sup> In one study, Cleverley and Williams examined twenty different barbituric and thiobarbituric acids by X-ray powder diffraction (XPD) and solid-state IR and found that nine of these barbituric acids exhibited polymorphism.<sup>155</sup> In the case of 5-ethyl-5-phenyl barbituric acid, six different polymorphs were observed to form by XPD. No correlation between molecular structure and the occurrence of polymorphism has been found for these compounds.

Craven reported previously that single crystals of three polymorphs of barbital—referred to as forms I, II, and IV—were obtained from the same ethanolic solution.<sup>65,71</sup> Not surprisingly, the crystal structures of forms I, II, and IV show that molecules of barbital form three different hydrogen-bonding motifs. Craven concluded that barbital I, which has the highest melting point of the three compounds (range 190 ° to 176 °C), is the most stable structure because of more effective van der Waals contacts. The fact that all three crystalline forms were obtained concomitantly under the same crystallization conditions suggests the hydrogen-bonded aggregates in these structures are close in energy.

In summary, we chose to study barbital for the following reasons:

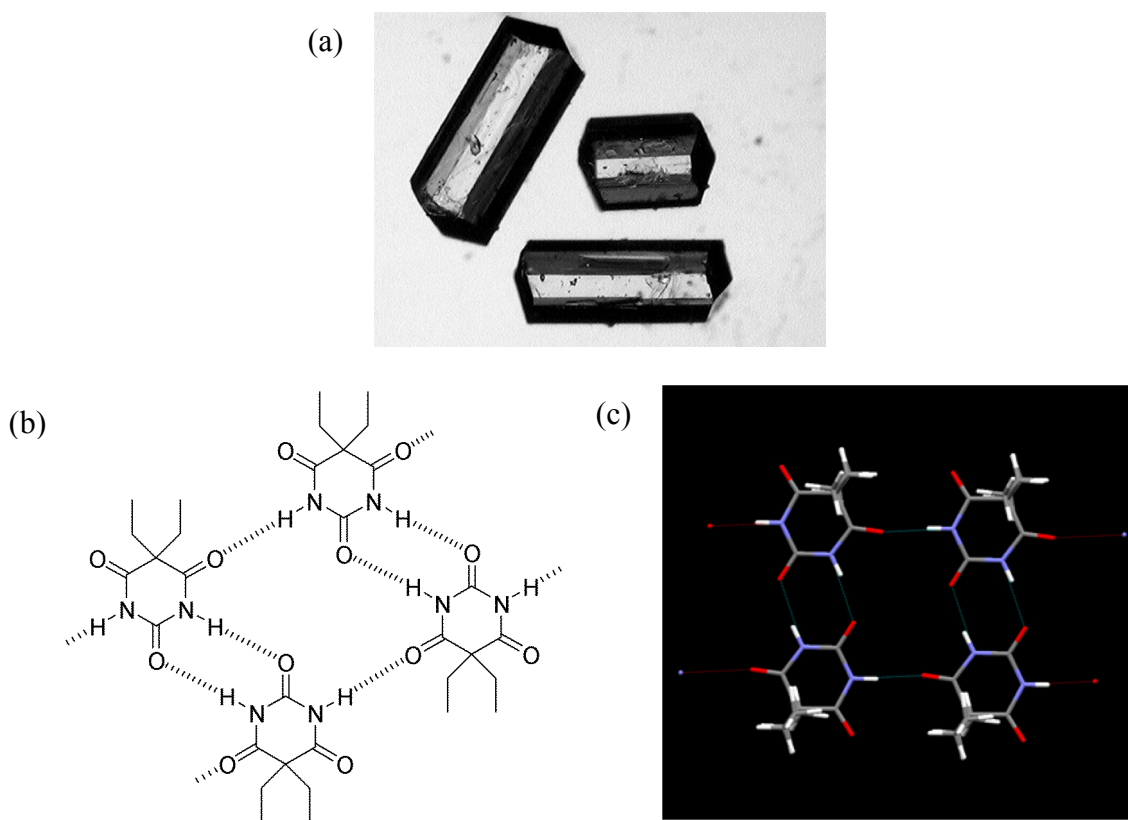
- Barbital has three known polymorphs (forms I, II and IV) that can form concomitantly.
- The polymorphs of barbital are stable enough to form and persist without undergoing rapid phase transformation.
- The crystal structures of all three polymorphs are known.<sup>65,71</sup>
- Barbital is soluble in solvents suitable for crystallizing on bulk SAMs and in microchannels.
- Barbital has hydrogen-bonding groups complementary to functional groups terminating SAMs that we studied.

Table 2.1 shows the melting point, crystal system and habit of each form. Figures 2.6, 2.7 and 2.8 show examples of crystals and hydrogen-bonding motifs of each form.

**Table 2.1** Melting point, crystal system and shape of forms for barbital.

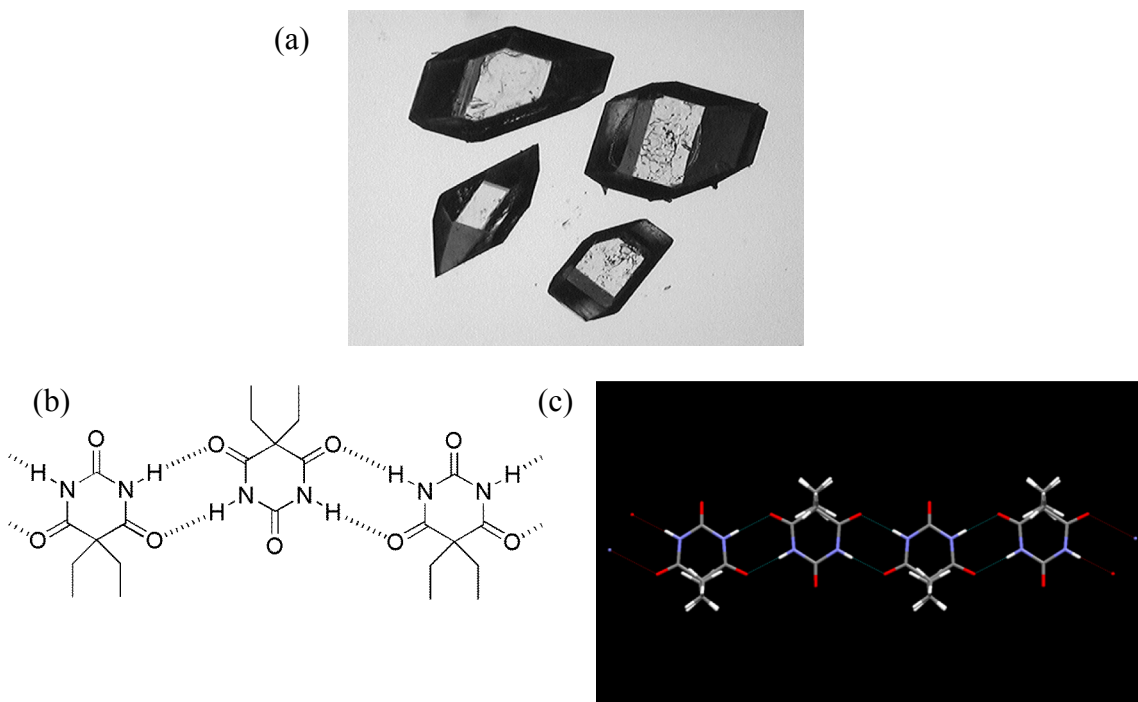
Form	I	II	IV
Melting Point	190 °C	183 °C	176 °C
Crystal System	Trigonal	Monoclinic	Monoclinic
Habit	Rhombohedral needles	Prisms	Twinned rectangular plates or flat pyramids

**Form I:**



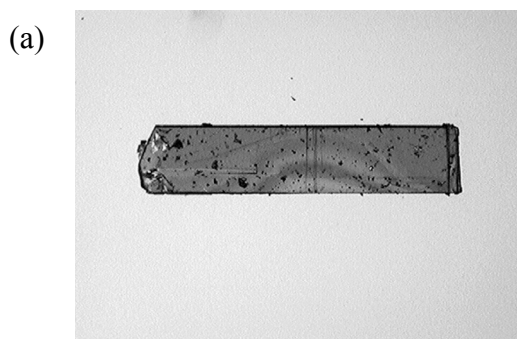
**Figure 2.6** Structure of form I of barbital (a) and the hydrogen-bonding motif of form I (a linear ribbon) illustrated with a ChemDraw diagram (b) and crystal packing diagram (c).

**Form II:**



**Figure 2.7** Structure of form II of barbitol (a) and the hydrogen-bonding motif of form II (a linear tape) illustrated with a ChemDraw diagram (b) and crystal packing diagram (c).

**Form III:**



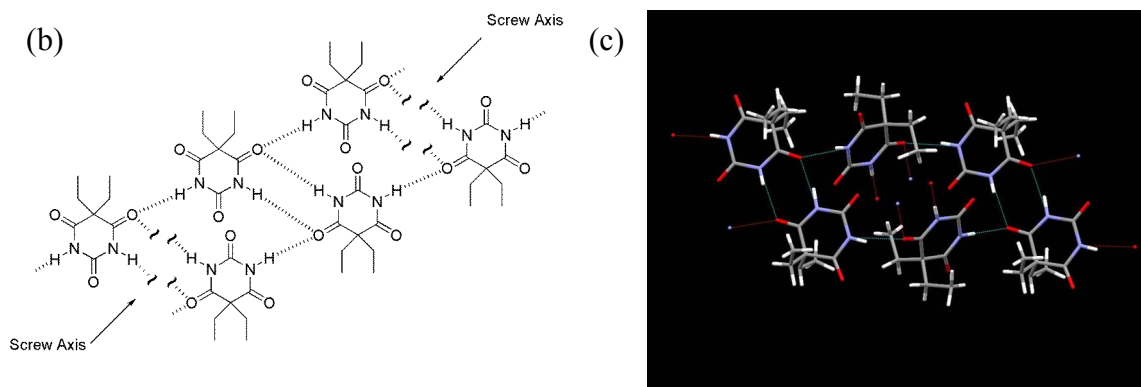


**Figure 2.8** Structure of form IV of barbital and the hydrogen-bonding motif of form IV (a sheet) illustrated with a ChemDraw diagram (b) and crystal packing diagram (c).

### 2.5.2 Acetaminophen

In addition to barbital, we identified acetaminophen as a model system for this study. The structure of acetaminophen is shown in Figure 2.9. We chose acetaminophen in large part based on the study described earlier by Metzger that showed that nucleation and growth of the two polymorphs of acetaminophen (forms I and II) could be controlled by crystallizing acetaminophen in the presence of different polymeric solids.<sup>51</sup> The presence of N-H and O-H donors and C=O and OH acceptors on acetaminophen introduces the potential for variability in the hydrogen-bonding motifs that result from different combinations of those functional groups as donors and acceptors.

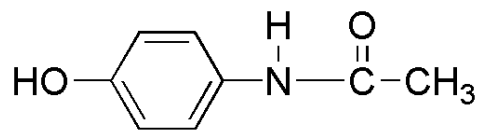


**Figure 2.9** Structure of acetaminophen.

We chose to use acetaminophen because:

- Acetaminophen has two known polymorphs.
- The polymorphs of acetaminophen are stable enough to form and persist without undergoing rapid phase transformation.
- The crystal structures of forms I and II of acetaminophen are known.<sup>68,69</sup>
- Acetaminophen is soluble in solvents suitable for crystallizing on bulk SAMs and in microchannels.
- Acetaminophen has hydrogen-bonding groups complementary to functional groups terminating SAMs that we studied.

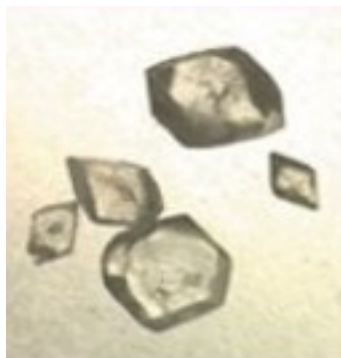
Table 2.2 shows the melting point, crystal system and habit of the two forms of acetaminophen. Figures 2.10 and 2.11 show examples of crystals and hydrogen-bonding motifs of each form.

**Table 2.2** Melting point, crystal system and shape of forms for acetaminophen.

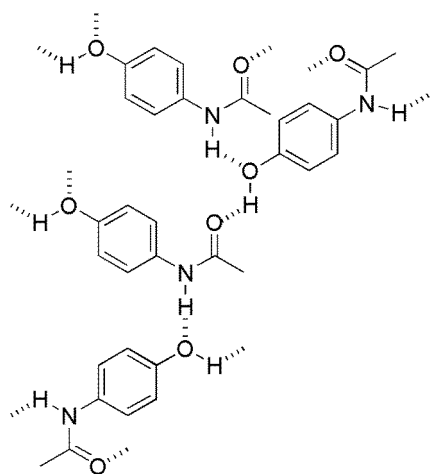
<b>Form</b>	<b>I</b>	<b>II</b>
Melting Point	171-172 °C	160-161 °C
Crystal System	Monoclinic	Orthorhombic
Habit (shape)	Block	Prism

**Form I:**

(a)



(b)



(c)

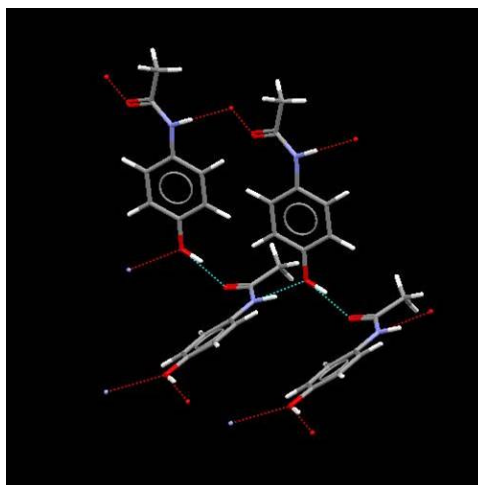


**Figure 2.10** Structure of form I of acetaminophen and the hydrogen-bonding motif of form I illustrated with a ChemDraw diagram (b) and crystal packing diagram (c).<sup>76</sup>

**Form II:**

(a)



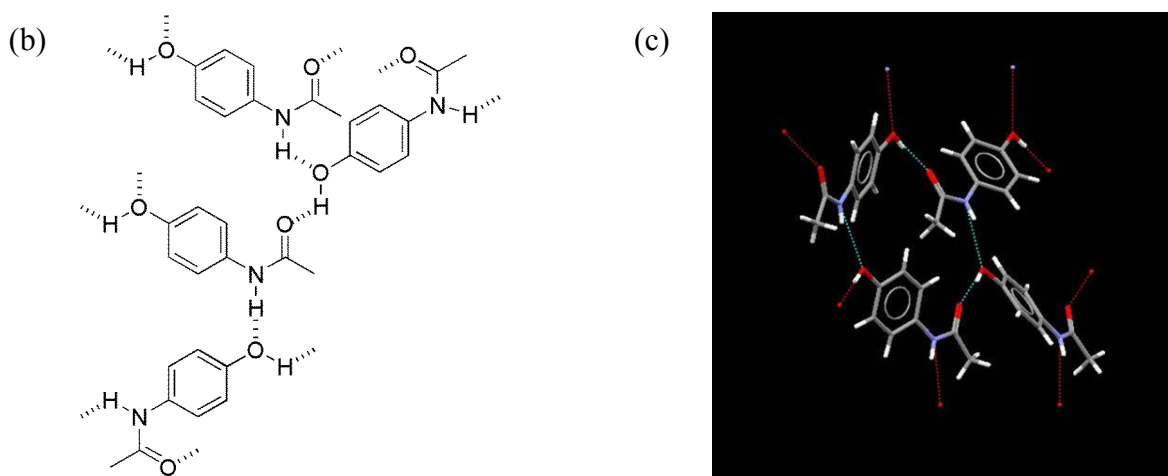


**Figure 2.11** Structure of form II <sup>76</sup> of acetaminophen and the hydrogen-bonding motif of form II (a sheet) illustrated with a ChemDraw diagram (b) and crystal packing diagram (c).

### 3. Self-Assembled Monolayers

#### 3.1 Introduction and background on self-assembled monolayers

Self-assembled monolayers (SAMs) are ordered assemblies of molecules the thickness of a single molecule formed by adsorption of molecules from solution or a gas onto a solid surface. In recent years, the field of SAMs has witnessed fantastic growth in the development of synthetic procedures to prepare SAMs, techniques to characterize surface structure, composition and properties of SAMs, and broad utilization of SAMs to chemical modify surfaces in biology, medicine, materials science, and manufacturing.<sup>77-87</sup> In 1946, Zisman published the first paper describing the preparation of a molecular monolayer by adsorption of a surfactant onto a clean metal surface.<sup>88</sup> Initial development of SAMs focused in large part on using chlorosilane derivatives to hydrophobize glass substrates.<sup>77,89,90</sup> More recently, efforts have focused predominantly on SAMs composed of substituted alkanethiolates on gold and other precious metals.<sup>91-109</sup> Gold is the



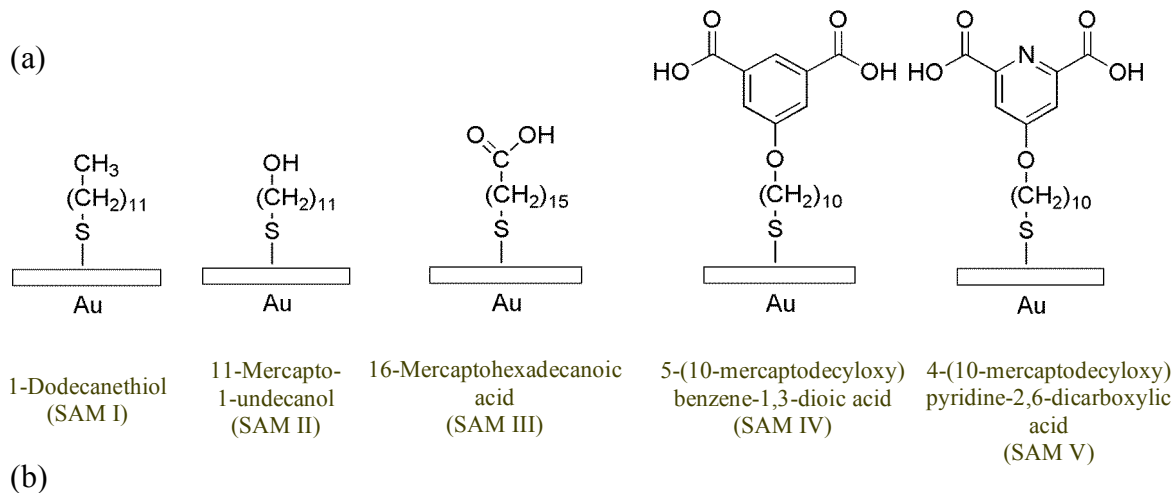
substrate used most commonly because it does not oxidize easily in air. Oxidation of the metal surface generally interferes with deposition of SAMs and results in poor coverage. SAMs of substituted alkanethiolates on gold are prepared by adsorption of the corresponding alkanethiols or the di-n-alkyl disulfides from dilute solutions.<sup>110</sup> SAMs continue to present exclusive opportunities to modify the properties of surfaces in order to investigate self-organization, structure-property relationships and interfacial phenomena. The ability to tailor both head and tail groups of the constituent molecules makes SAMs excellent systems to understand molecule-substrate, molecule-solvent and intermolecular interactions.<sup>78,111</sup> SAMs are highly ordered and oriented and can include different groups both within the alkyl chain and at the chain termini. SAMs can be used for corrosion prevention, wear protection and similar applications because of their dense and stable structure.<sup>87,112-117</sup>

SAMs also have been reported to serve as substrates that promote nucleation and growth of organic,<sup>14,56,57</sup> inorganic,<sup>10</sup> and protein crystals.<sup>16,17</sup> For example, SAMs with different chemical functional groups (e.g., carboxylic acids) influence the heterogeneous nucleation and growth of crystals of malonic acid.<sup>14</sup> Molecules of malonic acid crystallize by assembling into linear chains in which the molecules of malonic acid (HOOC-CH<sub>2</sub>-COOH) are joined by hydrogen bonds between the acid groups on adjacent molecules. The carboxylic acid groups of malonic acid are exposed at the (001) facet, or plane, on the surface of crystals of malonic acid as they form. Crystallization of malonic acid from solution in the presence of SAMs composed of [Au]-S(CH<sub>2</sub>)<sub>11</sub>COOH resulted in oriented nucleation and growth of crystals. Growth occurred with the (001) facet of the crystals oriented parallel to the surface of the SAM with the COOH groups on the surface of the

crystal in contact with the COOH groups of the SAM.<sup>14</sup> This study demonstrated that SAMs can serve as templates, or prenucleation sites, that influence aggregation of molecules from solution and subsequent nucleation and growth of crystals on those sites. An important finding of this work is that templated assembly of molecules and subsequent oriented nucleation and growth of crystals from solution onto a SAM requires hydrogen-bonding groups at the surface of the SAM that are complementary to those exposed on the surface of the crystal. In another study, SAMs of rigid biphenyl thiols were employed as heterogeneous templates for oriented crystallization of L-alanine and DL-valine.<sup>17</sup> Hydrogen bonding between the functional groups exposed on the surface of the monolayer such as hydroxyl groups and carboxylate groups on molecules of alanine was observed as a driving force for oriented nucleation and growth of crystals of alanine.<sup>17</sup> Whitesides also showed that face-selective nucleation of calcite occurred on SAMs of  $\omega$ -terminated alkanethiols patterned on the surface of gold and silver substrates.<sup>10</sup> Oriented growth of calcite crystals occurred preferentially on SAMs terminated with hydrophilic  $\text{CO}_2^-$ ,  $\text{SO}_3^-$ ,  $\text{PO}_3^{2-}$  and OH groups, while growth was inhibited on SAMs with hydrophobic  $\text{N}(\text{CH}_3)_3^+$  and  $\text{CH}_3$  groups. These studies demonstrate that SAMs provide a convenient tool to control or at least influence nucleation and growth of molecular crystals by varying the geometry, chemistry and pattern of functional groups presented on the surface of SAMs. Moreover, these studies provide the foundation and, in part, the motivation for the research described in this thesis—namely, utilizing SAMs as prenucleation sites, or templates, to promote and control heterogeneous nucleation and growth of polymorphs of pharmaceuticals such as barbital and acetaminophen.

### 3.2 SAMs used for crystallization

The different SAMs shown in Figure 3.1 were used for crystallization experiments with barbital and acetaminophen. All SAMs feature alkyl chains with ten or more methylene units because previous studies have shown that alkanethiols with ten or more carbon atoms pack more efficiently with greater order than alkanethiols with fewer than ten carbon atoms.<sup>118-121</sup> Alkanethiols are known to self-assemble on the (111) surface of gold substrates in a hexagonal or pseudo-hexagonal arrangement in which the alkyl chains tilt over 30° from perpendicular to the surface.<sup>120,122,123</sup> This commonly observed closest-packed structure in alkanethiols on Au(111) is referred to as an  $R30^\circ(\sqrt{3}\times\sqrt{3})$  packing arrangement. We expect SAMs I-III to adopt the  $R30^\circ(\sqrt{3}\times\sqrt{3})$  packing arrangement because those SAMs have small head groups that will not interfere with closest-packing of the alkyl chains.<sup>124-126</sup> In the case of SAMs IV and V; the head groups are wider than the underlying alkyl chains. Therefore, it is not clear what packing arrangement those SAMs will adopt.



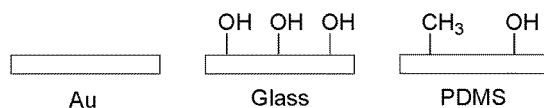


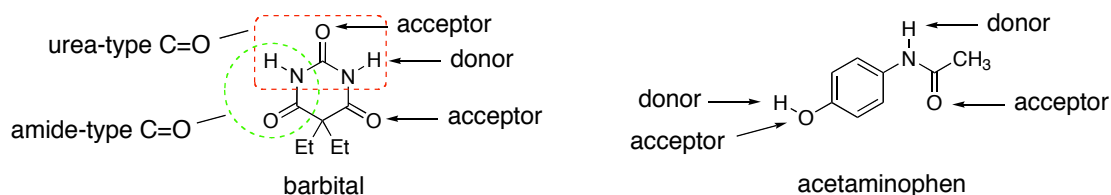
**Figure 3.1** (a) Chemical structures of SAMs I-V deposited on gold substrates for experiments. (b) Chemical structures used for control experiments.

The head groups of SAMs I-V were selected to provide both hydrophobic and hydrophilic surfaces with a range of surface energies. SAM I has a hydrophobic methyl head group, while other SAMs have hydrophilic OH, COOH and pyridine head groups that are capable of forming hydrogen bonds. For example, the protic OH group on SAM II can serve both as a hydrogen-bonding donor and as an acceptor at the lone pairs of electron on the oxygen atom, The carboxyl group on SAM III also can donate and accept hydrogen bonds via the acidic OH group and the C=O group. SAMs IV and V both feature two carboxyl groups. In addition, SAM V has a basic pyridine group that serves as an additional site for accepting hydrogen bonds. We chose to utilize SAMs II-V specifically because those SAMs are terminated with hydrogen-bonding donor and acceptor groups that are complementary to those present on barbital and acetaminophen.

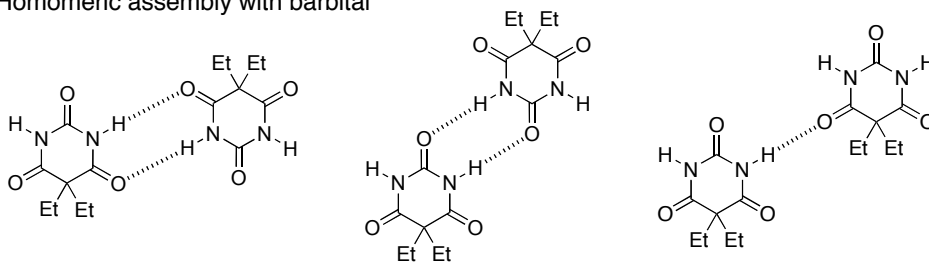
As shown in Figure 3.2a, barbital features a total of two N-H donors and three C=O acceptors. Both urea-type N-H donors and the two amide-type C=O acceptors of barbital are identical chemically because of two-fold symmetry within the molecule. The urea-type and amide-type C=O groups of barbital differ chemically. Acetaminophen contains a total of two donors and two acceptors. The O-H and N- H donors differ chemically as do the phenolic O-H and amide C=O acceptors of acetaminophen. Etter has established that chemically distinct organic hydrogen-bonding donors and acceptors generally show different hydrogen-bonding behavior with the strongest (most acidic)

donors and the strongest (most basic) acceptors selectively forming hydrogen bonds with each other.<sup>127</sup> In the absence of other hydrogen-bonding groups, molecules of barbital and acetaminophen undergo homomeric (self) assembly that can lead to different motifs of hydrogen bonding depending on which donors and acceptors interact to form hydrogen bonds. For example, dimeric aggregates of barbital with three different motifs (i.e., forms I, II and IV) are shown in Figure 3.2b. In the presence of other competing hydrogen-bonding groups, barbital and acetaminophen may undergo heteromeric rather than homomeric assembly to form hydrogen-bonded complexes when the best hydrogen-bonding donor and acceptor reside on different types of molecules. For example, as shown in Figure 3.2c, barbital can undergo heteromeric assembly with carboxylic acids and alcohols because those groups have donors that are more acidic than the urea-type N-H groups of barbital. Such heteromeric assembly can lead to complexes with several different structural motifs depending on which N-H and C=O groups of barbital are involved in hydrogen bonding. Acetaminophen similarly can undergo heteromeric assembly to form hydrogen-bonded complexes with carboxylic acids and alcohols that can adopt several different structural motifs.

a) donor & acceptor groups on barbital and acetaminophen



b) Homomeric assembly with barbital



c) Heteromeric assembly with barbital

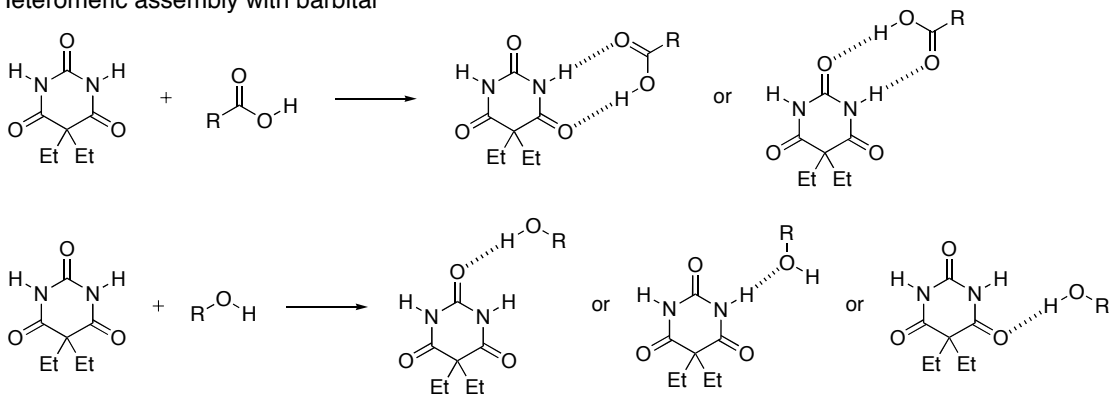


**Figure 3.2** a) Hydrogen-bonding donor and acceptor groups on barbital and acetaminophen. b) Examples of different hydrogen-bonding motifs that result from homomeric (self) assembly of barbital. c) Examples of different hydrogen-bonding motifs that can result from heteromeric assembly of barbital with carboxylic acids and alcohols.

We chose to crystallize barbital and acetaminophen on SAMs with head groups that contain different arrangements of hydrophilic OH, COOH and pyridine functional groups to promote heteromeric assembly with barbital and acetaminophen through hydrogen bonding on the surface. Figure 3.3 illustrates heteromeric assembly of barbital on SAMs

terminated with carboxylic acid and alcohol groups. The orientation of barbital on the surface of each SAM depends on which C=O group participates in hydrogen bonding, whether the molecules form a single hydrogen bond or two hydrogen bonds with the functional groups on the surface, and the tilt-angle, orientation and order of the head groups of the SAMs. For example, assembly of barbital via a single hydrogen bond on SAM II results in two different orientations of barbital on the surface, as shown on the right in Figure 3.3. Hydrogen bonding via the urea-type C=O orients the molecule with the ethyl substituents exposed on the surface, while hydrogen bonding via the amide-type C=O orients the molecule with the hydrogen-bonding groups exposed on the surface. Our goal is investigate whether formation of aggregates such as those shown in Figure 3.3 can be controlled on different SAMs and to determine if such templates will influence subsequent nucleation and growth of different polymorphs.

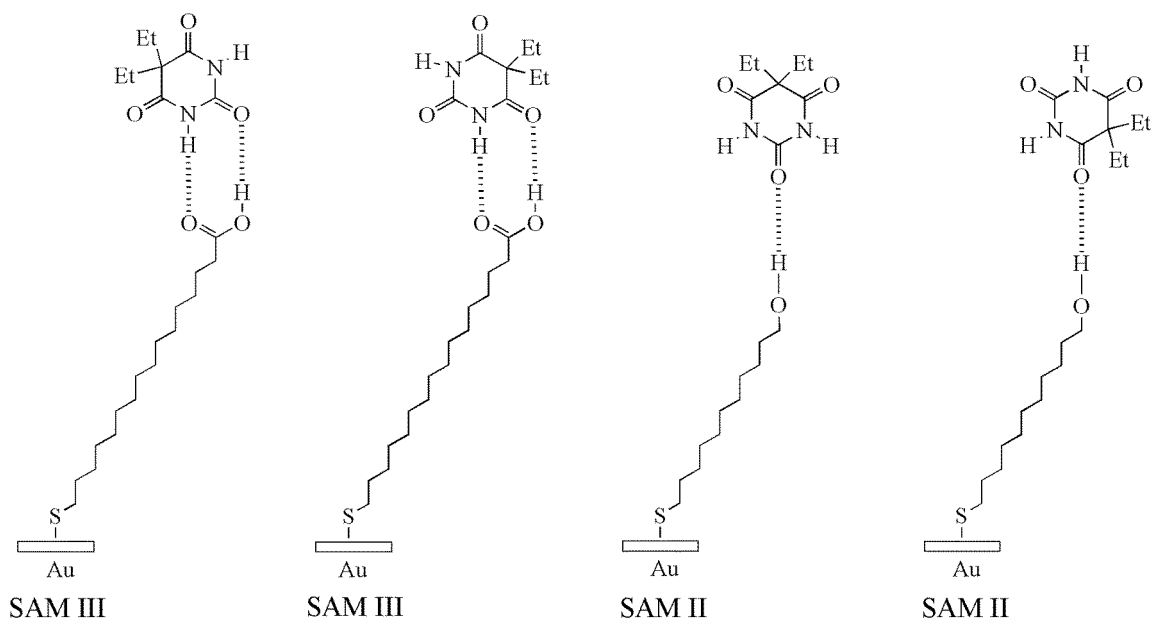
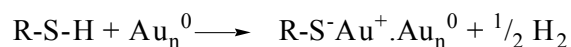


**Figure 3.3.** Illustration of different modes of hydrogen bonding interactions between barbital and SAMs terminated with COOH and OH groups.

### 3.3 Preparation of SAMs

Organosulfur compounds such as alkanethiols, di-n-alkyl sulfide, di-n-alkyl disulfides, mercaptopyridines and mercaptoanilines have a strong affinity for the surfaces of transition metals.<sup>118,128-131</sup> Of the SAM systems above, the most studied and best understood by far is that of alkanethiolates on Au surfaces. For alkanethiols, addition of the S-H bond to the gold surface may be considered as an oxidative addition according to the following equation.<sup>132</sup>



Although organosulfur compounds form SAMs by chemisorption on other substrates such as silver, copper, platinum, mercury, iron and GaAs, gold is the preferred substrate because it does not have a stable surface oxide.<sup>121</sup> Moreover, its surface can be cleaned chemically with Piranha solution (70% H<sub>2</sub>SO<sub>4</sub>/30% H<sub>2</sub>O<sub>2</sub>) to remove physically and chemically adsorbed impurities. SAMs of alkanethiols on gold can be prepared readily as shown in Figure 3.4. The resulting SAMs of alkanethiols on gold generally form with high surface coverage and are highly ordered.



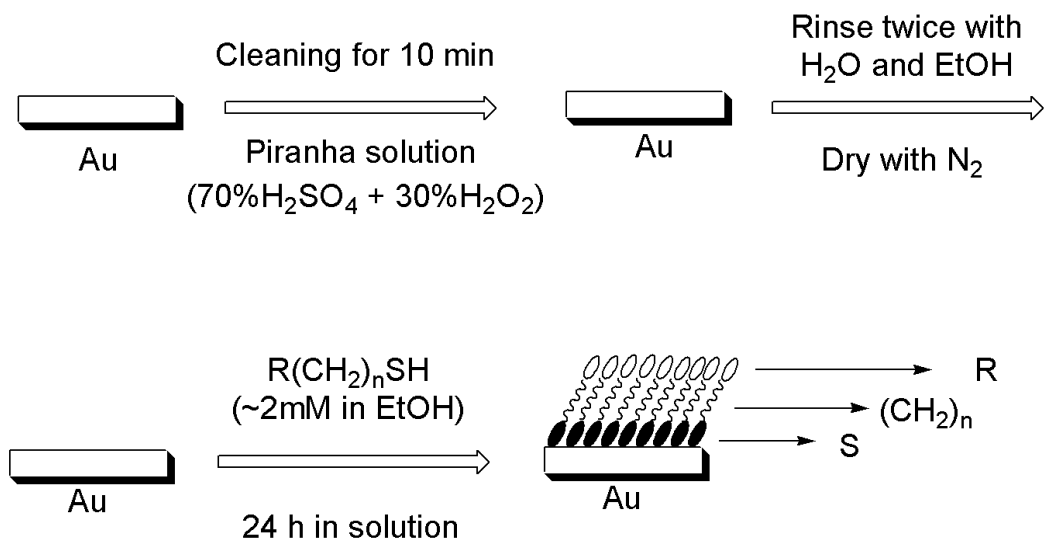


**Figure 3.4** Preparation of SAMs of alkanethiols on gold.

Two different adsorption kinetics predominate during adsorption of alkanethiols onto Au(111) surfaces in dilute solutions ( $\sim 1\text{mM}$ ). The initial and fastest step of adsorption occurs within a few minutes. For example, previous reports have shown that, the thickness of SAMs reaches 80-90 % of the maximum value and that the contact angle of water droplets approaches the limiting values during the first few minutes.<sup>133</sup> During the second and slower step, completion of adsorption takes several hours, at which time thickness and contact angle reach their maximum values. SAMs can be prepared from substituted alkanethiols as well as unsubstituted alkanethiols. It is important to note that several constraints apply, however, when SAMs are prepared from substituted alkanethiols with head groups containing reactive functional groups or dimensions larger than that of typical straight-chain alkanes. For example, the head group should not contain any chemical functionality that competes with the thiol in coordinating to gold. Second, the head group must not react with the thiol. Third, the head group must not be so sterically demanding as to cause poor packing of the underlying hydrocarbon chains.

### 3.3.1 Experimental procedures used to prepare SAMs on gold.

Glass slides with dimensions of 3 in. x 1 in. x 0.4 in. coated with 50 Å of chromium followed by 1000 Å of gold (Evaporated Metal Films) were cut into 1 in. x 1 in. squares that were cleaned in piranha solution (70% H<sub>2</sub>SO<sub>4</sub>, 30% H<sub>2</sub>O<sub>2</sub>) for 10 min, rinsed with deionized water and ethanol, and dried under nitrogen. Monolayers of ω-substituted alkanethiols were prepared by immersing the clean gold slides in 2 mM ethanolic solutions of the desired compound for 24 h at room temperature. Commercially available ω-substituted alkanethiols (i.e., 1-dodecanethiol, 11-mercapto-1-undecanol and 16-mercaptohexadecanoic acid) were purchased from Aldrich and used without further purification. 5-(10-mercaptodecyloxy)benzene-1,3-dioic acid and 4-(10-mercaptodecyloxy)-pyridine-2,6-dicarboxylic acid were prepared using synthetic procedures we reported previously.<sup>134,135</sup> 1-Dodecanethiol (SAM I), 11-mercapto-1-undecanol (SAM II), 16-mercaptohexadecanoic acid (SAM III), 5-(10-mercaptodecyloxy)benzene-1,3-dioic acid (SAM IV) and 4-(10-mercaptodecyloxy)-pyridine-2,6-dicarboxylic acid (SAM V) were deposited on gold substrates. The resulting SAMs on gold were rinsed with ethanol and dried with nitrogen just prior to being used for crystallization experiments.

## 3.4 Characterization of SAMs

### 3.4.1 Contact Angle Goniometry

The phenomenon of wetting or non-wetting at the surface of a solid by a liquid reflects the hydrophobic or hydrophilic nature of the surface and provides valuable insight into the interaction energy at the surface. The technique of contact angle

goniometry provides a convenient means to quantify the wettability of surfaces by measuring the wetting angle, or contact angle, when of a sessile drop of water (or other liquid) is placed in contact with the surface. The contact angle is measured by placing a 1  $\mu\text{L}$  drop of water onto the surface and then measuring the angle between the plane tangent to the surface of the drop of water where it meets the surface and the plane tangent to the surface of the solid. The contact angle is measured by viewing the profile of the drop on the surface through a magnifying lens equipped with a goniometer. This concept is illustrated in Figure 3.5.

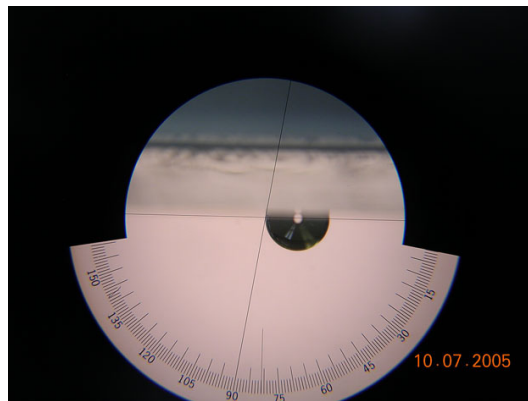


**Figure 3.5** Example of a contact angle measurement.

Contact angles offer an easy-to-measure indication of the chemical bonding between functional groups exposed on the surface of the substrate and molecules of water in the drop. This bonding determines wettability and adhesion, and also allows prediction of coating properties and detection. Contact angles also provide information about surface energy and surface tension of the drop. For our purposes, contact angle is a suitable

method to measure the relative hydrophobic or hydrophilic character of SAMs with different head groups.<sup>136,137</sup>

Contact angle measurements of SAMs I-V and bare gold were determined using a Rame-Hart Model 100-00 Goniometer (Mountain Lakes, NJ). Drops of water (1  $\mu\text{L}$ ) were deposited with a micropipette and viewed through a low-power microscope. The microscope produced a clear image of the profile of the sessile drops on each of the different substrates, as shown in Figure 3.6. The contact angles for SAMs I-V and bare gold are given in Table 3.1. The reported contact angles are the average of five independent readings. The contact angles we measured for SAM I, SAM II and SAM III were consistent with values reported previously in the literature.<sup>138</sup>

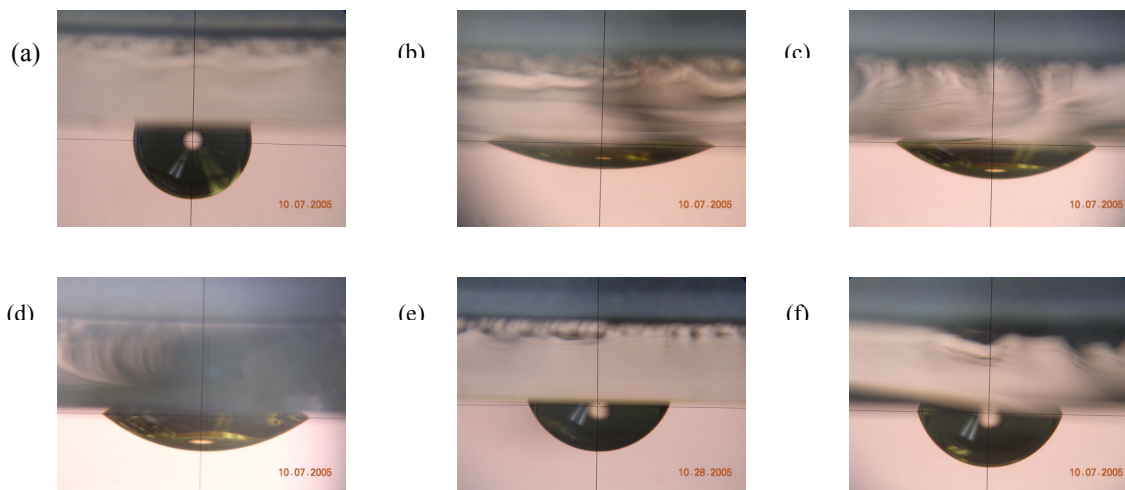


**Figure 3.6** Images of 1  $\mu\text{L}$  drops of water on SAMs I-V and bare gold viewed through a microscope equipped with a goniometer: (a) SAM I; (b) SAM II; (c) SAM III; (d) SAM IV; (e) SAM V and (f) bare gold.

**Table 3.1** Contact angle measurements of SAMs.

Surface	Contact angle (°)
Bare Au	78.6 ± 0.9
SAM I	113.8 ± 0.2
SAM II	35.2 ± 0.4
SAM III	42.9 ± 0.7
SAM IV	69 ± 0.5
SAM V	72.6 ± 0.5

### 3.4.2 Ellipsometry

Ellipsometry is a sensitive technique that uses polarized light to measure the thickness of thin films, surfaces, and microstructure of materials.<sup>110,139-141</sup> Polarized light is shone onto the surface of a sample at an oblique angle of incidence. The plane of incidence of the light is the plane that contains both incident and reflected beams. The polarization of light reflected parallel (p) and perpendicular (s) to the plane of incidence is measured. This polarization allows the relative phase change ( $\Delta$ ) and relative amplitude change ( $\Psi$ ) from the reflected surface to be determined. These values are related to the thickness of the SAM with refractive index (k) and extinction coefficient (n).

The thickness of SAMs I-V on the Au substrates was estimated using a Manual Photoelectric Rudolf 439L633P ellipsometer (Rudolph Instruments, Fairfield, NJ) (He-Ne laser,  $\lambda=632.8$  nm, angle of incidence  $70^\circ$ ). Readings were taken on bare gold to establish the optical constants (refractive index, k and extinction coefficient n) which

were compared to values previously reported in literature.<sup>142</sup> Four separate points were measured on each sample and the readings averaged using an assumed refractive index of 1.47. The thicknesses of SAMs I-V are shown in Table 3.2. All values of thickness were determined using the software package 439PCS11 Ellipsometry Analysis (rev. 1.0) from Rudolph Instruments.

**Table 3.2** Thickness of SAMs.

SAM	Thickness (nm)
SAM I	1.35
SAM II	1.5
SAM III	1.8
SAM IV	1.6
SAM V	1.5

### 3.4.3 Grazing angle FT-IR

The ideal method to obtain FT-IR spectra of SAMs on gold is the grazing angle technique. This technique includes the reflection of incoming light under a large angle of incidence (greater than 80°) relative to the surface normal. This technique has been used widely to study and characterize the adsorption of molecules on metal surfaces.<sup>91,92,110,119,143,144</sup> Grazing angle IR spectra are similar to IR spectra obtained using normal transmission techniques on bulk samples with one important difference; grazing angle IR spectra do not show all IR absorption bands expected for the compounds

because transition dipoles parallel to the surface generally are not observed. Grazing angle IR is a useful technique for our purpose of characterizing SAMs because characteristic absorption bands of the alkyl, alcohol and carboxylic acid functional groups present in the head groups of SAMs I-V are present and easily identified.

FT-IR surface spectra were obtained with a Nexus FT-IR model 670 spectrometer equipped with a ThermoNicolet grazing angle accessory and a liquid-nitrogen cooled MCTA detector. The IR beam was incident at  $75^\circ$  on the gold substrates. The optical path was purged with  $N_2$  gas before and during the collecting data. For each sample 64 scans were collected with a  $4\text{ cm}^{-1}$  resolution. The scan range was from  $4000$  to  $400\text{ cm}^{-1}$  with the range from  $4000$ - $680\text{ cm}^{-1}$  giving the most useful information for the SAMs used in this research. A clean gold substrate was used to obtain a background spectrum before collecting the spectra on the different SAMs. Grazing angle IR spectra obtained from SAMs I-V are shown in Figure 3.7.

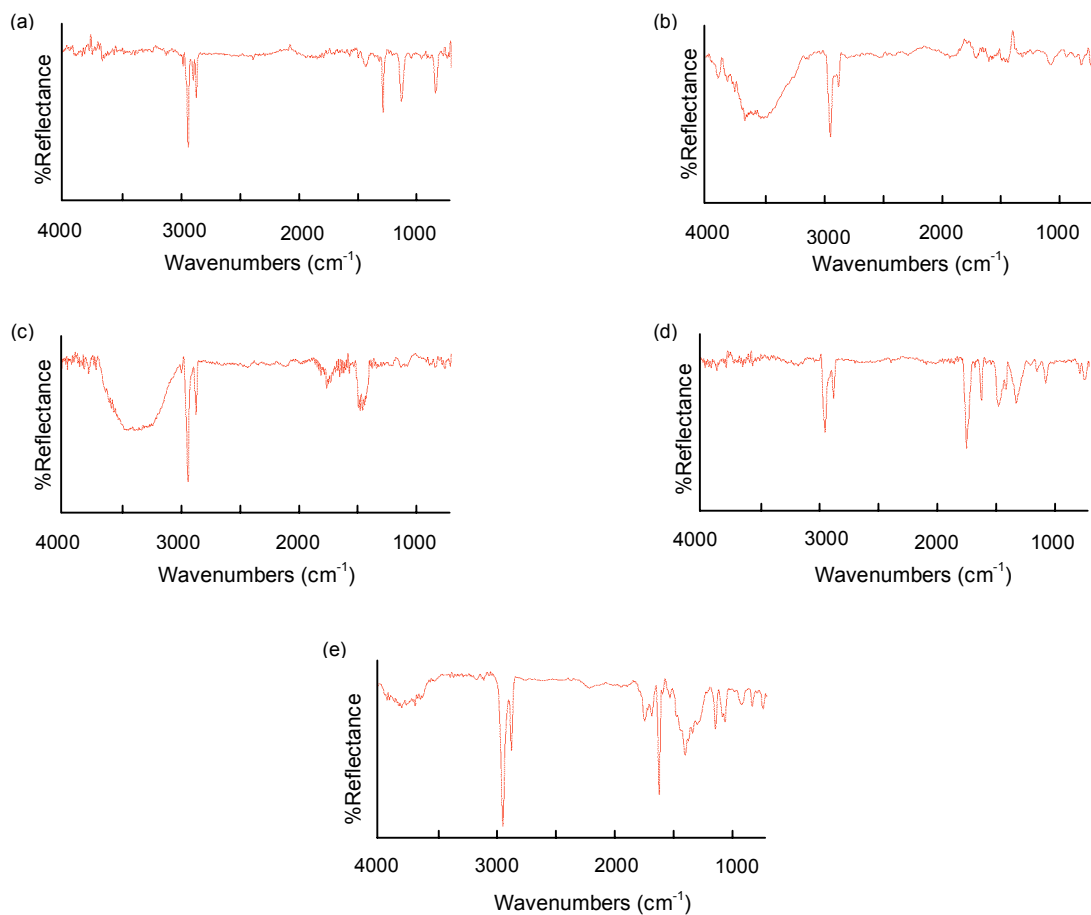


**Figure 3.7.** Grazing angle FT-IR spectra of SAMs that were used for crystallization experiments. (a) SAM I. (b) SAM IV. (c) SAM III. (d) SAM II. (e) SAM V.

### 3.4.4 Cyclic Voltammetry

Cyclic voltammetry (CV) is one of the most commonly used electrochemical techniques to investigate the surface coverage and order of SAMs by measuring the insulating behavior of well-packed monolayers.<sup>80,145-149</sup> CV measurements are made based on a linear potential waveform obtained by changing the potential as a linear function of time. The electrode potential is ramped linearly to a more negative potential,



and then ramped in reverse back to the starting voltage. The forward scan produces a current peak for any analytes that can be reduced through the range of the potential scan. The current will increase as the potential reaches the reduction potential of the analyte, but then falls off as the concentration of the analyte is depleted close to the electrode surface. As the applied potential is reversed, it will reach a potential that will reoxidize the product formed in the first reduction reaction, and produce a current of reverse polarity from the forward scan. This oxidation peak will usually have a similar shape to the reduction peak.

Cyclic voltammetry measurements were obtained using an EG&G Princeton Applied Research Potentiostat/Galvanostat Model 273. A platinum wire counter electrode, standard calomel reference electrode and SAM on gold as the working electrode were the electrodes used for measurements. The SAM coated gold substrate was connected with an alligator clamp and 1cm<sup>2</sup> of gold substrate was kept immersed in solution. Experiments were done in 1mM potassium ferricyanide as the redox active species with 0.1 M potassium chloride as a supporting electrolyte. To reduce electrical noise, the electrochemical cell was placed inside a Faraday cage. The cyclic voltammetry curves were obtained generally in the range of -0.5 to +0.7 V with a scan rate of 50 mV/s and a scan increment of 1mV. The cyclic voltammograms for SAMs I-V and bare gold are shown in Figure 3.8. The CV measurements show that the redox activity of Fe<sup>+2</sup>/Fe<sup>+3</sup> observed using bare gold as the working electrode went to zero when SAMs on gold were used as the working electrode. The absence of any redox activity of the ferricyanide mediator indicates that SAMs I-V cover the surface of the gold substrate uniformly with few defects.

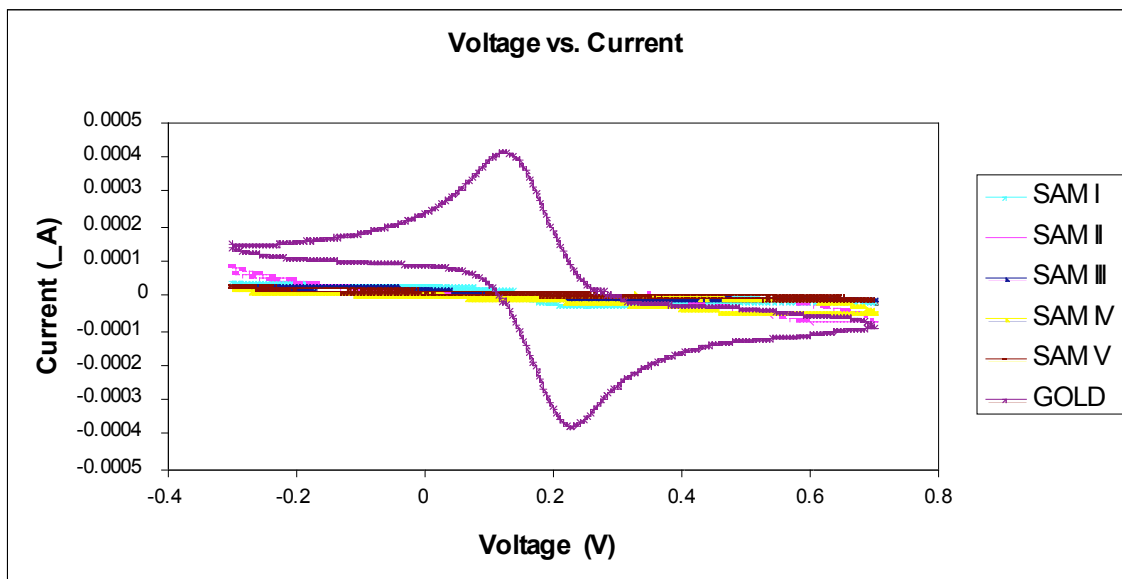


**Figure 3.8** Cyclic voltammograms of SAMs I-V and bare gold.

## 4. Crystallization on SAMs

### 4.1 Crystallization on SAMs on bulk surfaces

Nucleation, which is the first step of crystallization, generally is affected by a number of factors that include free energy of a surface, temperature, degree of supersaturation, solubility and concentration.<sup>1,14,17,42,57,156-158</sup> Changes to any one of these factors can alter the arrangement of molecules within aggregates and the structure of those aggregates on surfaces and in solution. Our hypothesis is that molecular aggregates that form on surfaces prior to nucleation will serve as prenucleation sites, or templates, that promote nucleation of crystals and influence the packing arrangement of molecules within nuclei as they form. Accordingly, our goal is to test whether we can control the incidence of different polymorphs of barbital and acetaminophen by changing these parameters systematically using a range of conditions for crystallization. For example, parameters such as free energy of the surface can be altered using a series of SAMs with different

head groups, while degree of supersaturation, solubility and concentration can be changed by varying the temperature, the type of solvent used and rate at which solvent evaporates during crystallization.

Accordingly, we employed three different methods to crystallize barbital and acetaminophen that we refer to as method 1, method 2 and method 3. Methods 1 and 2 involved using slow evaporation of solvent at two different rates to achieve slow nucleation and growth of crystals under thermodynamic conditions. Method 3 involved using rapid cooling of a solution to drive crystallization by changing the degree of supersaturation and achieve fast nucleation and growth of crystals under kinetic conditions.

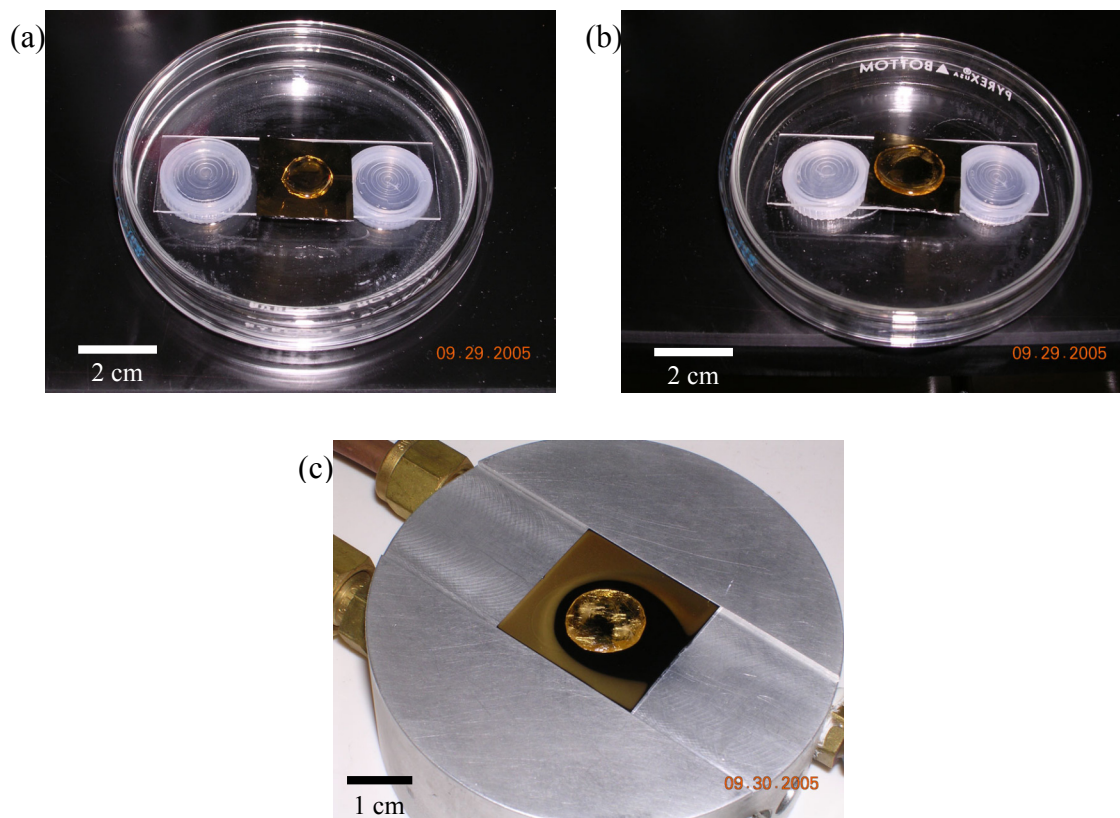


**Figure 4.1** (a) Crystallization set up for method 1 (solvent at the bottom of the Petri dish). (b) Method 2 (no solvent at the bottom of the Petri dish). (c) Method 3.

Each of the three methods was carried out with barbital using three different solvents—ethanol, water and ethyl acetate—to study the effects of changing polarity, solubility, rates of evaporation, the presence or absence of protic groups, and solvation of barbital, as well as the different SAMs, in controlling which polymorphs formed. The three solvents were chosen in part based on the requirement that barbital exhibit good solubility. We used ethanol and water because both are polar solvents with one or two protic OH groups capable of accepting and donating hydrogen bonds with protic donors and basic acceptors present on barbital as well as on the head groups of SAMs. Both ethanol and water were chosen because ethanol features both nonpolar hydrophobic and polar hydrophilic groups, while water features only polar hydrophilic groups. We used ethyl acetate as a representative polar aprotic solvent with no acidic groups capable of serving as hydrogen-bonding donors. Crystallization experiments with acetaminophen were carried out using only ethanol. The different solution concentrations of barbital and acetaminophen used are shown in Table 4.1.

**Table 4.1** Concentration of barbital and acetaminophen in solutions used for crystallization.

**Barbital**

<b>Solvent</b>	<b>Method 1</b>	<b>Method 2</b>	<b>Method 3</b>
Ethanol	0.35M	0.35M	0.7M
Ethyl Acetate	0.1M	0.1M	0.15M
Water	-	0.036M	0.07M

## Acetaminophen

Solvent	Method 1	Method 2	Method 3
Ethanol	0.1M	0.1M	0.2M

### 4.1.1 Method 1

For method 1, the substrate was placed on a glass microscope slide that was suspended on plastic caps in Petri dish. Solvent was then added to the Petri dish until the level of solvent reached half way between the bottom of the dish and the substrate suspended above. Ten drops of the drug solution at room temperature were delivered by syringe to the surface of the substrate. The Petri dish was then covered with the lid of the Petri dish. This setup allowed the solvent to evaporate slowly over days from small gaps between the Petri dish and cover. Excess solvent underneath the suspended substrate served to minimize the rate of evaporation by saturating the atmosphere inside the container with solvent vapor. Crystallization experiments were carried out on SAMs I-V and also on glass, gold and PDMS as control experiments for barbital. PDMS was not tested with acetaminophen because initial crystallization experiments in ethanol showed that acetaminophen was not a suitable choice for further study. We did not carry out crystallization experiments with acetaminophen in microchannels for the same reason. Five trials were carried out for each SAM and control surface. Crystallization from ethanol generally produced crystals in 1-2 days. Crystallization from ethyl acetate generally gave crystals in less than 24 hours. Water was not used for this method because of its low volatility. Whenever possible, samples of crystals were isolated from solution

prior to complete evaporation of all solvent to avoid possible contamination by crystals formed rapidly under kinetic conditions.

#### **4.1.2 Method 2**

The conditions used for method 2 were identical to those for method 1 except that no excess solvent was placed under the substrate. For method 2, the substrate was placed on a glass microscope slide that was suspended on plastic caps in Petri dish. Ten drops of the drug solution at room temperature were delivered by syringe to the surface of the substrate by syringe. The Petri dish was then covered with the lid of the Petri dish. This setup allowed the solvent to evaporate slowly over days from small gaps between the Petri dish and cover. Crystallization experiments were carried out on SAMs I-V and also on glass, gold and PDMS as control experiments for barbital. PDMS was not used for experiments with acetaminophen. Five trials were carried out for each SAM and control surface. Crystallization from ethanol generally produced crystals within 12 hours. Crystallization from ethyl acetate generally produced crystals within 1-2 hours. Water was not used for this method because of its low volatility. Whenever possible, samples of crystals were isolated from solution prior to complete evaporation of all solvent to avoid possible contamination by crystals formed rapidly under kinetic conditions.

#### **4.1.3 Method 3**

For method 3, the substrate was placed onto the surface of an aluminum block and cooled to 0 °C by circulating ice water through the block. The drug solution and syringe both were heated separately to 60 °C. It was necessary to heat the syringe prior to

introducing the drug solution to prevent crystallization inside of the syringe. Ten drops of the drug solution at 60 °C were delivered by syringe to the surface of the substrate. Crystallization experiments were carried out on SAMs I-V and also on glass and gold as control experiments for barbital. Cooling on an aluminum block could not be used in control experiments with PDMS as the substrate because of the insulating properties of PDMS. Accordingly, Method 3 was not used with PDMS as a substrate. Five trials were carried out for each SAM and control surface. Crystallization from all solvents generally produced crystals in less than 10 minutes. In all cases, samples of crystals were isolated from solution.

#### **4.2 Crystallization on SAMs in microfluidic channels**

Crystallization experiments also were carried out on SAMs in microfluidic channels. We have begun to investigate microfluidic devices that contain multiple channels composed of polydimethylsiloxane (PDMS) on SAMs as a means to develop high throughput methods to screen for polymorphs. Crystallization in microchannels offers several advantages over crystallization on bulk surfaces that include: (1) microchannels require very small quantities (micro or nanoliters) of solution for crystallization; (2) multiple channels can be used to carry out multiple crystallization experiments simultaneously on a single device; and (3) individual channels functionalized with different SAMs allow for crystallization experiments on a range of SAMs simultaneously. Two potential disadvantages of using microchannels instead of bulk surfaces are that methods involving slow evaporation cannot be used to drive crystallization because microchannels behave essentially as closed systems, and that characterization of different polymorphic forms can be difficult because microchannels

necessarily limit the size of crystals that can grow. The goals of this research include determining (1) if crystals of barbital will nucleate selectively on SAMs in microchannels, (2) whether nucleation of polymorphs occurs reproducibly in microchannels on surfaces functionalized with a range of hydrophobic and hydrophilic SAMs, (3) if PDMS in the walls of the channels competes with SAMs in promoting nucleation of polymorphs; (4) whether the incidence of specific polymorphs on SAMs in microchannels is similar to that on SAMs on bulk surfaces, and (5) whether microfluidic devices with multiple channels are practical as devices to grow crystals and to screen for polymorphs.

#### **4.2.1 Fabrication of microfluidic devices**

We chose to fabricate microfluidic devices using poly(dimethylsiloxane) (PDMS) because procedures to prepare and pattern microchannels are well established.<sup>159</sup> PDMS is ideal as a material for attaching to SAMs and studying crystallization. For example, PDMS is nontoxic; it cures at low temperatures; it is elastomeric so it releases easily from delicate features of a mold without damaging the mold or itself; it bonds well to SAMs and other surfaces and also releases with little force from those same surfaces; it is transparent optically, which allows crystallization to be monitored using an optical stereomicroscope.

Microfluidic devices in polydimethylsiloxane (PDMS) were prepared with a single 18 mm x 1 mm x 0.2 mm channel or multiple 18 mm x 0.7 mm x 0.1 mm channels, as shown in Figure 4.2.



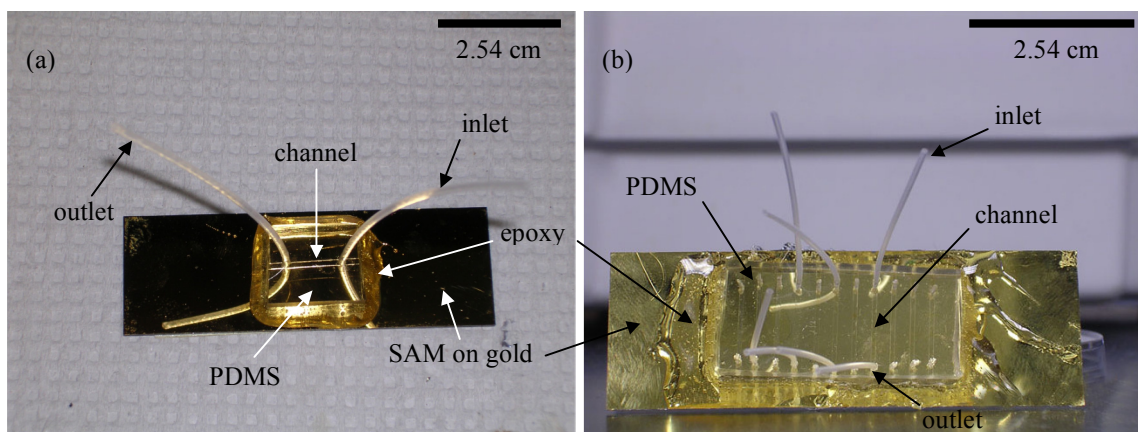


**Figure 4.2** (a) Microfluidic device with a single channel (1 mm x 18 mm x 0.2 mm).  
 (b) Microfluidic device with ten channels (0.7 mm x 18 mm x 0.1 mm).

Microchannels were fabricated using an elastomeric PDMS kit (SYLGARD-184, Dow Corning) consisting of a vinyl-terminated silicone base polymer that was mixed with a methyl hydrosiloxane crosslinking agent (10:1 w/w) and a platinum catalyst. After mixing and removing air bubbles under vacuum, the mixture was poured onto a silicon/SU-8 master and cured at 60 °C overnight. The resulting slab of PDMS was removed from the master, frozen in liquid nitrogen, holes were drilled at either end perpendicular to the channels, and polyethylene tubes (Becton Dickinson) with an inner diameter of 0.86 mm and an outer diameter of 1.52 mm were inserted into channels. The PDMS was then washed with soapy water, rinsed thoroughly with deionized water, dried and placed onto SAM-coated gold substrates. A bead of Epoxy was placed along all edges of the PDMS. The Epoxy served to seal the ends of the open channels exposed on the edges of the PDMS, and also to hold the PDMS in place on the SAM. Although we found that PDMS often showed weak sealing properties when placed in contact with

SAMs on gold, adhesion of PDMS to the SAMs generally was strong enough to prevent leakage of solution from individual microchannels.

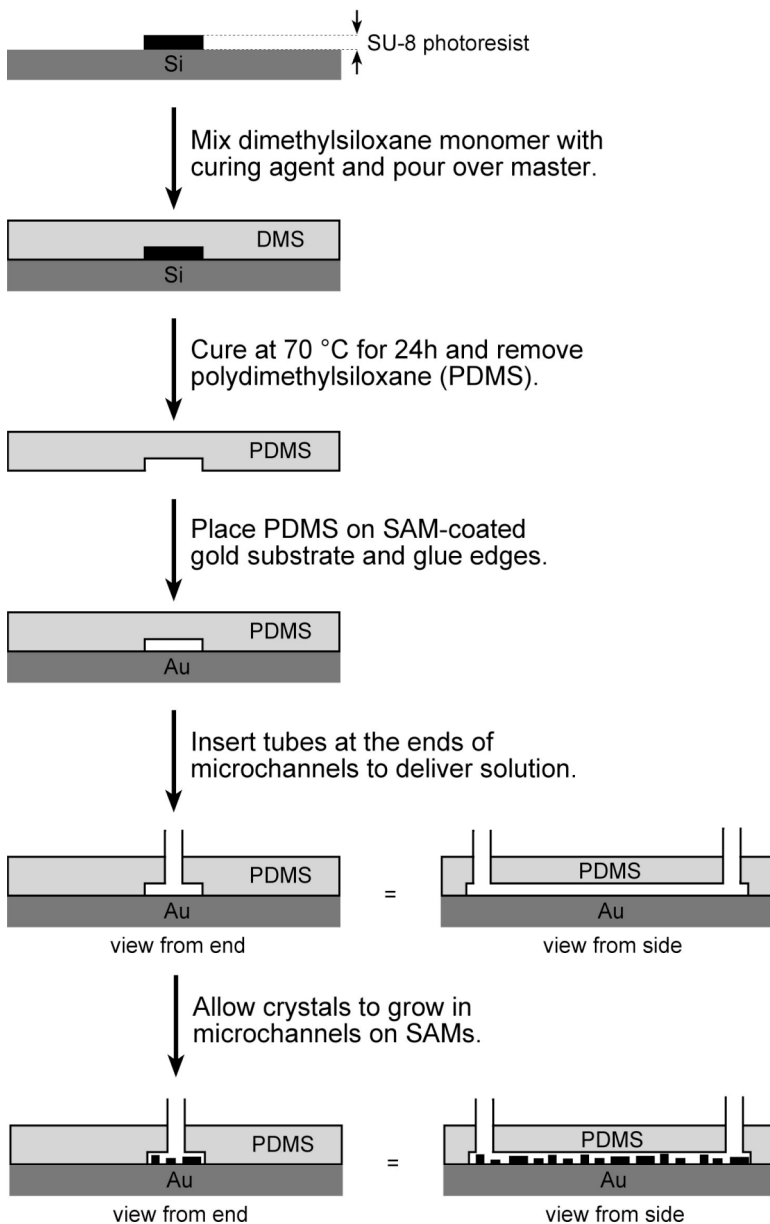


**Figure 4.3** Fabrication of microfluidic device and growth of crystals.

#### 4.2.2 Crystallization of barbital in microchannels

Barbital was crystallized in microchannels placed on SAMs I-V and also on PDMS as a control. Five separate experiments were carried out on each of these substrates.

Crystals were grown from solutions in absolute ethanol using the two general methods described below. We carried out crystallization experiments with just barbital because experiments with acetaminophen on bulk surfaces coated with SAMs gave only form I of acetaminophen. The different solvents and concentrations of barbital used for microfluidic device experiments are shown in Table 4.2.

**Table 4.2** Concentration of barbital solutions used for crystallization in microfluidic devices.

<b>Solvent</b>	<b>Method 1</b>	<b>Method 2</b>
Ethanol	0.35M	0.7M
Water	0.036M	0.07M

#### **4.2.2.1 Method 1**

Solutions of barbital were injected into microchannels with a syringe, the tubes were sealed, and the solution was allowed to sit undisturbed at room temperature. Ethyl acetate was not used for crystallization experiments in microchannels because that solvent causes significant swelling of the PDMS elastomer. Crystallization experiments were carried out on SAMs I-V and also on glass, gold and PDMS as control experiments for barbital. Five trials were carried out for each SAM and control surface. Crystals appeared in the microchannels within 24 hours from solutions containing ethanol or water.

#### **4.2.2.2 Method 2**

For method 2, the microfluidic device was placed onto the surface of an aluminum block and cooled to 0 °C by circulating ice water through the block. Cooling on an

aluminum block could not be used in control experiments with PDMS as the substrate because of the insulating properties of PDMS. Accordingly, the microfluidic device was placed into a freezer at -5 °C when PDMS was used as a substrate. The drug solution and syringe both were heated to 60 °C. It was necessary to heat the syringe prior to introducing the drug solution to prevent crystallization inside of the syringe. Solutions of barbital at 60 °C were injected into microchannels in the microfluidic device. Ethyl acetate was not used for crystallization experiments in microchannels because that solvent causes significant swelling of the PDMS elastomer. Crystallization experiments were carried out on SAMs I-V and also on glass, gold and PDMS as control experiments for barbital. Five trials were carried out for each SAM and control surface. Crystals generally appeared within several minutes. Individual crystals were isolated for characterization by removing the PDMS slab from the substrate.

### **4.3 Characterization of crystals**

Crystals grown on bulk surfaces and in microfluidic devices were isolated under an optical stereomicroscopy using fine tweezers or the sharp tip of an X-Acto blade. In most cases, the polymorphs of barbital could be identified and sorted based on the distinctive rod, block and plate morphologies exhibited consistently by forms I, II and IV, respectively. We found that form I of acetaminophen was the only polymorph that grew, and that form I was identified readily based on the distinctive block morphology. Crystals grown in microfluidic channels generally were smaller necessarily than those grown on bulk surfaces. Thus, it was more difficult to isolate and characterize crystals in

microchannels. Samples of individual crystals typically consisted of no more than 1 mg (typically less) of crystals regardless of the technique used.

Crystals of forms I, II and IV of barbital and forms I and II of acetaminophen can be characterized using a variety of analytical techniques that include melting point, optical microscopy, IR spectroscopy,  $^{13}\text{C}$  CP/MAS NMR and X-ray powder diffraction. Each of these techniques is described in the sections that follow. Although X-ray powder diffraction and  $^{13}\text{C}$  CP/MAS NMR spectroscopy commonly are used to identify and distinguish polymorphs, both techniques require approximately 50-100 mg of sample to achieve satisfactory signal-to-noise. Consequently, we utilized melting point, optical microscopy and infrared spectroscopy as the primary means to identify the polymorphs of barbital and acetaminophen.

#### **4.3.1 Melting point**

Pure, crystalline solids have a characteristic melting point, the temperature at which the solid melts to become a liquid. Each polymorph typically has a distinct melting point that differs from those of other polymorphs. The difference in magnitude between two melting points usually reflects the relative difference in lattice energies of two polymorphs with the more stable polymorph having the higher melting point. Thus, polymorphs with similar lattice energies may exhibit melting points that are close or even identical.<sup>160</sup> Forms I, II and IV of barbital have melting points of 190 °C, 183 °C and 176 °C, respectively, while forms I and II of acetaminophen have melting points of 171 °C and 160 °C. The relatively large differences make identification of the various polymorphs of barbital and acetaminophen straightforward using melting point.

### 4.3.2 Optical microscopy

Optical microscopy provides a rapid and convenient method to screen the homogeneity of samples of crystals visually and to record digital images of samples for analysis and comparison. Polymorphs frequently grow with unique morphologies, or habits, that allow different crystalline forms to be distinguished. It is important to note, however, that many compounds may crystallize in a single packing arrangement that exhibits different habits depending on the conditions used for crystallization. Moreover, different polymorphic forms may exhibit similar habits. Therefore, observation of crystals with different habits does not always indicate the presence of polymorphs. When crystals with different habits form, analysis by another analytical technique generally is required. In the case of barbital, forms I, II and IV form distinct rod, prism and plate morphologies (Figure 4.4) that have been reported previously by Craven.<sup>65</sup>

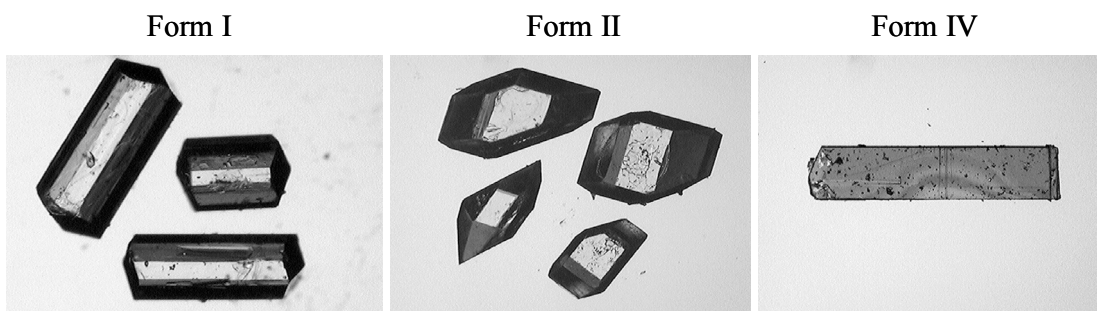


**Figure 4.4** Images of form I, II and IV of barbital.

Similarly, forms I and II of acetaminophen exhibit block and prism morphologies (Figure 4.5) by which the forms can be distinguished visually.<sup>68,69,76</sup>

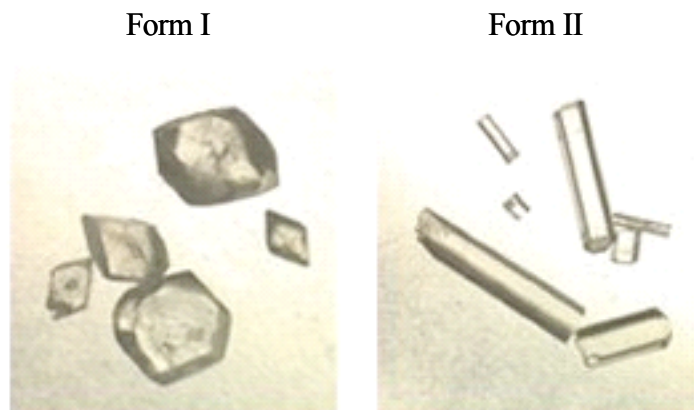


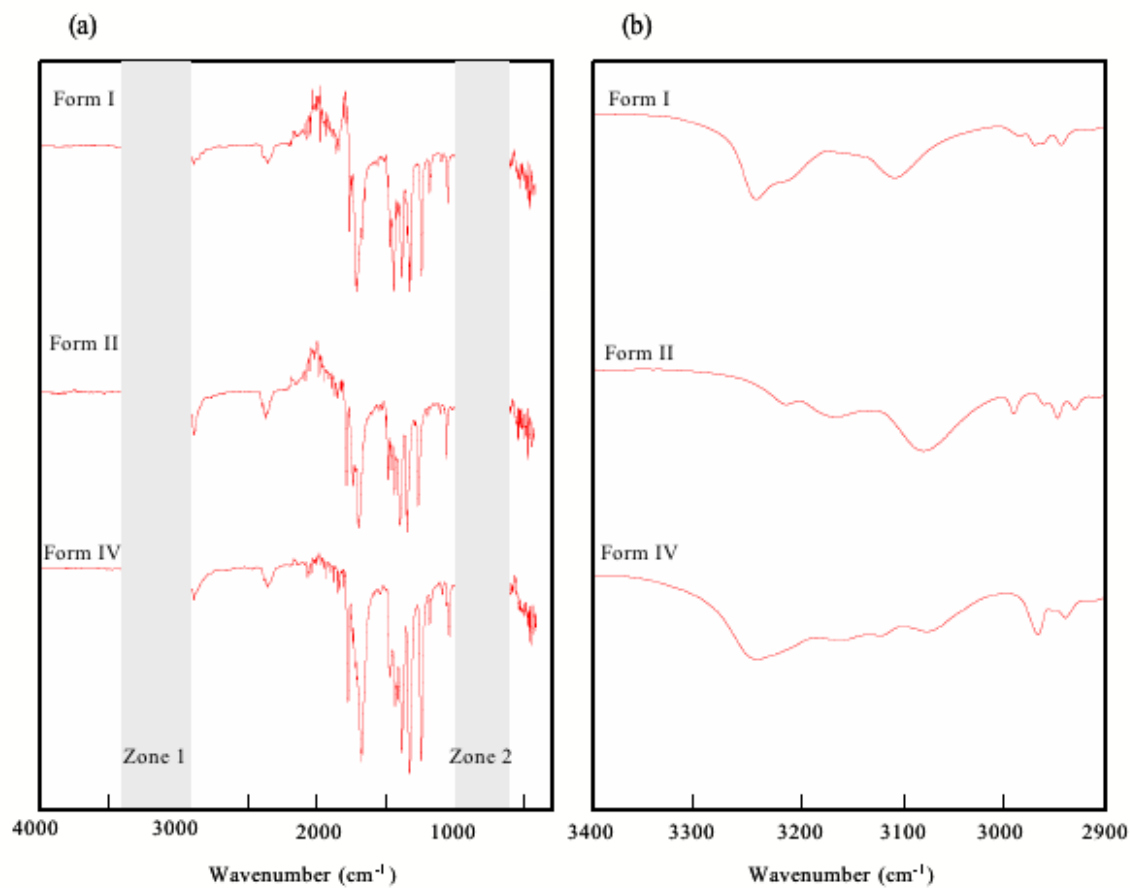
**Figure 4.5** Images of form I and II of acetaminophen.<sup>76</sup>

Prior to removing crystals from bulk substrates and microchannels, images were taken of both bulk samples and individual crystals using a low-power optical stereomicroscope equipped with a digital camera. The images were then compared to those of the various polymorphs grown previously using normal methods of recrystallization of slow evaporation and rapid cooling of solutions in Pyrex beakers.

### **4.3.3 Infrared Spectroscopy**

Infrared spectroscopy provides one of the more useful analytical methods to identify polymorphs. IR spectroscopy is particularly well suited to distinguish polymorphs of compounds that contain hydrogen-bonding functional groups. The stretching frequencies of hydrogen-bonding donors such as O-H and N-H groups and acceptors such as C=O groups vary significantly depending on type and number of hydrogen bonding interactions and differences in crystal packing. One advantage of IR over other analytical techniques is that spectra can be collected on small amounts of sample using an attenuated total internal reflection (ATR) accessory. For example, most of the IR spectra

collected in this study were obtained from single crystals less than 1 mg in mass in order to unambiguously identify which polymorph was present. The three polymorphs of barbital can be distinguished readily by IR as reported previously by Craven.<sup>65</sup> Shown in Figure 4.6 are the IR spectra of forms I, II and IV of barbital.





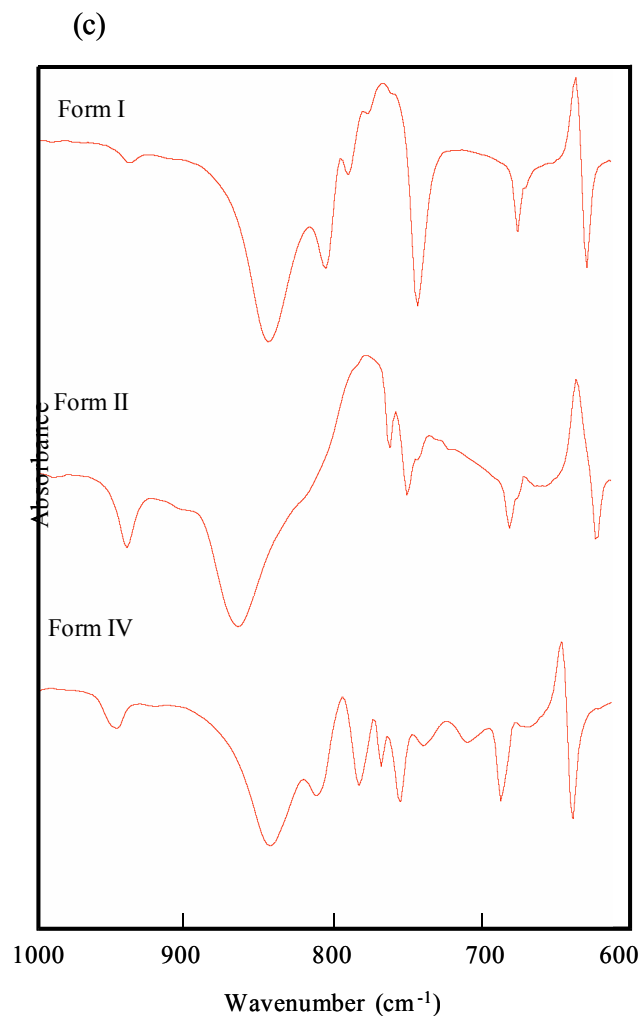


**Figure 4.6** (a) IR spectra for forms I, II and IV of barbitol. (b) Expanded IR spectra of zone 1. (c) Expanded IR spectra of zone 2.

Forms I, II and IV of barbitol were assigned to individual samples primarily based on characteristic differences in the N-H stretching absorptions in the range 3250-3050 cm<sup>-1</sup> and in the fingerprint region in the range 850-750 cm<sup>-1</sup>. Shown in Figure 4.7 are the IR spectra of forms I and II of acetaminophen.

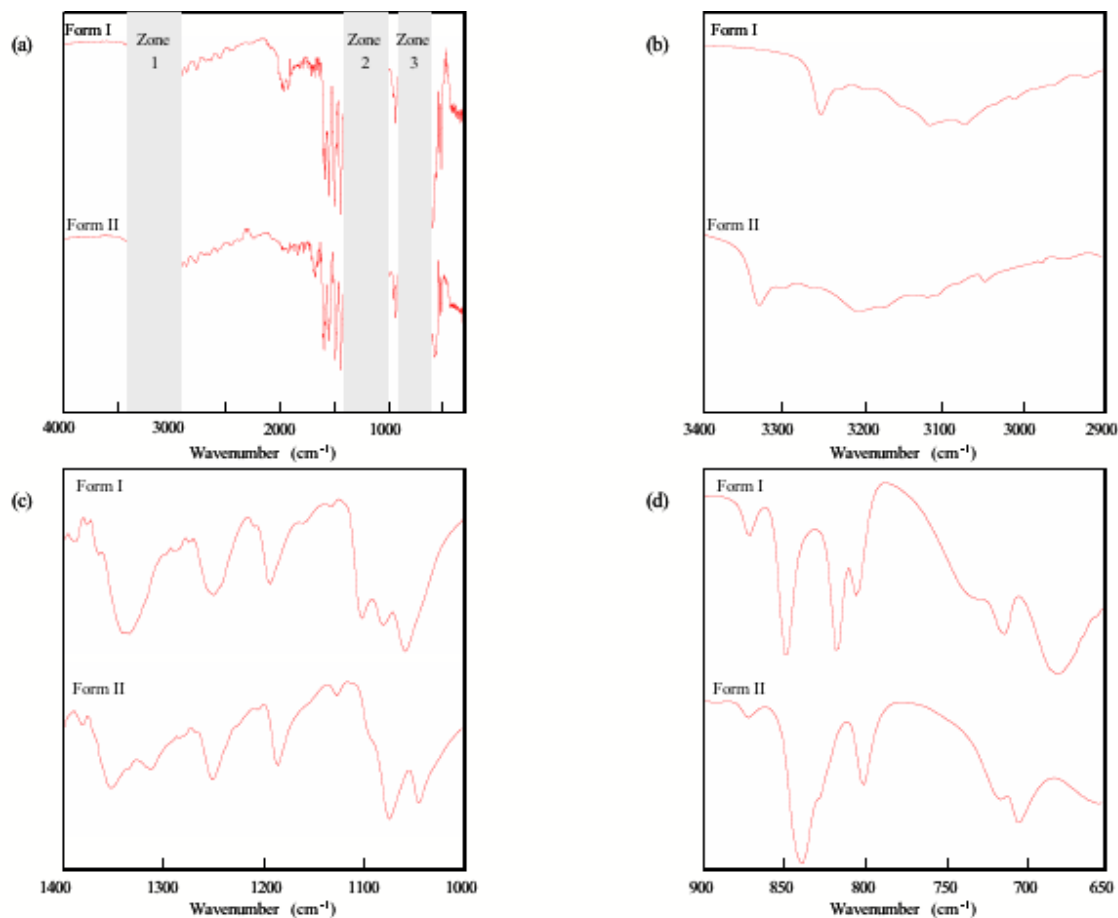


**Figure 4.7** (a) IR spectra for forms I and II of acetaminophen. (b) Expanded IR spectra of zone 1. (c) Expanded IR spectra of zone 2. (d) Expanded IR spectra of zone 3.

Forms I and II of acetaminophen were assigned to samples primarily based on characteristic differences in the N-H and O-H stretching absorptions in the range 3350-3000  $\text{cm}^{-1}$  but also differences in the fingerprint region in the ranges 1400-1300  $\text{cm}^{-1}$ , 1100-1000  $\text{cm}^{-1}$ , 850-800  $\text{cm}^{-1}$  and 750-650  $\text{cm}^{-1}$ . The differences in the N-H and O-H stretching absorptions arise because of differences in the strengths of hydrogen bonds involving those groups.<sup>161</sup>

#### 4.3.4 $^{13}\text{C}$ CP/MAS NMR

$^{13}\text{C}$  cross-polarization/magic angle spinning (CP/MAS) NMR spectroscopy is an analytical method used with increasing frequency to investigate and characterize polymorphs.<sup>162,163</sup> The  $^{13}\text{C}$  CP/MAS technique is sensitive to subtle differences in crystal packing, molecular conformations and hydrogen bonding in solids. For example, it has been shown that formation of a hydrogen bond to a carbonyl group generally causes the chemical shift of the carbonyl to move downfield by approximately 3 ppm.<sup>164</sup> Accordingly; we have used  $^{13}\text{C}$  CP/MAS NMR to characterize and identify the polymorphs of barbital. The  $^{13}\text{C}$  CP/MAS NMR spectra of forms I, II and IV of barbital are shown in Figure 4.8 and the corresponding chemical shift values for resonances for the three spectra are shown Table 4.3.

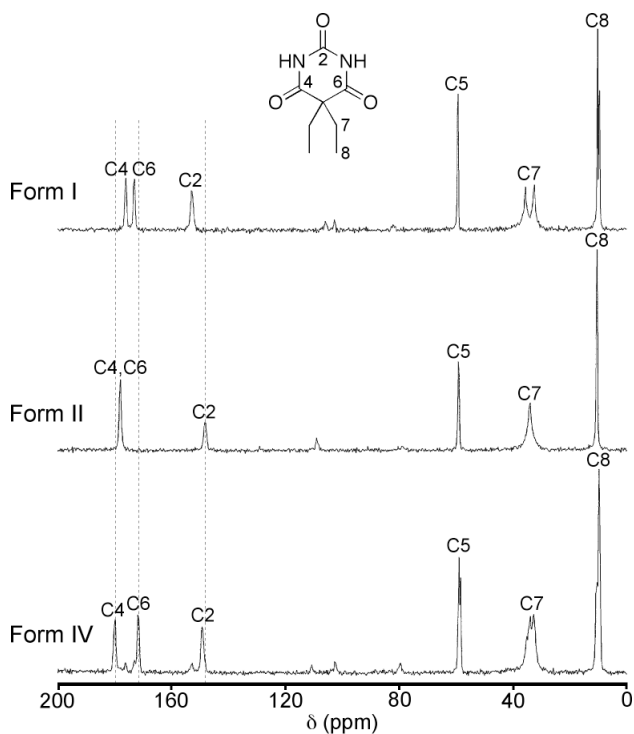
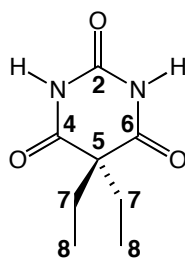


**Figure 4.8**  $^{13}\text{C}$  CP/MAS NMR spectra of forms I, II and IV of barbital.

**Table 4.3** Chemical shifts from  $^{13}\text{C}$  CP/MAS NMR spectra of forms I, II and IV of barbital.



Atom	Form I (ppm)	Form II (ppm)	Form IV (ppm)
C(2)	152.8	148.0	149.2
C(4)	176.1	178.1	180.0
C(5)	58.8	58.8	58.1, 58.6
C(6)	173.2	178.1	172.0
C(7)	31.9, 35.0	33.3	32.1, 33.3
C(8)	9.0, 9.8	10.0	9.3

As shown in Figures 2.6, 2.7 and 2.8, the carbonyl group at C4 forms a hydrogen bond while the carbonyl group at C6 is not involved in hydrogen bonding. The  $^{13}\text{C}$  CP/MAS spectrum shows two separate resonances for C4 and C6 with the peak for C4 shifted downfield by 3 ppm. The carbonyl group at C2 of form I, which also forms a hydrogen bond, is shifted downfield by 3 ppm when compared to the carbonyl group at C2 in the spectrum of form 2, which is not involved in hydrogen bonding. In the spectrum of form II, the carbonyl groups at C4 and C6 both form one hydrogen bond, and thus have identical chemical shift and give just one resonance. In the  $^{13}\text{C}$  CP/MAS spectrum of form IV, the resonances for C4 and C6 are separated by about 6 ppm ( $2 \times 3$  ppm), reflecting the fact that the carbonyl group at C4 forms two hydrogen bonds, while the carbonyl group is not involved in hydrogen bonding. Comparison of the three spectra also reveals differences in the number and chemical shift values of resonances for C5, C7

and C8 that arise because the molecules adopt reside in different conformations and crystal packing arrangements in the three forms.  $^{13}\text{C}$  CP/MAS spectroscopy was not used to characterize forms I and II of acetaminophen.

#### 4.3.5. X-Ray Powder Diffraction

X-ray powder diffraction (XPD) is the most widely used technique for identifying polymorphs.<sup>165-167</sup> The XPD pattern from a crystalline solid results satisfying the Bragg equation,  $n\lambda = 2d \sin\theta$ , where  $n$  is an integer,  $\lambda$  is the wavelength of radiation,  $d$  is the spacing between parallel planes of electron density in the crystal lattice, and  $\theta$  is the angle at which X-rays diffract.<sup>168</sup> The different  $d$  spacings within a given unit cell give rise to diffraction peaks that are plotted as values of  $2\theta$  along the x-axis in the XPD pattern. The  $2\theta$  values of the peaks reflect the different lattice spacings and thus the dimensions of the unit cell. Thus, each polymorph generates a unique XPD pattern because the dimensions of the unit cells differ considerably. For example, shown in Figure 4.9 are the XPD traces for forms I, II and IV of barbital. Comparison of the XPD patterns reveals that each form gives rise to a XPD pattern with unique peaks that do not overlap with those of the other polymorphs.

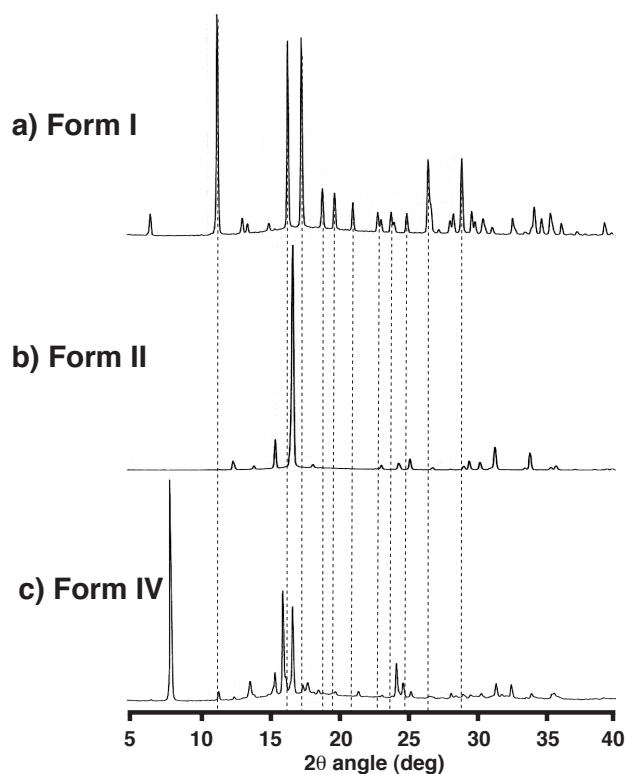


**Figure 4.9** X-ray powder diffraction traces of forms I, II and IV of barbital (a-c, respectively). The dotted lines mark the positions of the more intense peaks in the trace of form I (a). Overlap of these peaks with peaks in the trace of form IV (c) indicate contamination of form IV by approximately 5% of form I.

#### 4.4 Results and Discussion

Crystallization using methods 1, 2 and 3 on bulk surfaces was carried out with barbital using ethanol, water and ethyl acetate as solvents, and with acetaminophen using just ethanol as the solvent. Crystallization in microfluidic channels was carried out with just barbital using methods 1 and 2. The results of these experiments are presented below and are broken down hierarchically by drug, substrate (i.e., bulk surface or microfluidic channel), and solvent system used.

The crystallization behavior of acetaminophen and barbital in this study can be broadly summarized as follows. Crystals of form I for acetaminophen dominated the results from ethanolic solutions on all surfaces. For barbital, form IV unexpectedly dominated on many of the surfaces in all three solvent systems, but especially from ethanolic solutions. The different polymorphic forms of acetaminophen and barbital were identified primarily using optical microscopy and infrared spectroscopy.

Forms I, II and IV of barbital exhibited distinct rod, prism and plate morphologies or habits, respectively, similar to those reported by Craven, as shown previously in Figures 2.6, 2.7, 2.8 and 4.4.<sup>68,69</sup> Shown in Figure 4.10 are representative examples of the morphologies, of forms I, II and IV of barbital that were collected from crystallization experiments on SAMs (Form I on SAM III, form II on SAM II, and form IV from SAM IV in a microchannel) in ethanolic solutions. Slight differences in morphology are evident when images of polymorphs grown on SAMs are compared to those grown from methanolic solution in a glass beaker. For example, form I grows as flattened rods or thick plates as shown on the left in Figure 4.10. This morphology differs from that normally observed (left in Figure 4.4) where the rods exhibit nearly uniform thickness that reflects the high symmetry (R-3) of the space group. Form II grows as elongated prisms with parallelogram or truncated parallelogram shapes. This morphology differs significantly from the block-like prisms shown in the center in Figure 4.4. The plate morphology of form IV grown on SAMs is similar to the plate morphology grown in glass beakers.

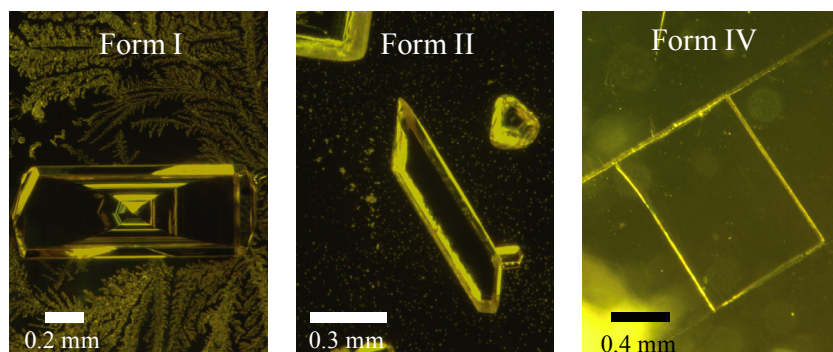


**Figure 4.10** Forms I, II and IV of barbital from different substrates.

Similarly, forms I and II of acetaminophen exhibit block and prism morphologies (Figure 4.5) by which the forms can be distinguished visually.<sup>76</sup> Shown in Figure 4.11 are representative examples of forms I and II of acetaminophen from bulk surface experiments (both grown on SAM III). We found that form I grew as blocks (left in Figure 4.11) with morphology similar to that observed previously. In contrast, form II formed polycrystalline films (right in Figure 4.11) on SAMs in the few experiments where form II appeared instead of single crystals with the expected prism morphology.

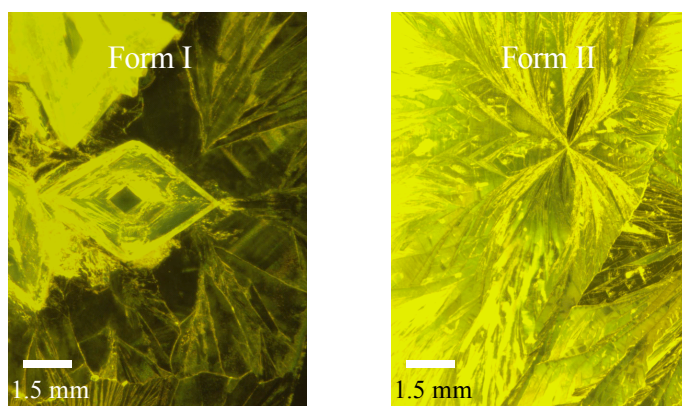


**Figure 4.11** Forms I and II of acetaminophen from different substrates.



Examples of crystal forms of acetaminophen and barbital grown on SAMs I-V and on control surfaces that are glass, gold and PDMS are shown for each drug with each solvent. The results of the experiments with acetaminophen are summarized and presented first, followed by the results of experiments with barbital. The experiments with barbital on bulk surfaces and microchannels are presented separately. Each section is divided in subsections according to the solvents used.

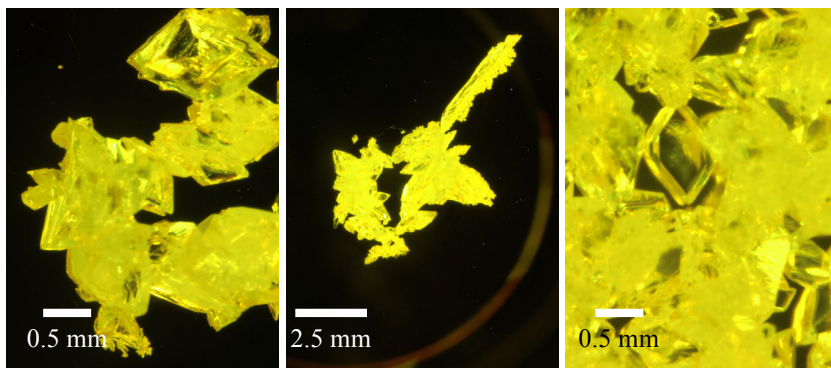
#### **4.4.1 Acetaminophen**

##### **4.4.1.1 Bulk Surfaces**

###### **4.4.1.1.1 Ethanol**

Acetaminophen crystallization experiments were done only in ethanol on SAMs I-V and also on gold and glass as control experiments. Form I (the common form) is more stable at room temperature than form II (but is not suitable commercially for direct compression into tablets<sup>74,75</sup>). Because of that SAMs with different polar and nonpolar head groups used to control the nucleation of acetaminophen to get the less common form II. Examples from each surface are shown in Figure 4.12.

SAM I

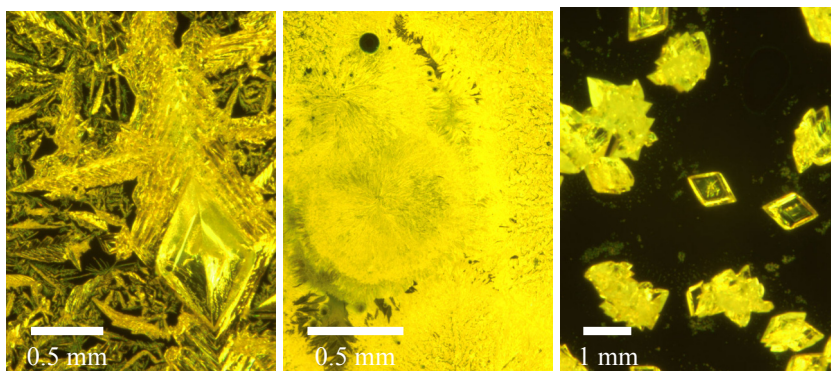


method 1

method 2

method 3

SAM II

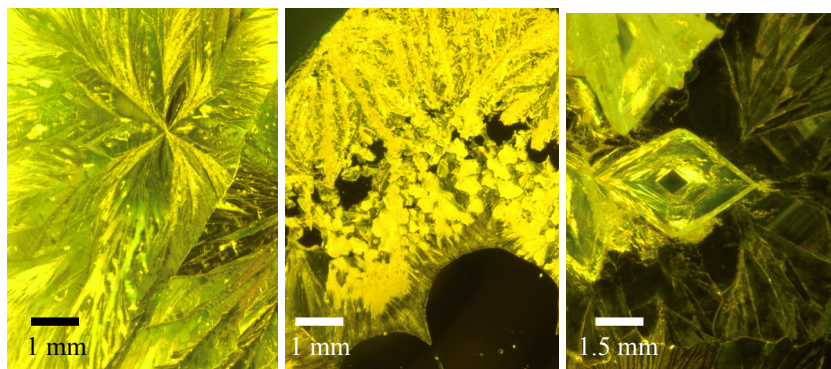


method 1

method 2

method 3

SAM III

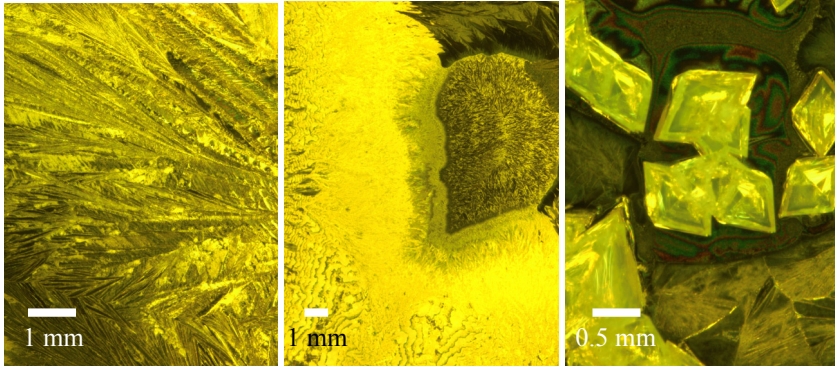


method 1

method 2

method 3

SAM IV

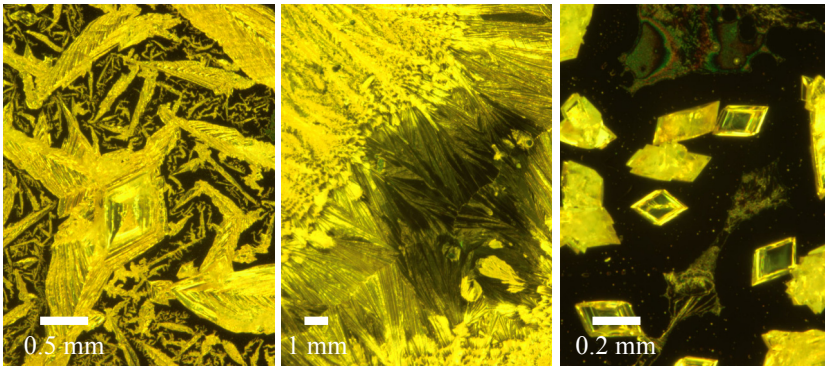


method 1

method 2

method 3

SAM V

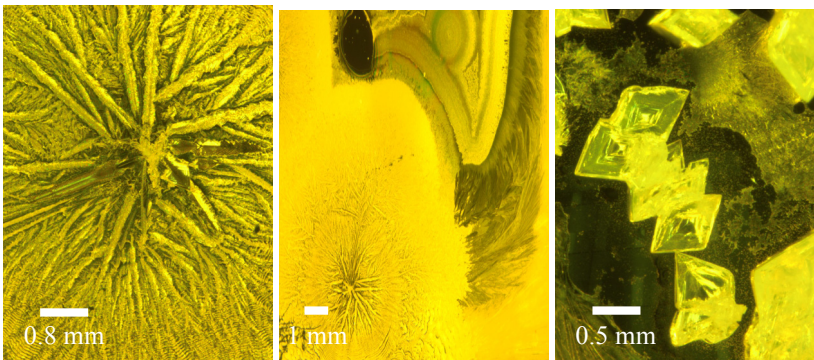


method 1

method 2

method 3

Bulk Gold



method 1

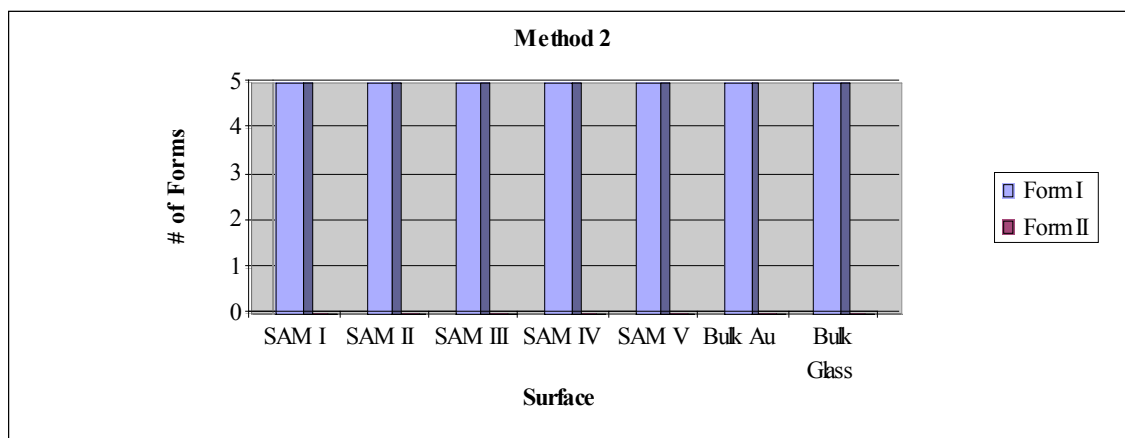
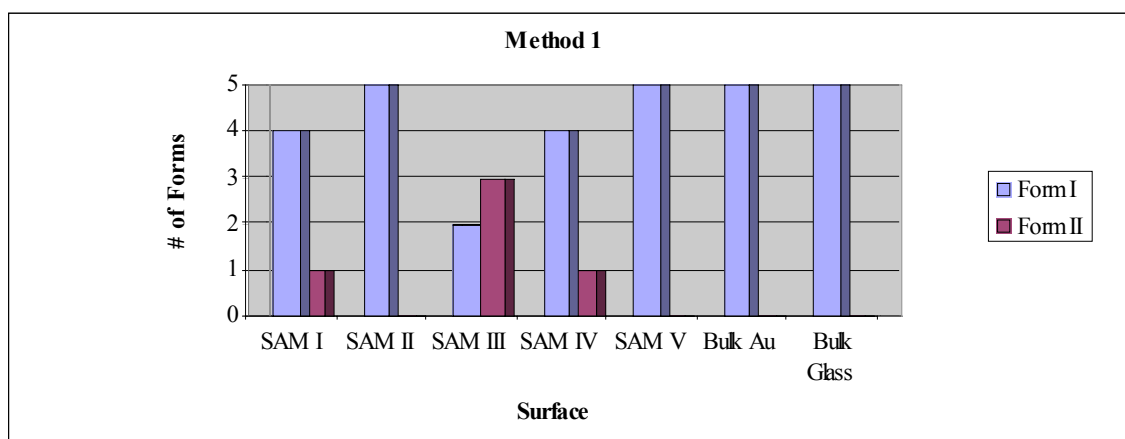
method 2

method 3

**Figure 4.12** Examples of acetaminophen crystal pictures on each surface for each method.

Characterization of crystals by optical microscopy and infrared spectroscopy, revealed that form I was the predominant polymorph of acetaminophen that formed on SAMs I-V and the control surfaces. The results of these experiments using all three methods are summarized in Figure 4.13. Form II appeared only in one out of five runs on SAMs I and IV, and in three out of five runs on SAM III when acetaminophen was crystallized using method 1. This selectivity for form I was even more pronounced for method 2, which gave only form I, and for method 3, which gave form II in one out of five runs on SAM II. In summary, form II appeared only six times out of a total of 105 runs on different surfaces using methods 1-3. These results indicate that, at least for the surfaces and methods we utilized, the crystallization behavior of acetaminophen did not deviate from that normally observed in the absence of SAMs. Ultimately, we were not able to determine why acetaminophen crystallized predominantly as form I on SAMs I-V and the control surfaces. Although we can propose several explanations for this behavior, none can be substantiated without further investigation. For example, it is possible that the surfaces we examined do act as templates that promote aggregation of acetaminophen on the surface, and that all of the surfaces simply favor aggregates that nucleate form I preferentially instead of form II. Alternatively, nucleation may occur in solution on dust or other airborne contaminants. The fact that form II appeared in just 6 of 105 runs on SAMs or control surfaces was surprising, especially considering that Lang, Grzesiak and Matzger found that form II nucleated readily on a range of solid polymers.<sup>51</sup> One

important difference between the two studies is that SAMs present essentially two-dimensional surfaces that have lower interaction energy with molecules in solution than three-dimensional surfaces such as those presented on solids of polymers. Consequently, three-dimensional surfaces may be necessary to achieve high enough interaction energy for templating of form II of acetaminophen to occur.



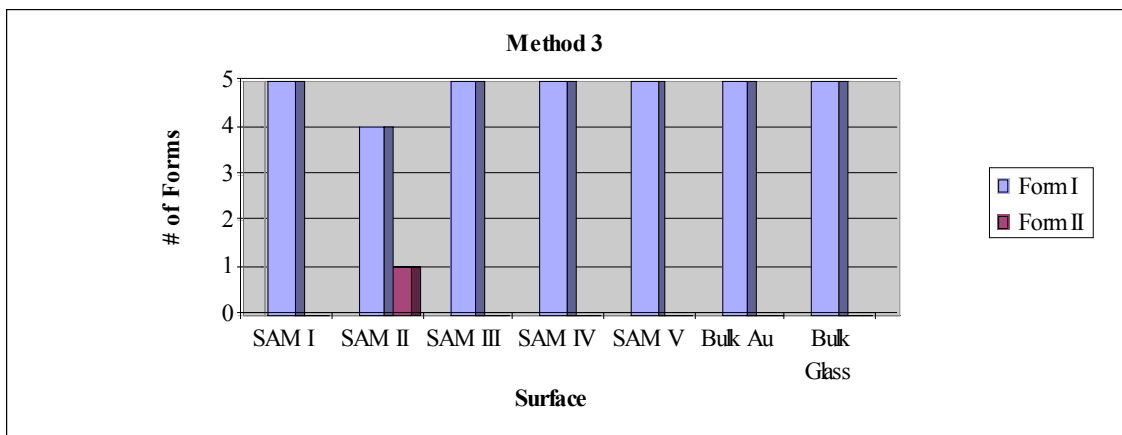


**Figure 4.13** Results of acetaminophen crystallization experiments for each method.

After completing the crystallization experiments with acetaminophen in ethanol and finding no evidence of form II, we decided to stop experiments with acetaminophen and focus our efforts instead on crystallization experiments with barbital.

## 4.4.2 Barbital

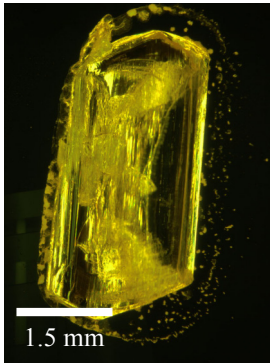
### 4.4.2.1 Bulk surfaces

#### 4.4.2.1.1 Ethanol

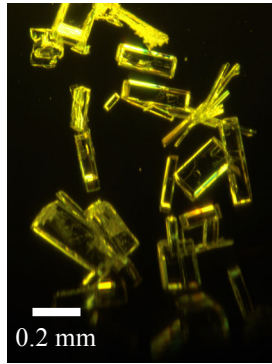
Examples of crystals grown from each different surface are shown in Figure 4.14. The results are summarized in Figure 4.15 as a graph for each method.



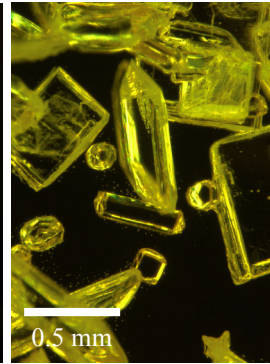
SAM I



method 1

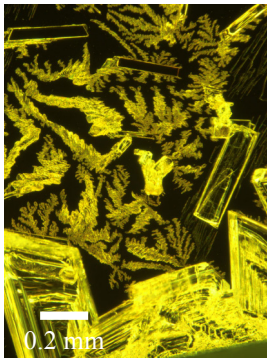


method 2

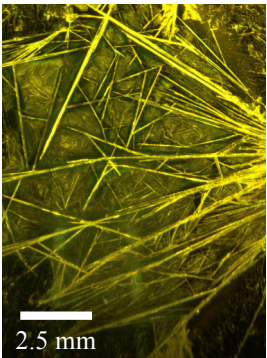


method 3

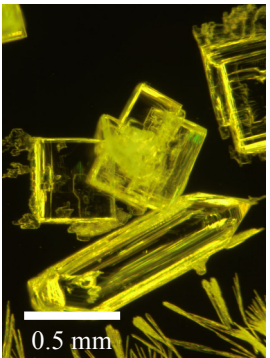
SAM II



method 1

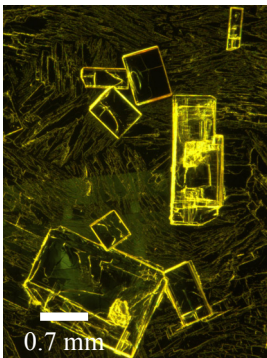


method 2

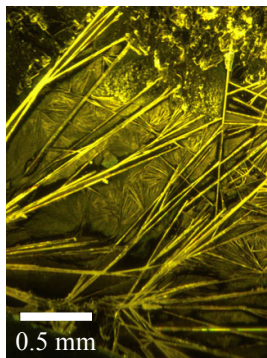


method 3

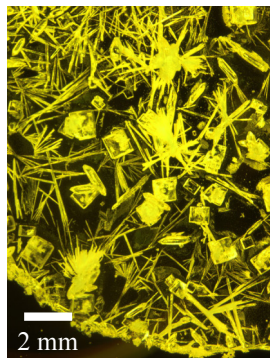
SAM III



method 1

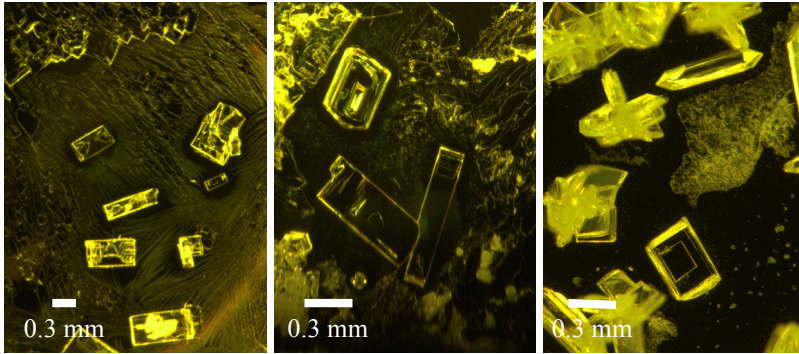


method 2



method 3

SAM IV

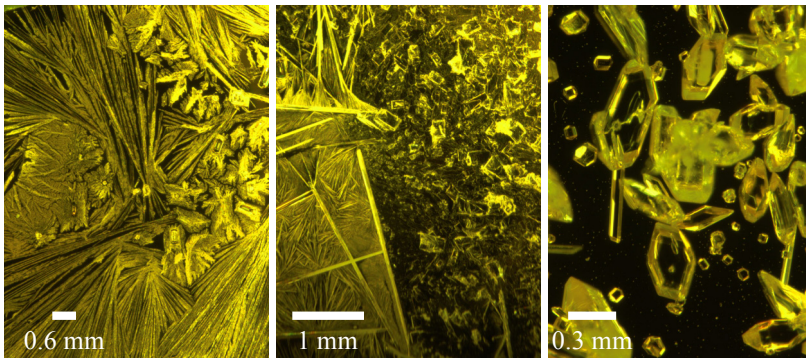


method 1

method 2

method 3

SAM V

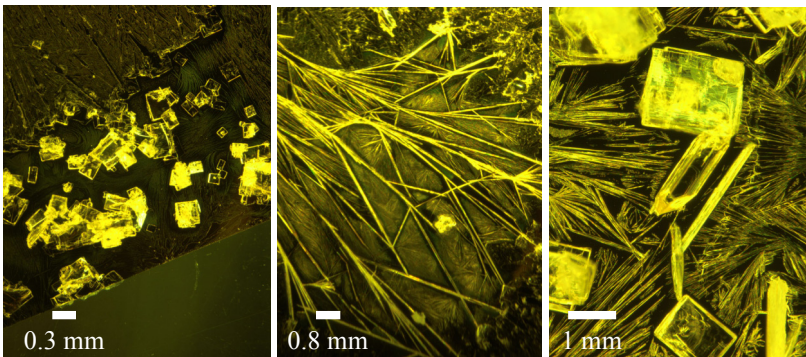


method 1

method 2

method 3

Bulk Gold



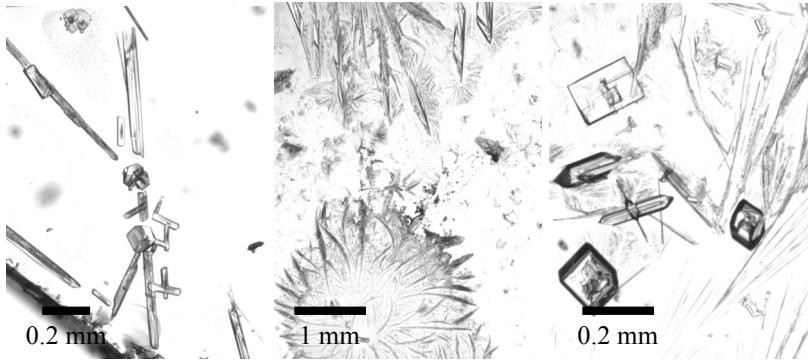
method 1

method 2

method 3



Glass

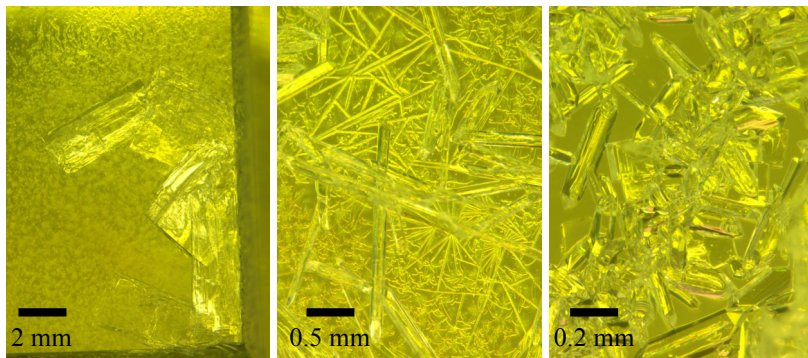


method 1

method 2

method 3

PDMS



method 1

method 2

method 3

**Figure 4.14** Examples of barbital crystal pictures on each surface for each method from ethanolic solution.

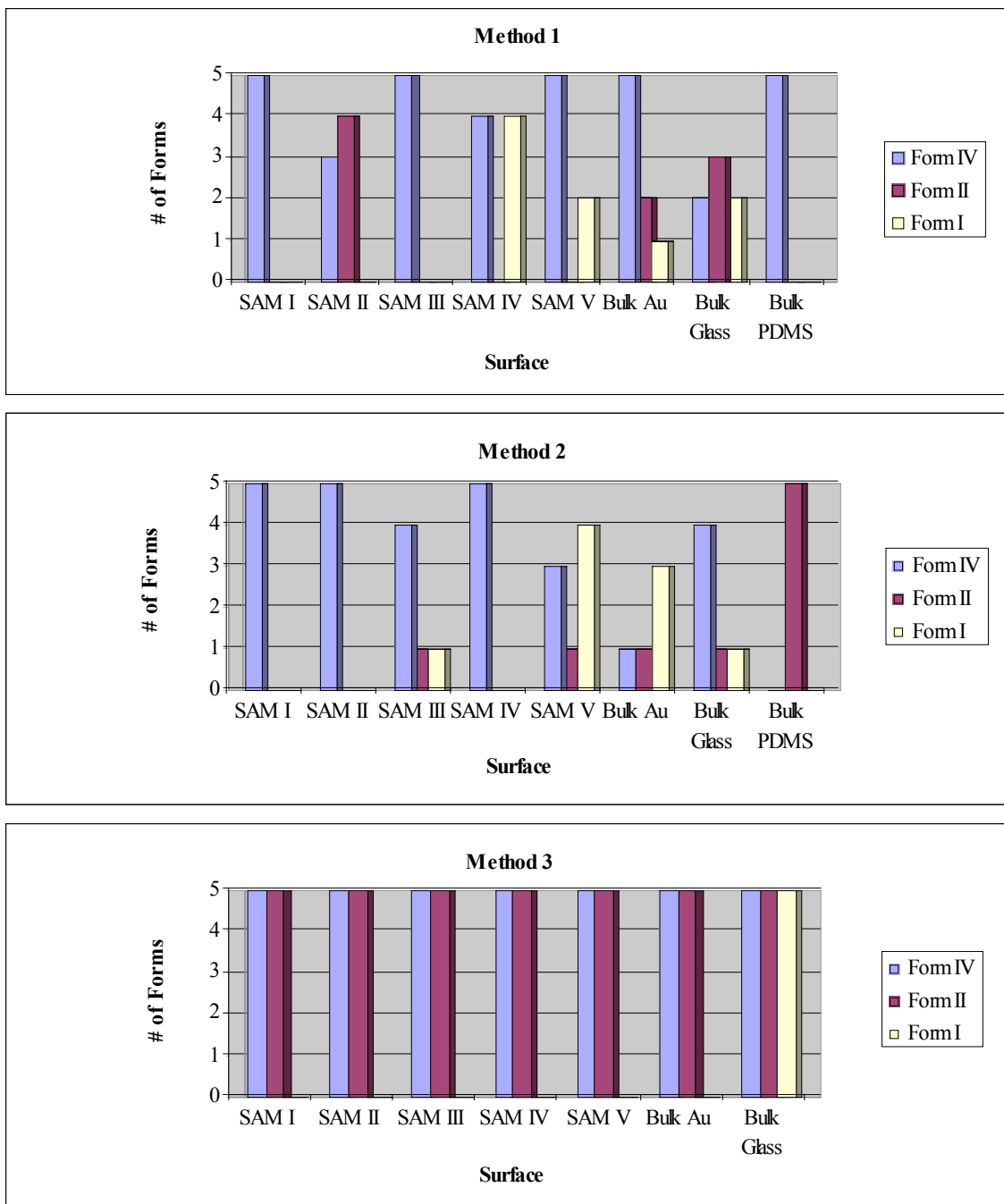


**Figure 4.15** Results of barbital crystallization experiments for each method from ethanolic solution.

The experiments on SAMs in ethanol clearly show that form IV of barbital was the dominant polymorph for methods 1 and 2 on SAMs I-V, with form IV appearing as the only polymorph on SAMs I and III by method 1 and on SAMs I, II and IV by method 2. Exceptions occurred on SAMs II and IV by method 1 and SAM IV by method 2. In those cases, form I or II appeared concomitantly with form IV in equal or slightly greater frequency. In contrast, form II appeared concomitantly with form IV on all SAMs by Method 3. In the control experiments, gold and glass substrates always gave mixtures of the three polymorphs concomitantly by methods 1-3 with the exception that form I did not appear on bare gold by method 3. These results show crystallization under thermodynamic conditions by methods 1 and 2 generally give greater selectivity for one form than crystallization under kinetic conditions by method 3. Moreover, the greater selectivity under thermodynamic conditions generally favors form IV over forms I and II on SAMs. This result is surprising considering that SAM IV is the least stable polymorph of the three forms of barbital. More surprising is the fact that form IV appears with approximately equal frequency on all SAMs. Although we anticipated that the different functional groups exposed on the surface of SAMs I-V would lead to selective nucleation of forms I, II and IV, we did not expect that nucleation of form IV would predominate on all SAMs.

Plates of form IV grew consistently oriented on all SAMs with the large rectangular 010 face in contact with SAMs. This behavior suggested that preferential orientation might occur because of favorable interaction between functional groups exposed on the 010 face of the crystal and those on the surface of the SAM. Analysis of the crystal packing in the crystal structure of form IV revealed that the hydrogen-bonded layers of

molecules stack on top of one another along the 010 direction in the crystals. As shown in Figure 4.16, that packing arrangement exposes the polar hydrogen-bonding groups on individual molecules of barbital at the small facets presented on the edges of the plates and the nonpolar ethyl groups (colored magenta in Figure 4.16) at the surface of the large 010 facet. Thus, the large 010 face on plates of form IV are hydrophobic. The fact that the hydrophobic 010 faces of crystals of form IV always contact the surface of SAMs I-V in ethanol suggests that hydrogen bonding is not involved in promoting oriented growth. Rather, we hypothesize that molecules of ethanol solvent bind to the surface of SAMs II-V by forming strong hydrogen bonds to the OH, CO<sub>2</sub>H and pyridine groups, thereby creating ordered layers of solvent that generate a hydrophobic surface. This concept is illustrated in Figure 4.16. Alcohols are known to be good hydrogen-bonding donors and acceptors that generally form strong hydrogen bonds.<sup>169</sup> As shown in Figure 4.16, aggregation of ethanol onto the surface via hydrogen bonding necessarily results in oriented assembly with the ethyl groups exposed at the surface. Ordered solvation in this manner would effectively block the hydrogen-bonding groups of the SAMs and present a hydrophobic surface of ethyl groups similar to that presented on the 010 face of crystals of form IV. In the absence of exposed hydrogen-bonding groups on the surface, templating of molecules onto the surface via hydrogen bonding should not occur. Moreover, the hydrogen-bonded layers in form IV maximize hydrogen-bonding contacts between molecules of barbital within layers while eliminating hydrogen bonding between adjacent layers and to surfaces. It follows that form IV should be favored in the presence of surfaces with no exposed hydrogen-bonding groups because hydrogen bonding is favored within layers. Conversely, forms I and II may be favored when in the presence of

surfaces with exposed hydrogen-bonding groups if hydrogen-bonded contacts between molecules of barbital and the surface are more energetically favorable than those between molecules of barbital. Accordingly, we hypothesize that oriented growth of form IV with the 010 face in contact with SAMs occurs as a result of maximizing favorable hydrophobic interactions between molecules of barbital in hydrogen-bonded layers and the solvated surface as layers form. Solvation of SAMs II-V by ethanol in this manner would give hydrophobic surfaces essentially similar to that of hydrophobic SAM I, and would explain why the crystallization behavior is similar on all five SAMs.

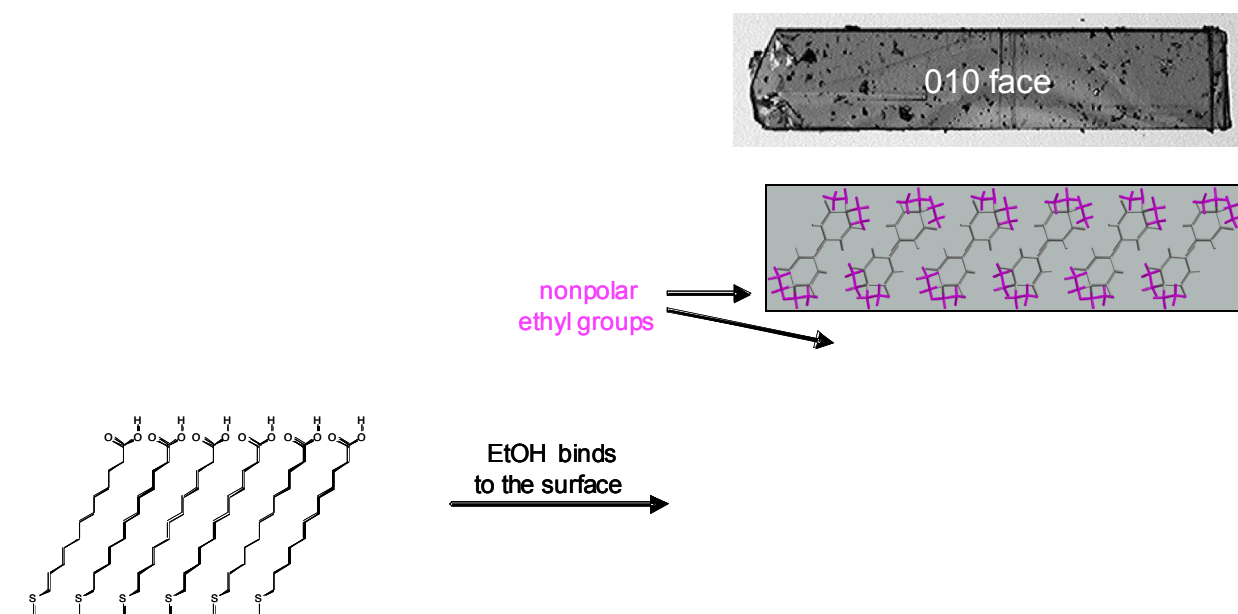
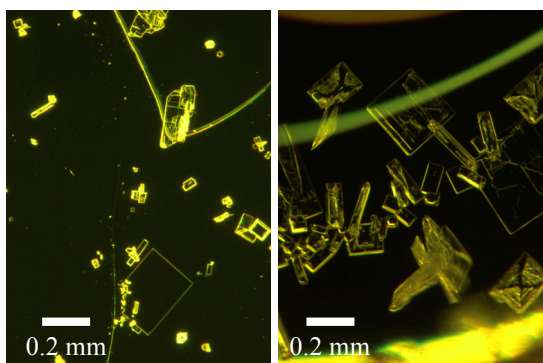


**Figure 4.16** Top: Image of a crystal of form IV showing the large 010 face of the plate morphology in the plane of the page. Middle: View of a single hydrogen-bonded layer of barbital molecules view from the side showing the ethyl groups (magenta) exposed above and below the layer on the 010 surfaces. Bottom: Illustration showing how solvation of a carboxylic acid terminated SAM by an ordered layer of ethanol molecules could result in exposure of ethyl groups to create a hydrophobic surface.

#### 4.4.2.1.2 Water

We chose to investigate the crystallization behavior of barbital in water in order to test our hypothesis in the previous section that solvation of surfaces by ethanol minimizes or eliminates hydrogen bonding between barbital and the surface. We reasoned that hydrogen bonding of water to the OH, CO<sub>2</sub>H and pyridine headgroups of SAMs II-V should still present hydrophilic surfaces with exposed OH groups capable of hydrogen bonding to barbital and, thus, capable of templating aggregation of barbital on the surface. In contrast to the ethanol, the solubility of barbital in water was very low. In combination with the low volatility of water, the low solubility of barbital eliminated method 1 as a choice for growing crystals in a timely manner. Consequently, only methods 2 and 3 were utilized for growing crystals. Examples of crystals grown from each different surface are shown in Figure 4.17. The results are summarized in Figure 4.18 as a graph for both methods.

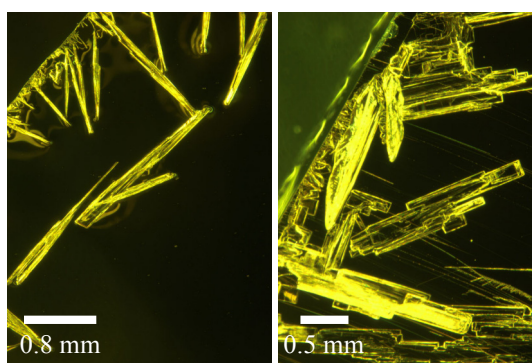
SAM I



method 2

method 3

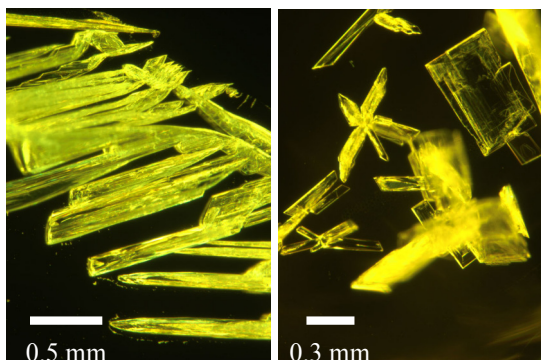
SAM II



method 2

method 3

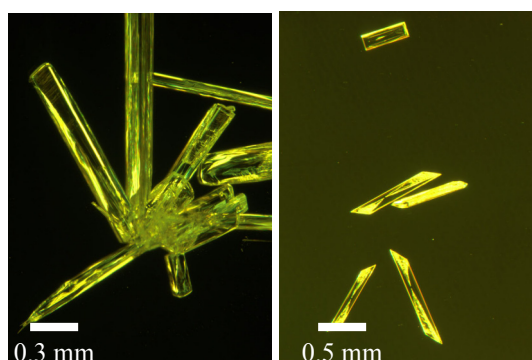
SAM III



method 2

method 3

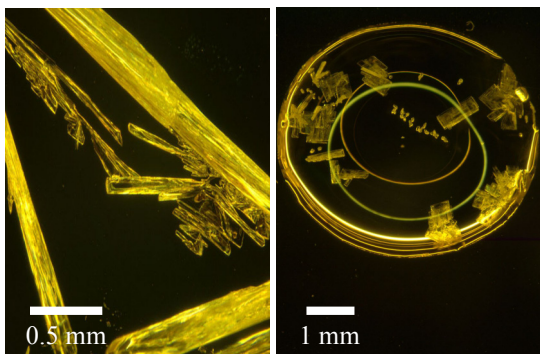
SAM IV



method 2

method 3

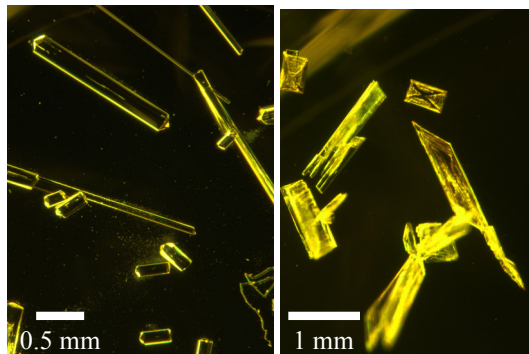
SAM V



method 2

method 3

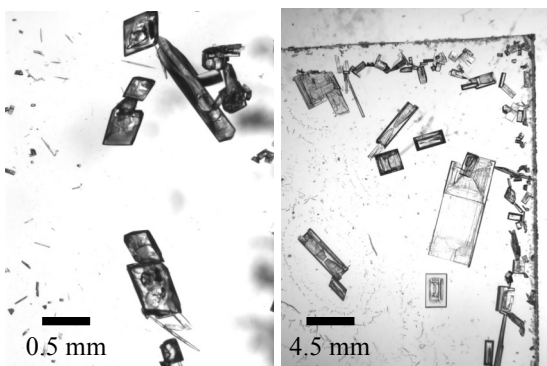
Bulk Gold



method 2

method 3

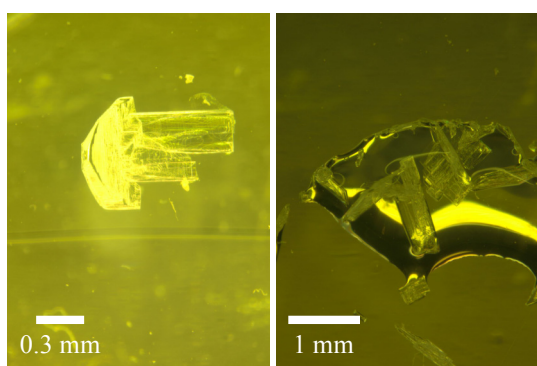
Glass



method 2

method 3

PDMS



method 2

method 3

**Figure 4.17** Examples of barbital crystal pictures on each surface for each method from water solution.



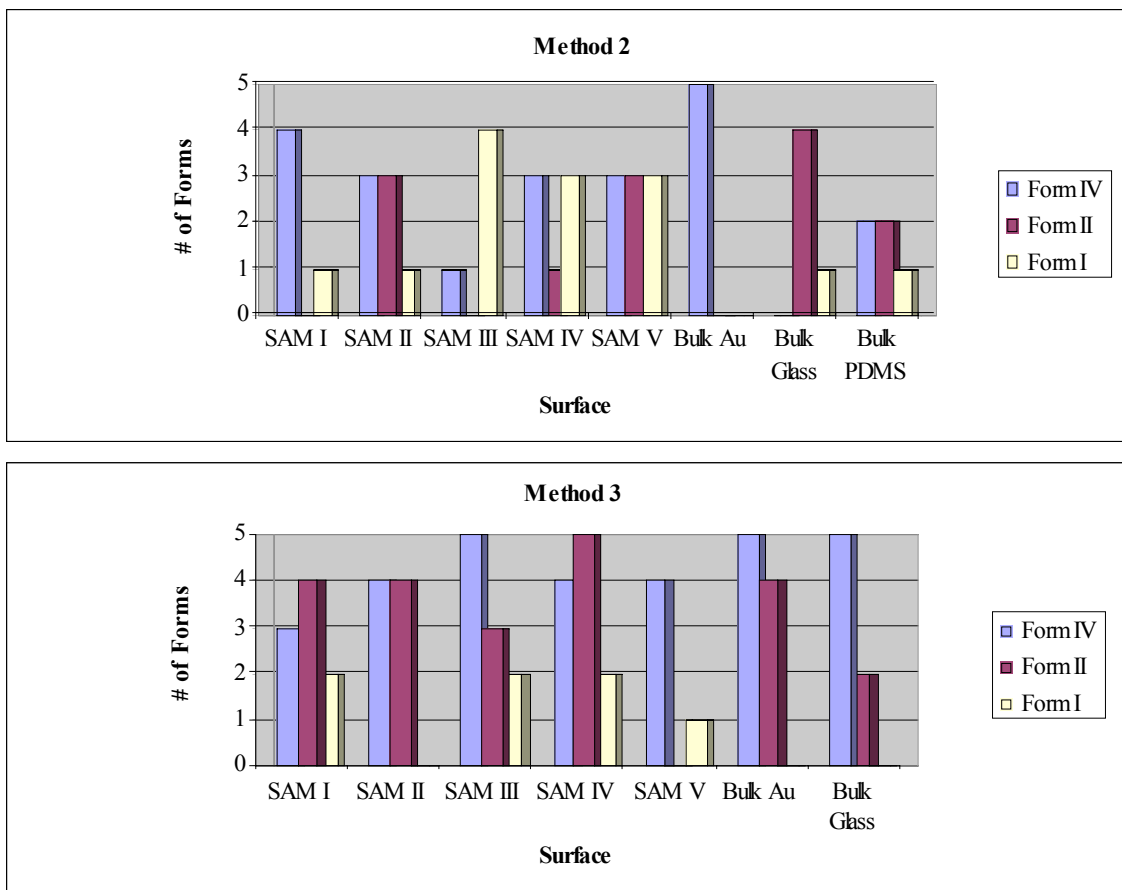


**Figure 4.18** Results of barbital crystallization experiments for each method from water solution.

The experiments on SAMs in water show greater variability with slightly lower selectivity for form IV and a higher incidence of form I by both methods when compared to the results from ethanol. Forms I and IV both appeared concomitantly on SAMs I and III with form I predominating on SAM III by method 2. All three forms appeared concomitantly on SAMs II, IV and V by method 2. It is notable that form IV is the only polymorph to appear on the bare gold control surface because gold behaves as a hydrophobic surface. This result supports our hypothesis that hydrophobic surfaces promote nucleation of form IV. Even more notable is the fact that bare glass gave only



forms I and II in water by method 2. This data contrasts sharply with the experiments in ethanol where form IV predominated. This result supports our claim that hydrophilic surfaces with exposed OH groups can promote templating of forms I and II where the molecules bind to the surface via hydrogen bonding. Similar to experiments in ethanol, method 3 gave a much higher incidence of form II. In contrast to experiments in ethanol, however, method 3 did not appear to lower selectivity. For example, only two forms appeared on SAMs II and V by method 3, while all three forms appeared on SAMs I, III and IV by method 3. This level of selectivity is comparable to that observed by method 2. Although the ratio of forms II and IV by method 3 varied slightly from SAM to SAM in water compared to ethanol, the ratio of forms II and IV summed over all SAMs remained constant at 1:1 in both solvents by method 3. These results show that while crystallization under thermodynamic conditions in water still favors metastable form IV, it also gives a considerably higher incidence of form I, which is the most stable polymorph. Together, with the data from experiments in ethanol, these results also indicate that crystallization under kinetic conditions generally gives a higher incidence of form II than under thermodynamic conditions independent of the SAM that is used. Perhaps most importantly, the fact that form IV predominates only on hydrophobic SAM I supports our claim that templated nucleation via hydrogen bonding to surfaces can promote different polymorphs than those that appear on hydrophobic surfaces.

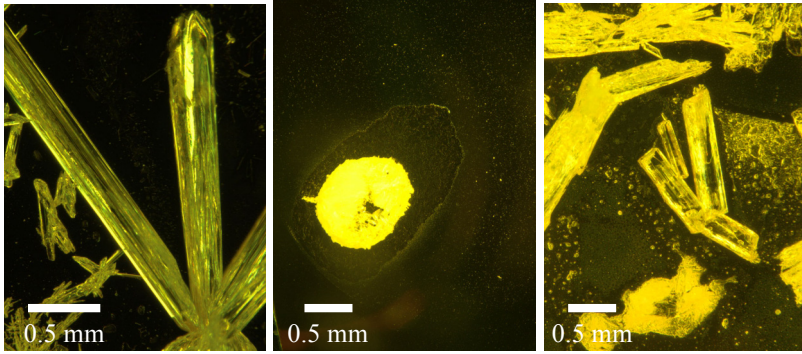
It is worth noting that crystals of form IV frequently appeared oriented with the large rectangular 010 face in contact with SAMs. In a several cases, plates of form IV were observed growing on hydrophilic SAMs attached at the edge of the plate with the 010 face orientated at an oblique angle to the plane of the surface. In that orientation, a plate

necessarily attached to the surface with the hydrogen-bonding groups of barbital at the edge of the plate in contact with the hydrogen-bonding groups on the surface of the SAM. These results suggest that hydrogen bonding plays a role in determining the orientation of crystals of barbital with respect to the surfaces. The fact that form IV appeared at all on hydrophilic SAMs indicates, however, that templated nucleation via hydrogen bonding of molecules on SAMs can lead to more than one polymorph.

#### **4.4.2.1.3 Ethyl Acetate**

In addition to ethanol and water, we chose investigate the crystallization behavior of barbital in ethyl acetate to examine the influence of a polar aprotic solvent with no acidic hydrogen-bonding donors on the crystallization behavior of barbital. We also wanted to further test our hypothesis that solvation of surfaces inhibits hydrogen bonding between barbital and the surface. We expected that a hydrogen bonding might still occur between ethyl acetate and the OH and CO<sub>2</sub>H groups on SAMs II-V because they contain acidic donors capable of bonding to the carbonyl oxygen acceptors on ethyl acetate. Considering that the carbonyl groups of esters usually are weak acceptors compared to hydroxyl groups, we expected solvation of SAMs, if it occurred at all, to form weak intermolecular contacts that resulted in poor coverage. Examples of crystals grown on each different surface are shown in Figure 4.19. The results are summarized in Figure 4.20 as a graph for the three crystallization methods.

SAM I

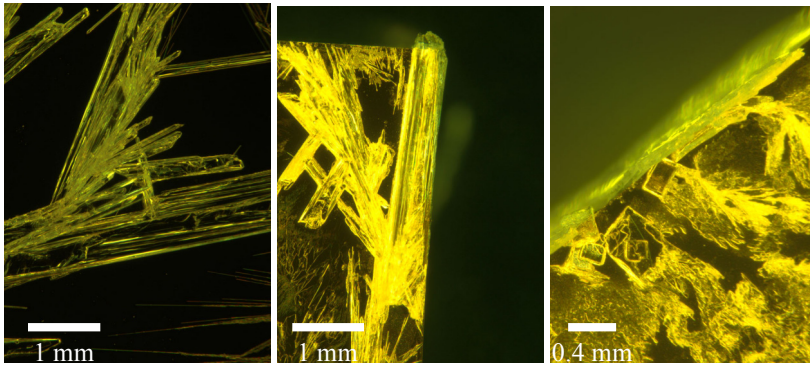


method 1

method 2

method 3

SAM II

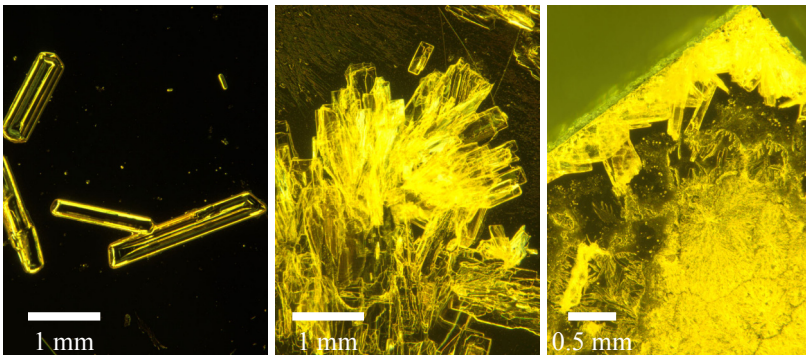


method 1

method 2

method 3

SAM III

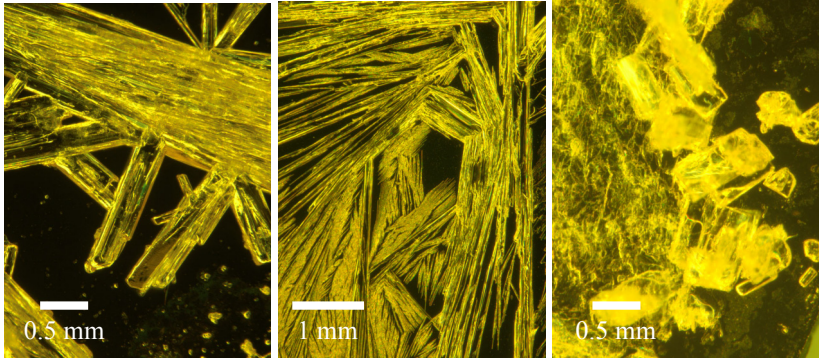


method 1

method 2

method 3

SAM IV

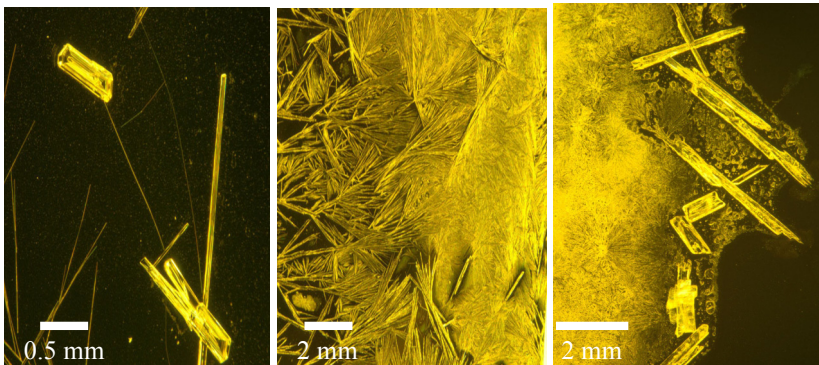


method 1

method 2

method 3

SAM V

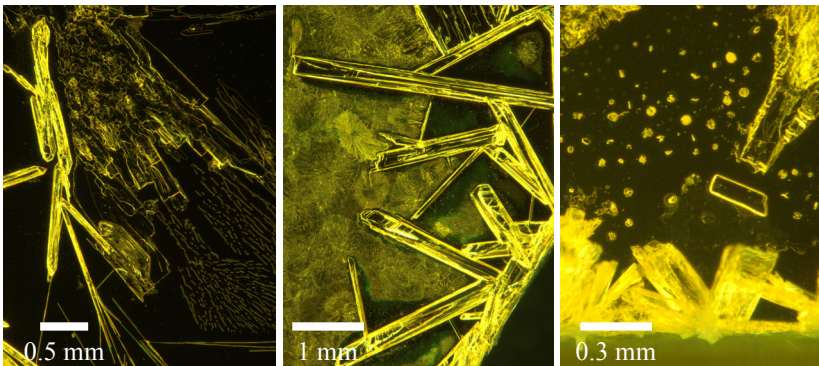


method 1

method 2

method 3

Bulk Gold



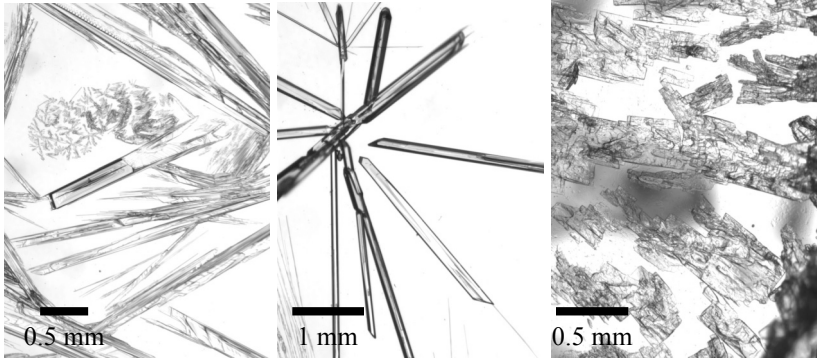
method 1

method 2

method 3



Glass

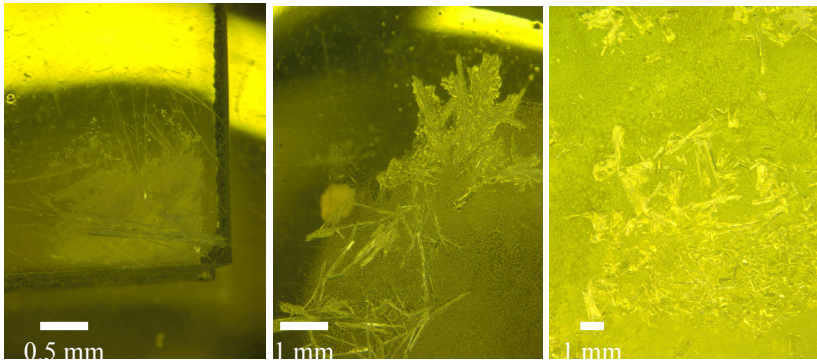


method 1

method 2

method 3

PDMS



method 1

method 2

method 3

**Figure 4.19** Examples of barbital crystal pictures on each surface for each method from ethyl acetate solution.

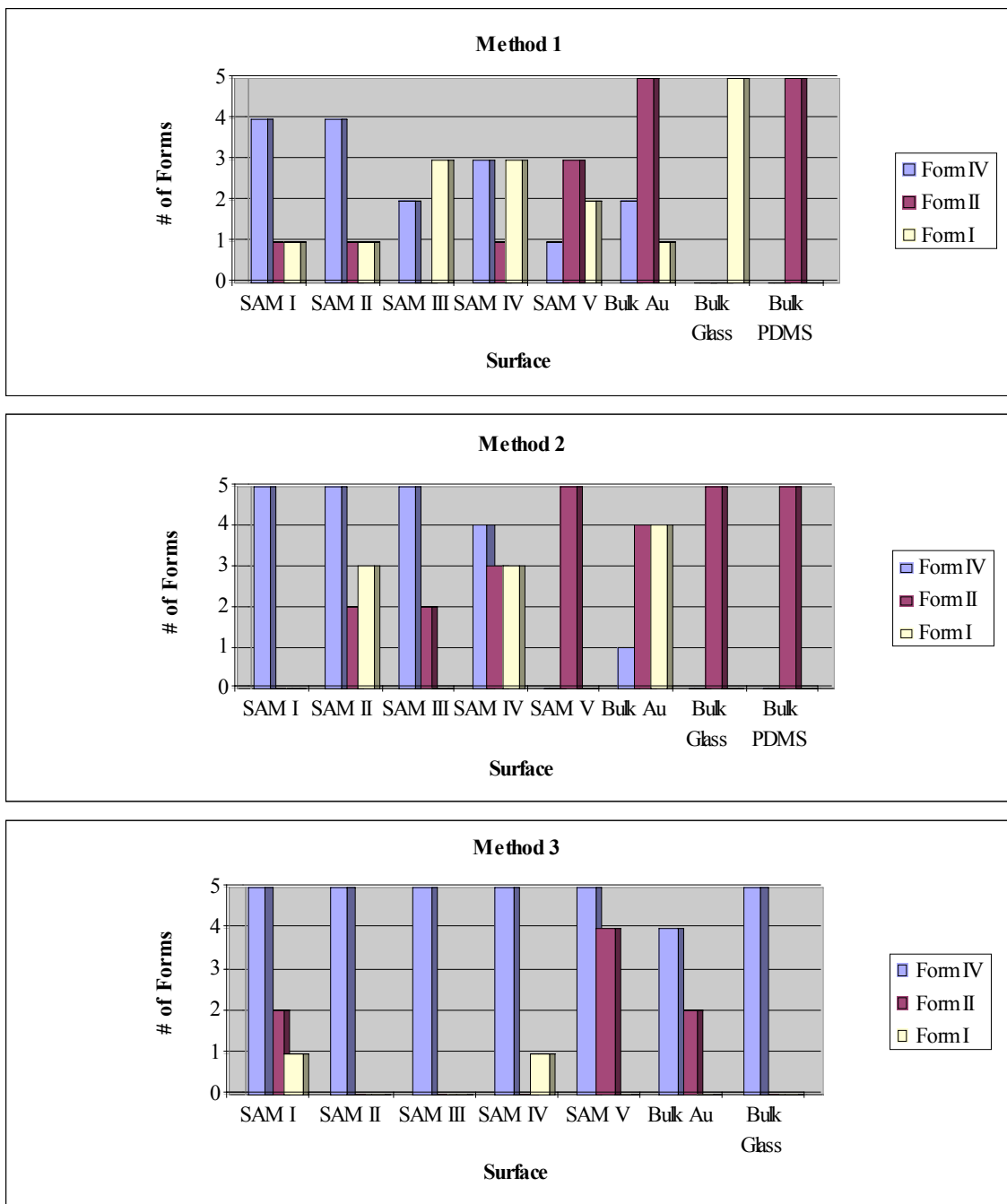


**Figure 4.20** Results of barbital crystallization experiments for each method from ethyl acetate solution.

The experiments in ethyl acetate also show greater variability with slightly lower selectivity for form IV and a higher incidence of forms I and II when compared to the

results from ethanol. Forms I, II and IV appeared concomitantly on SAMs I, II, IV and V with form IV appearing most frequently by method 1. Overall, the results from method 1 on SAMs in ethyl acetate were similar to those obtained in water from using method 2. Method 2 showed greater selectivity for form IV, which predominated on SAMs I-III. Form II was the only polymorph to appear on SAM V by method 2, which interestingly was the only set of conditions that produced form II in the absence of other polymorphs. It should be noted that form I predominated on SAM I by method 1 and was the only polymorph by method 2. These results are consistent with the results in ethanol and water, and provide further evidence that hydrophobic surfaces favor nucleation of form IV under thermodynamic conditions. The results of crystallization by method 3 in ethyl acetate deviate significantly from those in ethanol and water. Method 3 clearly favored form IV on all SAMs with form IV appearing exclusively on SAMs II and III, concomitantly with forms I and II on SAMs IV and V, respectively, and concomitantly with both forms I and II on SAM I.

#### **4.4.2.2 Microfluidic Device**

Crystallization experiments with barbital were carried out on SAMs I-V in microfluidic channels in addition to SAMs on bulk surfaces in an effort to develop methods for high throughput crystallization on surfaces. These experiments differ necessarily from those on bulk surfaces in that evaporation by methods 1 and 2 were not possible. Instead, crystallization was carried out as described earlier by allowing solutions of barbital to sit over SAMs in microchannels either at room temperature (method 2) or by rapidly cooling of more concentrated solutions (method 3). Experiments

in microchannels were carried on in ethanol and water. Ethyl acetate could not be used because it caused PDMS in the walls of the microchannels to swell. One of the goals of these experiments was to determine if polymorphs nucleated on SAMs in microchannels had the same habit as those nucleated on bulk surfaces. We found that the habits of the different polymorphs in microfluidic channels remained consistent with those observed on SAMs on bulk surfaces. We also aimed to determine if PDMS in the walls of the microchannels influenced nucleation crystals in competition with SAMs. Plates of form IV in particular generally grew oriented with the large rectangular 010 face in contact with SAMs as observed earlier on bulk surfaces. The high frequency with which crystals of form IV grew in this manner indicates that oriented growth on the underlying SAM probably occurs during nucleation. Crystals often first appeared at the edges of channels. Models for heterogeneous nucleation and growth of molecular crystals have established that molecular aggregation from solution is most favorable at high energy surfaces at kink sites (corners) and step edges.<sup>170</sup> Therefore; it was not surprising to find crystals of barbital often appearing at the edges of channels where SAMs come into contact with PDMS. Even though repeated attempts were made to observe under the microscope the location of initial growth, it was not possible to discern whether nucleation occurred selectively on SAMs or on PDMS. In all cases, crystals appeared to form at the interface between the two.

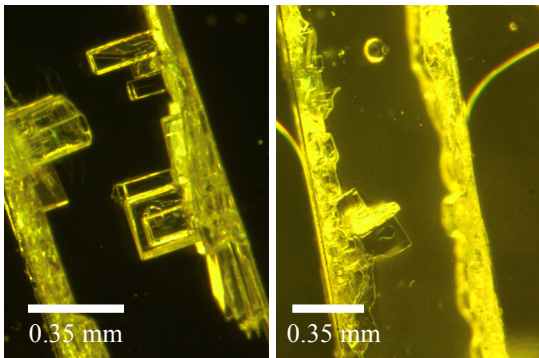
#### **4.4.2.2.1 Ethanol**

Examples of crystals grown on each different surface are shown in Figure 4.21. Shown in Figure 4.22 are the distributions of forms I, II and IV of barbital that grew from



ethanolic solutions in microchannels over SAMs I-V and PDMS under thermodynamic conditions (method 1) and kinetic conditions (method 2). Also shown for comparison are the distributions of polymorphs that appeared on bulk gold, glass and PDMS substrates in the absence of microchannels.

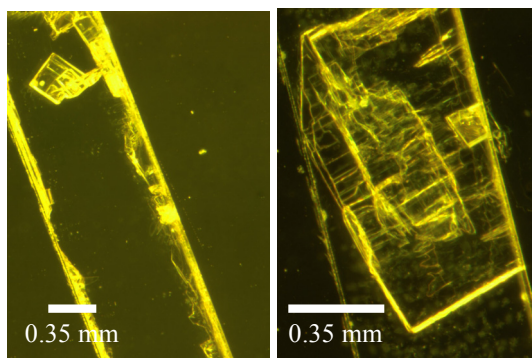
SAM I



method 2

method 3

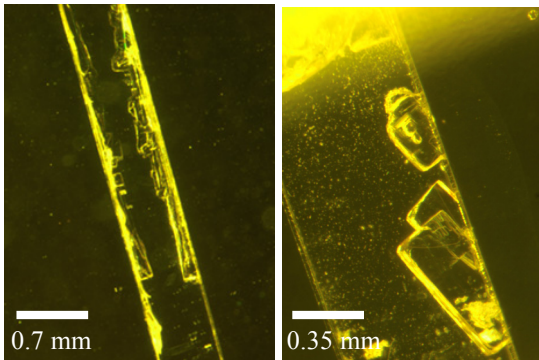
SAM II



method 2

method 3

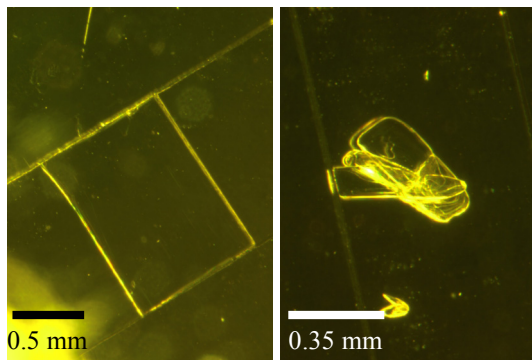
SAM III



method 2

method 3

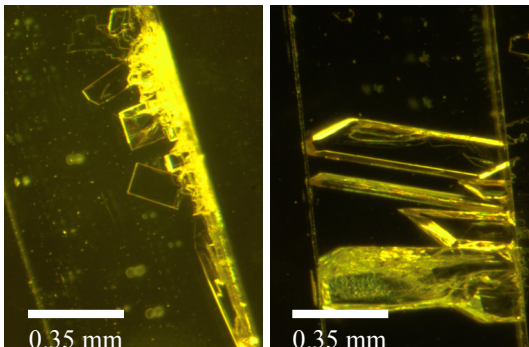
SAM IV



method 2

method 3

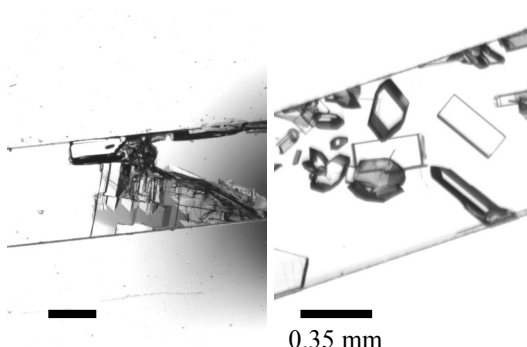
SAM V



method 2

method 3

PDMS

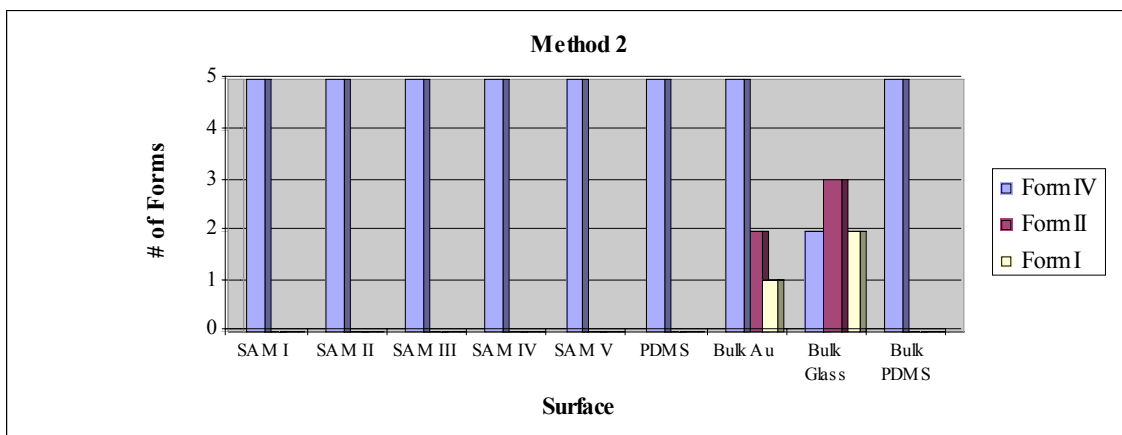


method 2

method 3

**Figure 4.21** Examples of barbital crystal pictures in microchannels from ethanolic solution.

Shown in Figure 4.22 are the distributions of forms I, II and IV of barbital that grew in microchannels over SAMs I-V and PDMS under thermodynamic conditions (method 1) and kinetic conditions (method 2). Also shown for comparison are the distributions of polymorphs that appeared on bulk gold, glass and PDMS substrates in the absence of microchannels.



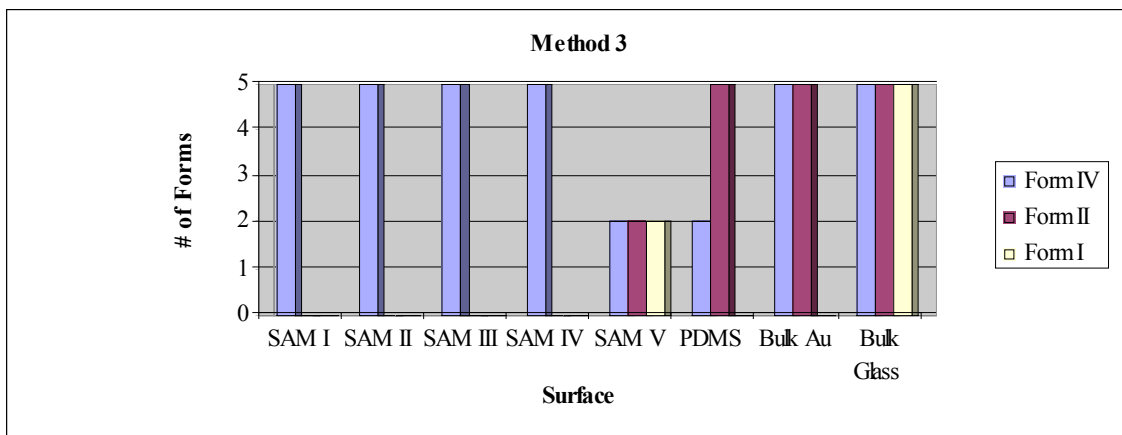


**Figure 4.22** Results of barbital crystallization experiments in microchannels from ethanolic solution. The distribution of forms I, II and IV that grew on bulk Au, glass and PDMS substrates are shown for comparison.

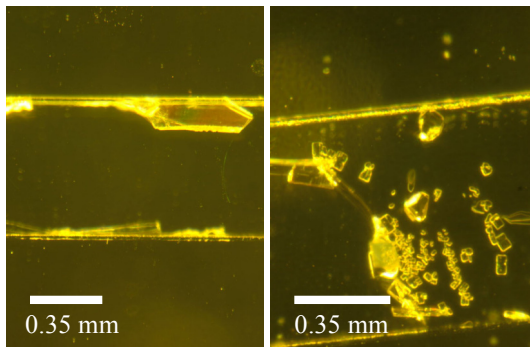
Form IV of barbital clearly was the dominant polymorph regardless of the substrate and crystallization method used with ethanol. For ethanolic solution under thermodynamic conditions (method 1), form IV was the only polymorph that appeared in microchannels. This result was unexpected for the following reasons: (1) form IV generally is the most difficult polymorph to prepare by conventional methods of crystallization from solution, (2) form IV is the least stable of the three polymorphs, and (3) concomitant crystallization of all three forms from bulk ethanolic solutions usually favors forms I and II. For example, all three polymorphic forms appear when barbital is crystallized over bare gold and glass substrates, as shown in Figure 4.22. Even more surprising was the lack of variation in selectivity across the range of different functional groups presented at the surface of SAMs I-V. These results differ slightly from those on SAMs on bulk surfaces where form IV predominated in ethanol, but did not always form exclusively. It is noteworthy that form IV was the only polymorph observed in

microfluidic channels under thermodynamic conditions with PDMS as the substrate. Form IV also was the only polymorph observed in the absence of microchannels when barbital was crystallized by slow evaporation of ethanolic solutions over bulk PDMS substrates. These results suggest that PDMS probably plays a significant role in promoting nucleation of form IV, and that the influence of PDMS likely is as important (if not more important) than that of SAMs under thermodynamic conditions. Crystallization of barbital under kinetic conditions (method 2) on SAMs also showed high selectivity for form IV. For example, Figure 4.22 shows that form IV appeared exclusively in microchannels over SAMs I-IV, while all three forms appeared in microchannels over SAM V. The high selectivity for the least stable polymorph in the presence of SAMs again was surprising, especially considering that kinetic conditions often lower selectivity and promote formation of multiple polymorphic forms. A decrease in selectivity in fact was observed for method 2 compared to method 1 on bulk gold, glass and PDMS surfaces as well as in microchannels over PDMS.

#### **4.4.2.2.2 Water**

Examples of crystals grown from aqueous solutions on each different surface are shown in Figure 4.23. Shown in Figure 4.24 are the distributions of forms I, II and IV of barbital that grew in microchannels over SAMs I-V and PDMS under thermodynamic conditions (method 1) and kinetic conditions (method 2). Also shown for comparison are the distributions of polymorphs that appeared on bulk gold, glass and PDMS substrates in the absence of microchannels.

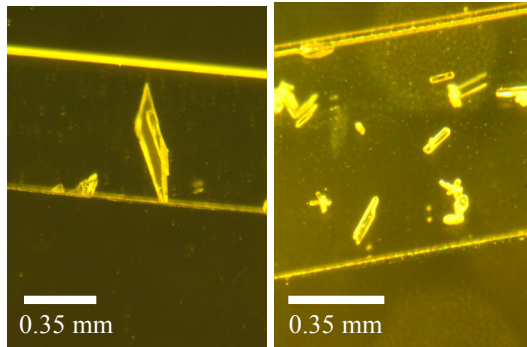
SAM I



method 2

method 3

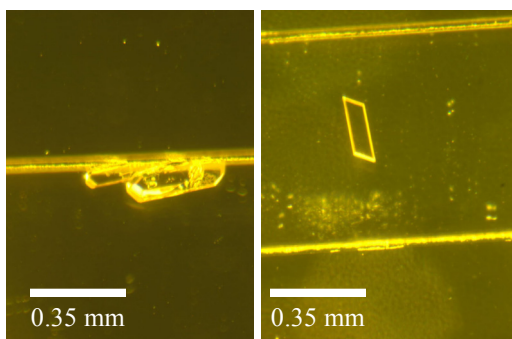
SAM II



method 2

method 3

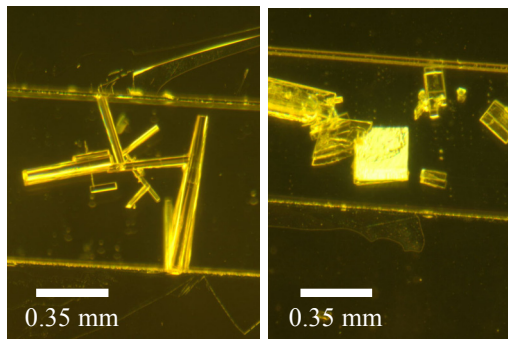
SAM III



method 2

method 3

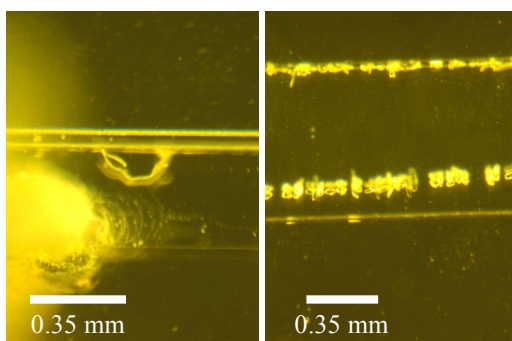
SAM IV



method 2

method 3

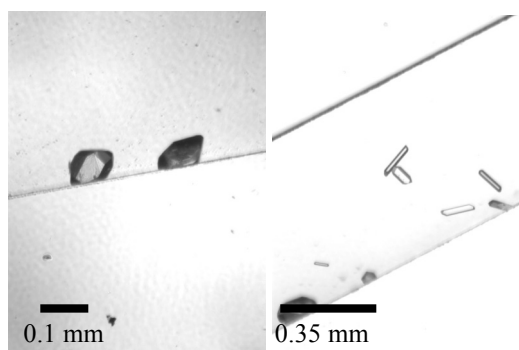
SAM V



method 2

method 3

PDMS



method 2

method 3

**Figure 4.23** Examples of barbital crystal pictures in microchannels from water solution.

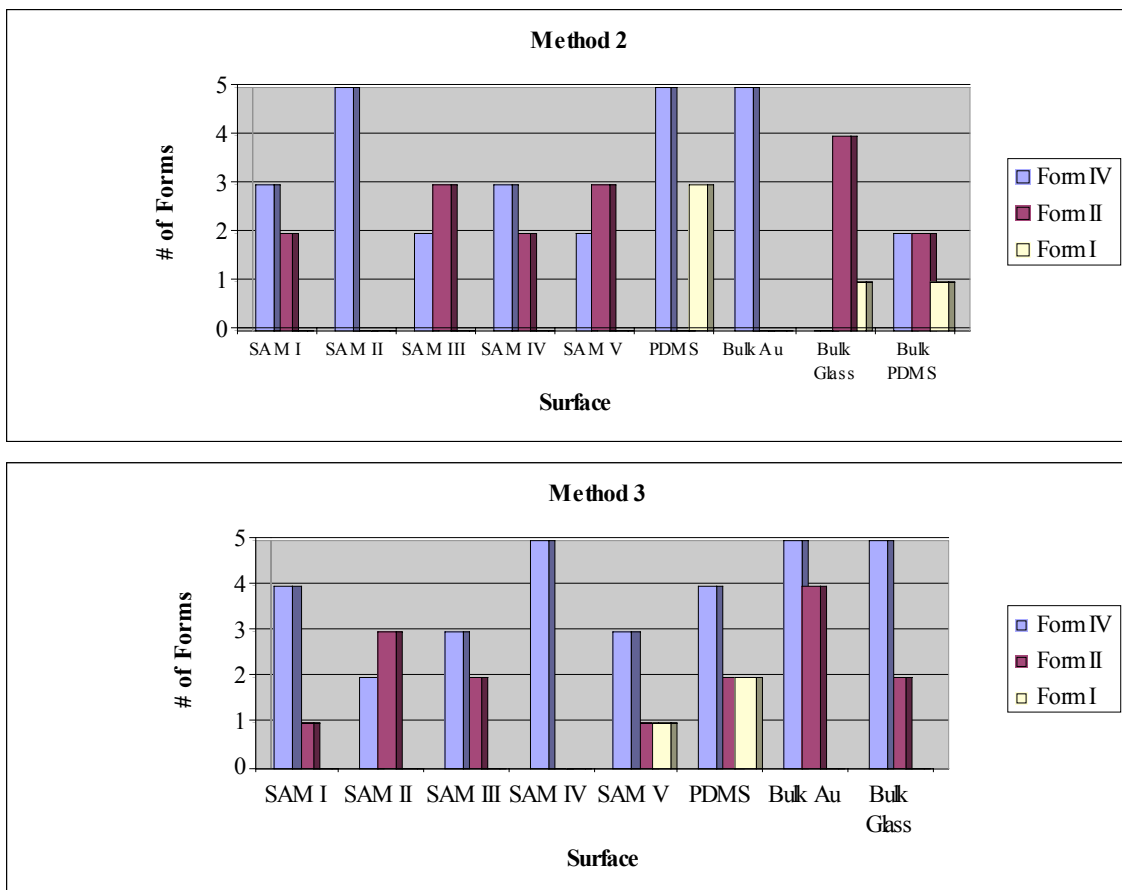


**Figure 4.24** Results of barbital crystallization experiments in microchannels from water solution. The distribution of forms I, II and IV that grew on bulk Au, glass and PDMS substrates are shown for comparison.

The results from crystallizing barbital on SAMs in microfluidic channels from water differ from those from ethanol. Whereas form IV was the only polymorph that crystallized from ethanol by method 2, crystallization from water gave approximately equal amounts of forms II and IV concomitantly on SAMs I, III, IV and V. SAM II was the only surface that gave form IV exclusively in water by method 2. Notably, form IV appeared in all experiments on the PDMS control surface with form I appearing concomitantly in 3 of 5 experiments by method 1. Interestingly, form I of barbital

appeared only in the PDMS control experiments in microchannels by method 1. Crystallization by method 3 gave form IV exclusively on SAM IV, forms II and IV concomitantly on SAMs I-III, and all three forms on SAM V. Overall, forms II and IV predominated with form IV appearing with slightly higher frequency than form II.

#### **4.5 Conclusions**

We have demonstrated that SAMs appear to exert little or no influence over the nucleation and growth of forms I and II of acetaminophen from ethanol on bulk surfaces. In contrast, we found that SAMs clearly influence the nucleation and growth of polymorphic forms I, II and IV of barbital both on bulk surfaces and in microfluidic channels. Crystallization of barbital over SAMs in general showed a high selectivity for form IV, which is surprising because form IV is the least stable of the three polymorphs. This finding differs from the normally observed crystallization behavior of barbital on glass substrates where all three polymorphs crystallize concomitantly with forms I and II dominating. Surprisingly, the selectivity for form IV persists across the series of SAMs despite differences in the hydrophobic and hydrophilic head groups. An important finding of this study was that crystallization under thermodynamic conditions of slow evaporation generally resulted in greater selectivity for one or more forms of barbital when compared to crystallization under kinetic conditions by rapid cooling. Another unexpected result was that solvation of SAMs by polar solvents such as ethanol appears to render hydrophilic surfaces more hydrophobic, thereby favoring oriented nucleation of form IV of barbital. This finding is significant in that it shows that solvents likely play a significant role in promoting or inhibiting templating of molecules on surfaces through

hydrogen-bonding interactions, and thus in controlling nucleation of one polymorph over another. Although we were not able to control selectivity between forms I, II and IV of barbital exclusively based on the choice of SAMs, we showed that crystallization of barbital on bulk surfaces and in microchannels over SAMs provides a way to prepare the least stable polymorph reproducibly and that crystallization under thermodynamic conditions leads to greater selectivity. These studies also provide evidence that PDMS in the walls of the microchannels may influence nucleation of barbital to a greater extent than SAMs.



#### 4.6 References

1. Bernstein, J. *Polymorphism in Molecular Crystals*, Clarendon Press, Oxford, **2002**.
2. Desiraju, G.R. *Crystal Engineering: The Design of Organic Solids*, Materials Science Monographs, Elsevier, New York, **1989**.
3. Byrn, S.R.; Pfeiffer, R.; Ganey, M.; Hoiberg, C.; Poochikian, G. *Pharm. Res.* **1995**, *12*, 945.
4. Rodriguez-Hornedo, N.; Murphy, D. *J. Pharm. Sci.* **1999**, *88*, 651.
5. Heywood, B.R; Mann, S. *Adv. Mater.* **1994**, *16*, 9.
6. Meldrum, F. C.; Flath, J.; Knoll, W. *Langmuir* **1997**, *13*, 2033.
7. Bandyopadhyay, K.; Vijayamohan, K. *Langmuir* **1998**, *14*, 6924.
8. Popovitz-Biro, R.; Lahav, M.; Leiserowitz, L. *J. Am. Chem. Soc.* **1991**, *113*, 8943.
9. Travaille, A. M.; Kaptijn, L.; Verwer, P.; Hulsken, B.; Elemans, J. A. A. W.; Nolte, R. J. M.; van Kempen, H. *J. Am. Chem. Soc.* **2003**, *125*, 11571.
10. Aizenberg, J.; Black, A.J.; Whitesides, G.M. *J. Am. Chem. Soc.* **1999**, *121*, 4500.
11. Kuther, J.; Seshadri, R.; Knoll, W.; Tremel, W. *J. Mater. Chem.* **1998**, *8*, 641.
12. Banno, N.; Nakanishi, T.; Matsunaga, M.; Asahi, T.; Osaka, T. *J. Am. Chem. Soc.* **2004**, *126*, 428.
13. Briseno, A.L.; Aizenberg, J.; Han, Y.-J.; Penkala, R.A.; Moon, H.; Lovinger, A.J.; Kloc, A.; Bao, Z. *J. Am. Chem. Soc.* **2005**, *127*, 12164.
14. Frostman, M.L.; Bader, M.M.; Ward, M.D. *Langmuir* **1994**, *10*, 576.

15. Kang, J.F.; Zaccaro, J.; Ulman, A.; Myerson, A. *Langmuir* **2000**, *16*, 3791.
16. Lee, A.Y.; Ulman, A.; Myerson, A.S. *Langmuir* **2002**, *18*, 5886.
17. Pham, T.; Lai, D.; Ji, D.; Tuntiwechapikul, W.; Friedman, J.M.; Lee, T.R.;  
*Coll. Surf. B: Biointerfaces* **2004**, *34*, 191.
18. Ji, D.; Arnold, C.M.; Graupe, M.; Beadle, E.; Dunn, R.V.; Phan, M.N.;  
Villazana, R.J.; Benson, R.; Colorado Jr., R.; Lee, T.R.; Friedman, J.M. *J. Cryst. Growth* **2000**, *218*, 390.
19. Hiremath, R.; Varney, S.W.; Swift, J.A. *Chem. Commun.*, **2004**, *23*, 2676.
20. Hiremath, R.; Basile, J.A.; Varney, S.W.; Swift, J.A. *J. Am. Chem. Soc.* **2005**,  
*127*, 18321.
21. Zheng, B.; Roach, L.S.; Ismagilov, R.F. *J. Am. Chem. Soc.* **2003**, *125*, 11170.
22. Chen, D.L.; Gerdts, C.J.; Ismagilov, R.F. *J. Am. Chem. Soc.* **2005**, *127*, 9672.
23. Ha, J.-M.; Wolf, J.H.; Hillmyer, M.A.; Ward, M.D. *J. Am. Chem. Soc.* **2004**,  
*126*, 3382.
24. Hilden, J.L.; Reyes, C.E.; Kelm, M.J.; Tan, J.S.; Stowell, J.G.; Morris, K.R.  
*Cryst. Growth Des.* **2003**, *3*, 921.
25. Chyall, L.J.; Tower, J.M.; Coates, D.A.; Houston, D.L.; Childs, S.L. *Cryst. Growth Des.* **2002**, *2*, 505.
26. Peterson, M.L.; Morissette, S.L.; McNulty, C.; Goldsweig, A.; Shaw, P.;  
LeQuesne, M.; Monagle, J.; Encina, N.; Marchionna, J.; Johnson, A.; Cima,  
M.J.; Almarsson, O. *J. Am. Chem. Soc.* **2002**, *124*, 10858.

27. McCrone, W.C. *Polymorphism in Physics and Chemistry of the Organic Solid State*, Eds. Fox, D.; Labes, M.M.; Weisseberg, A. Interscience, New York, **1965**, Vol. II, 726.
28. DeCamp, W.H. *Crystal Growth of Organic Materials*, Myerson, A.S.; Green, D.A.; Meenan, P. Eds. (ACS Proceedings Series, American Chemical Society, Washington, DC, **1996**.
29. Etter, M.C.; Macdonald, J.C.; Bernstein, J. *Acta Cryst. Sect. B, Struct. Commun.* **1990**, 46, 256.
30. Etter, M.C.; Reutzel, S.M. *J. Am. Chem. Soc.* **1991**, 113, 2586.
31. Desiraju, G.R. *Angew. Chem. Int. Ed. Engl.* **1995**, 34, 2311.
32. Moulton, B.; Zaworotko, M.J. *Chem. Rev.* **2001**, 101, 1629.
33. Desiraju, G.R. *Accounts Chem. Res.* **2002**, 35, 565.
34. Aksay, I.A.; Trau, M.; Manne, S.; Honma, I.; Yao, N.; Zhou, L.; Fenter, P.; Eisenberger, P.M.; Gruner, S.M. *Science* **1996**, 273, 892.
35. Towler, C.S.; Davey, R.J.; Lancaster, R.W.; Price, C.J. *J. Am. Chem. Soc.* **2004**, 126, 13347.
36. Busing, W.R. *Acta Cryst.* **1983**, A39, 340.
37. Bernstein, J.; Davey, R. J.; Henck, J.-O. *Angew. Chem. Int. Ed.* **1999**, 38, 3440.
38. Barnett, S.A.; Blake, A.J.; Champness, N.R. *CrystEng-Comm* **2003**, 5, 134.
39. Shekunov, B.Y.; York, P. J. *Cryst. Growth* **2000**, 211, 122.

40. Rodriguez-Hornedo, N.; Sinclair, B.D. *Crystallization : Significance in Product Development, Processing, and Performance, Encyclopedia of Pharmaceutical Technology*, Marcel Dekker, New York, **2002**, pp 671-690
41. Davey, R.J.; Allen, K.; Blagden, N.; Cross, W.I.; Lieberman, H.F.; Quayle, M.J.; Righini, S.; Seton, L.; Tiddy, G.J.T. *Cryst. Eng. Commun.* **2002**, *4*, 257.
42. Lahav, M.; Leiserowitz, L. *Chem. Eng. Sci.* **2001**, *56*, 2245.
43. Veessler, S.; Lafferrere, L.; Garcia, E.; Hoff, C. *Org. Proc. Res. Dev.* **2003**, *7*, 983.
44. Boistelle, R.; Astier, J. P.; Marchis-Mouren, G.; Desseaux, V.; Haser, R. *J. Cryst. Growth* **1992**, *123*, 109.
45. Lafont, S.; Veessler, S.; Astier, J. P.; Boistelle, R. *J. Cryst. Growth* **1994**, *143*, 249.
46. Ostwald, W. *Z. Phys. Chem.* **1897**, *22*, 289.
47. Hamiaux, C.; Perez, J.; Prange', T.; Veessler, S.; Ries-Kautt, M.; Vachette, P. *J. Mol. Biol.* **2000**, *297*, 697.
48. Weissbuch, I.; Popovitz-Biro, R.; Lahav, M.; Leiserowitz, L. *Acta Crystallogr.* **1995**, *B51*, 115.
49. Zbaida, D.; Weissbuch, I.; Shavit-Gati, E.; Addadi, L.; Leiserowitz, L.; Lahav, M. *React. Polym.* **1987**, *6*, 241.
50. Staab, E.; Addadi, L.; Leiserowitz, L.; Lahav, M. *Adv. Mater.* **1990**, *2*, 40.
51. Lang, M.; Grzesiak, A. L.; Matzger, A. J. *J. Am. Chem. Soc.* **2002**, *124*, 14834.

52. Li, M.; Wang, A. F.; Mao, G. Z.; Daehne, L. *J. Phys. Chem. B* **1999**, *103*, 11161.
53. Bonafede, S. J.; Ward, M. D. *J. Am. Chem. Soc.* **1995**, *117*, 7853.
54. Last, J. A.; Hilier, A. C.; Hooks, D. E.; Maxson, J. B.; Ward, M.D. *Chem. Mater.* **1998**, *10*, 422.
55. Rapaport, H.; Kuzmenko, I.; Berfeld, M.; Kjaer, K.; Als-Nielsen, J.; Popovitz-Biro, R.; Weissbuch, I.; Lahav, M.; Leiserowitz, L. *J. Phys. Chem. B.* **2000**, *104*, 1399.
56. Carter, P.W.; Ward, M.D. *J. Am. Chem. Soc.* **1994**, *116*, 769.
57. Hiremath, R.; Varney, S.W.; Swift, J. A. *Chem. Mater.* **2004**, *16*, 4948.
58. Yu, L.; Stephenson, G.A.; Mitchell, C.A.; Bunnell, C.A.; Snorek, S.V.; Bowyer, J.J.; Borchardt, T.B.; Stowell, J.G.; Byrn, S.R. *J. Am. Chem. Soc.* **2000**, *122*, 585.
59. Kuhnert-Brandstatter, M. *Pure Appl. Chem.* **1966**, *10*, 136.
60. Huang, T. *Acta Pharm. Int.* **1961**, *2*, 95.
61. Huang, T. *Acta Pharm. Int.* **1961**, *2*, 43.
62. Brandstatter, M. *Phys. Chem.* **1942**, *A191*, 227.
63. Fischer, R.; Kofler, A. *Ber. Dtsch. Pharm. Ges.* **1932**, *270*, 207.
64. Fischer, R. *Ber. Dtsch. Pharm. Ges.* **1932**, *270*, 149.
65. Craven, B. M.; Vizzini, E. A.; Rodrigues, M. M. *Acta Cryst.* **1969**, *B25*, 1978.
66. Nichols, G.; Frampton, C. S. *J. Pharm. Sci.* **1998**, *87*, 684.
67. Burger, A. *Acta Pharm. Technol.* **1982**, *28*, 1.
68. Haisa, M.; Kashino, S.; Maeda, H. *Acta Cryst.*, **1974**, *B30*, 2510.

69. Haisa, M.; Kashino, S.; Kawai, R.; Maeda, H. *Acta Cryst.*, **1976**, B32, 1283.
70. Beyer, T.; Day, G. M.; Price, S. L. *J. Am. Chem. Soc.* **2001**, 123, 5086.
71. Craven, B.M.; Vizzini, E.A. *Acta Cryst.* **1971**, B27, 1917.
72. Macdonald, J.C.; Whitesides, G.M. *Chem. Reviews* **1994**, 94, 2383.
73. Martino, P.D.; Conflant, P.; Drache, M.; Huvenne, J.-P.; Guyot-Hermann, A.-M. *J. Therm. Anal.* **1997**, 48, 447.
74. Duberg, M.; Nystrom, C. *Powder Technol.* **1994**, 46, 67.
75. Martino, P.D.; Guyot-Hermann, A.M., Conflant, P.; Drache, M.; Guyot, J.C. *Int. J. Pharm.* **1996**, 128, 1.
76. Goho, A. *Science News* Aug. 21, **2004**, 166, No.8, 122.
77. Ulman, A. *An Introduction to Ultrathin Organic Films*, Academic Press; Boston, **1991**.
78. Kuhn, H.; Ulman, A. *In Thin Films*; Ulman A., Ed.; Academic Press; New York, **1995**; Vol 20.
79. Evans, S.D.; Ulman, A.; Goppert-Berarducci, K.E.; Gerenser, L.J. *J. Am. Chem. Soc.* **1991**, 113, 5866.
80. Hong, H.G.; Mallouk, T.E. *Langmuir* **1991**, 7, 2362.
81. Yang, H.C., Aoki, K.; Hong, H.G.; Sackett, D.D.; Arendt, M.F.; Yau, S.L.; Bell, C.M.; Mallouk, T.E. *J. Am. Chem. Soc.* **1993**, 115, 11855.
82. O'Brien J.T.; Zeppenfeld, A.C.; Richmond, G.L.; Page, C.J. *Langmuir* **1994**, 10, 4657.
83. Fang, M.; Kaschak, D.M.; Sutorik, A.C.; Mallouk, T.E. *J. Am. Chem. Soc.* **1997**, 119, 12184.

84. Hatzor, A.; Moav, T.; Cohen, H.; Matlis, S.; Libman, J.; Vaskevich, A.; Shanzer, A.; Rubinstein, I. *J. Am. Chem. Soc.* **1998**, *120*, 13469.
85. Deng, W.; Fujita, D.; Yang, L.; Neji, H.; Bai, C. *Japanese J. App. Phys., Part 2: Letters* **2000**, *39*, L751.
86. Ulman, A.; Evans, S.D.; Shnidman, Y.; Sharma, R.; Eilers, J.E.; Chang, J.C. *J. Am. Chem. Soc.* **1991**, *113*, 1499.
87. Kumar, A.; Biebuyck, H.A.; Whitesides, G.M. *Langmuir* **1994**, *10*, 1498.
88. Bigelow, W.C.; Pickett, D.L.; Zisman, W.A. *J. Colloid Interface Sci.* **1946**, *1*, 513.
89. Maoz, R.; Sagiv, J. *J. Colloid Interface Sci.* **1984**, *100*, 465.
90. Silberzan, P.; Leger, L.; Ausserre, D.; Benattar, J. *J. Langmuir* **1991**, *7*, 1647.
91. Allara, D.L., Nuzzo, R.G. *Langmuir* **1985**, *1*, 45
92. Allara, D.L., Nuzzo, R.G. *Langmuir* **1985**, *1*, 52.
93. Ogawa, H.; Chihera, T.; Taya, K. *J. Am. Chem. Soc.* **1985**, *107*, 1365.
94. Schlotter, N.E.; Porter, M.D.; Bright, T.B.; Allara, D.L. *Chem. Phys. Lett.* **1986**, *132*, 93.
95. Sagiv, J. *J. Am. Chem. Soc.* **1980**, *102*, 92.
96. Wasserman, S.R.; Tao, Y.T.; Whitesides, J.M. *Langmuir* **1989**, *5*, 1074.
97. Le Grange, J. D.; Markham, J. L.; Kurjian, C. R. *Langmuir* **1993**, *9*, 1749.
98. Gun, J.; Sagiv, J. *J. Colloid Interface Sci.* **1986**, *112*, 457.
99. Gun, J.; Iscovici, R.; Sagiv, J. *J. Colloid Interface Sci.* **1984**, *101*, 201.
100. Tillman, N.; Ulman, A.; Schildkraut, J. S.; Penner, T. L. *J. Am. Chem. Soc.* **1988**, *110*, 6136.

101. Brandriss, S.; Margel, S. *Langmuir* **1993**, *9*, 1232.
102. Mathauser, K.; Frank, C. W. *Langmuir* **1993**, *9*, 3002.
103. Mathauser, K.; Frank, C. W. *Langmuir* **1993**, *9*, 3446.
104. Carson, G.; Granick, S. *J. Appl. Polym. Sci.* **1989**, *37*, 2767.
105. Kessel, C. R.; Granick, S. *Langmuir* **1991**, *7*, 532.
106. Schwartz, D. K.; Steinberg, S.; Israelachvili, J.; Zasadzinski, Z.A.N. *Phys. Rev. Lett.* **1992**, *69*, 3354.
107. Finklea, H. O.; Robinson, L. R.; Blackburn, A.; Richter, B.; Allara, D. L.; Bright, T. *Langmuir* **1986**, *2*, 239.
108. Rubinstein, I.; Sabatani, E.; Maoz, R.; Sagiv, J. *Proc. Electrochem. Soc.* **1986**, *86*, 175.
109. Rubinstein, I.; Sabatani, E.; Maoz, R.; Sagiv, J. *Electroanal. Chem.* **1987**, *219*, 365.
110. Nuzzo, R. G.; Allara, D. L. *J. Am. Chem. Soc.* **1983**, *105*, 4481.
111. Ball, P. *Designing the Molecular World*; Princeton University Press, Princeton, **1994**.
112. Carpick, R.W.; Salmeron, M. *Chem. Rev.* **1997**, *97*, 1163.
113. Kumar, A.; Abbott, N.L.; Kim, E.; Biebuyck, H.A.; Whitesides, G.M. *Accounts of Chemical Research* **1995**, *28*, 219.
114. Mrksich, M. *Chemical Society Reviews* **2000**, *29*, 267.
115. Gupta, V.K.; Abbott, N.L. *Science* **1997**, *276*, 1533.
116. Itoh, M.; Nishihara, H.; Aramaki, K. *J. of the Electrochem. Soc.* **1995**, *142*, 1839.



117. Zamborini, F.P.; Crooks, R.M. *Langmuir*, **1997**, *13*, 122.
118. Bain, C.D.; Whitesides, G.M. *Adv. Mater.* **1989**, *1*, 506.
119. Porter, M.D., Bright, T.B., Allara, D.L., Chidsey, C.E.D. *J. Am. Chem. Soc.* **1987**, *109*, 3559.
120. Strong, L.; Whitesides, G.M. *Langmuir* **1988**, *4*, 546.
121. Somorjai, G.A. *Chemistry in Two Dimensions-Surfaces*; Cornell University Press: Ithaca, New York, **1982**.
122. Chidsey, C.E.D.; Loiacono, D.N. *Langmuir* **1990**, *6*, 709.
123. Dubois, L.H.; Zegarski, B.R.; Nuzzo, R.G. *J. Chem. Phys.* **1993**, *98*, 678.
124. Fenter, P.; Eisenberger, P.; Liang, K.S. *Phys. Rev. Lett.* **1993**, *70*, 2447.
125. Camillone, N.; Chidsey, C.E.D.; Liu, G.Y.; Scoles, G. *J. Phys. Chem.* **1993**, *98*, 3503.
126. Poirier, G.E.; Tarlov, M. J. *Langmuir* **1994**, *10*, 2859.
127. Etter, M. C. *J. Phys. Chem.* **1991**, *95*, 4601; Etter, M. C. *Acc. Chem. Res.* **1990**, *23*, 120.
128. Dubois, L.H.; Nuzzo, R.G. *Ann. Phys. Chem.* **1992**, *43*, 437.
129. Folkers, J.P.; Zerkowski, J.A.; Laibinis, P.E.; Seto, C.T.; Whitesides, G.M. Supramolecular architecture; Bein, T. Ed.; *ACS Symposium Series 499*; American Chemical Society: Washington, DC, **1992**; pp 10-23
130. Lee, T.R.; Laibinis, P.E.; Folkers, J.P.; Whitesides, G. M. *Pure Appl. Chem.* **1991**, *63*, 821.
131. Whitesides, G.M.; Ferguson, G.S. *Chemtracts-Org. Chem.* **1988**, *1*, 171.
132. Ulman, A. *Chem Rev.* **1996**, *96*, 1533.

133. Bain, C.D.; Troughton, E.B.; Tao, Y.T.; Evall, J.; Whitesides, G.M.; Nuzzo, R.G. *J. Am. Chem. Soc.* **1989**, *111*, 321.
134. Soto, E.; MacDonald, J. C.; Cooper, C. G. F.; McGimpsey, W. G. *J. Am. Chem. Soc.* **2003**, *125*, 2838.
135. Cooper, C. G. F.; MacDonald, J. C.; Soto, E.; McGimpsey, W. G. *J. Am. Chem. Soc.* **2004**, *126*, 1032.
136. Bain, C.D., Whitesides G.M. *J. Am. Chem. Soc.* **1988**, *110*, 3665.
137. Folkers J.P., Laibinis, P.E., Whitesides, G.M. *Langmuir* **1992**, *8*, 1330.
138. Ahn, H.-S.; Cuong, P.D.; Park, S.; Kim, Y.-W.; Lim, J.-C. *Wear* **2003**, *255*, 819.
139. Chechik V., Stirling C. J. M. Gold-thiol self-assembled monolayers. In: Patai S, Rappoport Z, eds. *The Chemistry of Organic Derivatives of Gold and Silver*. New York: John Wiley & Sons, **1999**: pp 551-640
140. Tillman N., Ulman A., Penner T.L. *Langmuir* **1989**, *5*, 101.
141. Sastry, M. A. *Bulletin of Materials Science* **2000**, *23*, 159.
142. Ordal M.A., Long L.L., Bell R.J., Bell, S.E., Bell, R.R., Alexander, R.W., Jr, Ward C.A. *Applied Optics* **1983**, *22*, 1099.
143. Allara, D.L., Swalen, J.D. *J. Phys. Chem.* **1982**, *86*, 2700.
144. Troughton, E.B., Bain, C.D., Whitesides, G.M., Nuzzo, R.G., Allara, D.L., Porter, M.D. *Langmuir* **1988**, *4*, 365.
145. Beulen, M.W.J., Kastenbergh, M.I., Van Veggel, F.C.J.M., Reinhoudt, D.N. *Langmuir* **1998**, *14*, 7463
146. Boubour, E., Lennox, R.B. *Langmuir* **2000**, *16*, 4222.

147. Boubour, E., Lennox, R.B. *J. Phys. Chem. B* **2000**, *104*, 9004.
148. Boubour, E., Lennox, R.B. *Langmuir* **2000**, *16*, 7464.
149. Sondag-Huethorst, J.A.M., Fokkink, L.G. *Langmuir* **1995**, *11*, 2237.
150. Fischer, R. *Ber. Dtsch. Pharm. Ges.* **1932**, *270*, 149.
151. Fischer, R.; Kofler, A. *Ber. Dtsch. Pharm. Ges.* **1932**, *270*, 207.
152. Brandstatter, M. *Phys. Chem.* **1942**, *A191*, 227.
153. Huang, T. -Y. *Acta Pharm. Intern.* **1951**, *2*, 43.
154. Huang, T. -Y. *Acta Pharm. Intern.* **1951**, *2*, 95.
155. Cleverly, B.; Williams, P. P. *Tetrahedron*, **1959**, *7*, 277-288.
156. Spong, B.R.; Price, C.P.; Jayasankar, A.; Matzger, A.J.; Hornedo, N.R. *Adv. Drug Delivery Reviews* **2004**, *56*, 241.
157. Lee, A.Y.; Lee, I.S.; Dette, S.S.; Boerner, J.; Myerson, A.S. *J. Am. Chem. Soc.* **2005**, *127*, 14982.
158. Dunitz, J.D.; Bernstein, J. *Acc. Chem. Res.* **1995**, *28*, 193.
159. McDonald, J.C.; Duffy, D.C.; Anderson, J.R.; Chiu, D.T.; Wu, H.; Schueller, O.J.A.; Whitesides, G.M. *Electrophoresis* **2000**, *21*, 27.
160. Borcka, L. *Pharma. Acta Helv.* **1991**, *66*, 16. [95, 240, 241]
161. Wang, Shun-Li; Lin, Shan-Yang; Wei, Yen-Shan *Chem. Pharm. Bull.* **2002**, *50(2)*, 153.
162. Byrn, S. R.; Pfeiffer, R. R.; Stephenson, G.; Grant, D. J. W.; Gleason, W. B. *Chem. Mater.* **1994**, *6*, 1148.
163. Zumbulyadis, N.; Antalek, B.; Windig, W.; Scaringe, R. P.; Lanzafame, A. M.; Blanton, T.; Helber, M. *J. Am. Chem. Soc.* **1999**, *121*, 11554.

164. Etter, M. C.; Hoye, R. C.; Vojta, G. M. *Cryst. Rev.* **1988**, *1*, 281.
165. Azaroff, L. V. and Burger, M.J. *The powder method in x-ray crystallography*. McGraw-Hill Book Company, New York, U.S.A, **1958**.
166. Bish, D.L. and Reynolds, R.C. *Sample preparation for x-ray diffraction. Reviews in mineralogy, modern powder diffraction, Vol. 20* (ed. D.L. Bish and J.E. Post), pp. 73-99. Mineralogy Society of America, Washington D.C., **1989**.
167. Jenkins, R. and Snyder, R.L. *Introduction of X-ray powder diffractometry. In Chemical Analysis: A series of monographs on analytical chemistry and its applications, Vol.138* (ed. J.D. Winefordner), pp. 324-35. Wiley-Interscience, New York, **1996**.
168. Glusker, J.P.; Lewis, M. and Rossi, M. *Crystal structure analysis for chemists and biologists*. VCH Publishers, New York, **1994**.
169. Jeffrey, G.A. *An Introduction to hydrogen bonding*, Oxford Press, USA, 1997.
170. Ward, M.D. *Chem. Rev.* **2001**, *101*, 1697.
171. Landau, E.M.; Levanon, M.; Leiserowitz, L.; Lahav, M.; Sagiv, J. *Nature* **1985**, *318*, 353.
172. Landau, E.M.; Wolf, S.G.; Levanon, M.; Leiserowitz, L.; Lahav, M.; Sagiv, J. *J. Am. Chem. Soc.* **1989**, *111*, 1436.
173. Zhao, X.K.; McCormick, L.D. *Appl. Phys. Lett.* **1992**, *61*, 849.
174. Heywood, B.R.; Mann, S. *Adv. Mater.* **1994**, *6*, 9.
175. Frostman, L.M.; Ward, M.D. *Langmuir* **1997**, *13*, 330.
176. Addadi, L.; Weiner, S. *Proc. Natl. Acad. Sci. U.S.A.* **1985**, *82*, 4110.

177. Addadi, L.; Moradian, J.; Shay, E.; Maroudas, N.G.; Weiner, S. *Proc. Natl. Acad. Sci. U.S.A.* **1987**, *84*, 2732.
178. Feng, S.; Bein, T. *Science* **1994**, *265*, 1839.
179. Berman, A.; Ahn, D.J.; Lio, A.; Salmeron, M.; Reichert, A.; Charych, D. *Science* **1995**, *269*, 515.